

Elaboration of a positioning elbow orthosis for patients suffering from spasticity

Auteur : Gevaert, Lou

Promoteur(s) : Duchene, Laurent; 13444

Faculté : Faculté des Sciences appliquées

Diplôme : Master en ingénieur civil biomédical, à finalité spécialisée

Année académique : 2020-2021

URI/URL : <http://hdl.handle.net/2268.2/11530>

Avertissement à l'attention des usagers :

Tous les documents placés en accès ouvert sur le site le site MatheO sont protégés par le droit d'auteur. Conformément aux principes énoncés par la "Budapest Open Access Initiative"(BOAI, 2002), l'utilisateur du site peut lire, télécharger, copier, transmettre, imprimer, chercher ou faire un lien vers le texte intégral de ces documents, les disséquer pour les indexer, s'en servir de données pour un logiciel, ou s'en servir à toute autre fin légale (ou prévue par la réglementation relative au droit d'auteur). Toute utilisation du document à des fins commerciales est strictement interdite.

Par ailleurs, l'utilisateur s'engage à respecter les droits moraux de l'auteur, principalement le droit à l'intégrité de l'oeuvre et le droit de paternité et ce dans toute utilisation que l'utilisateur entreprend. Ainsi, à titre d'exemple, lorsqu'il reproduira un document par extrait ou dans son intégralité, l'utilisateur citera de manière complète les sources telles que mentionnées ci-dessus. Toute utilisation non explicitement autorisée ci-avant (telle que par exemple, la modification du document ou son résumé) nécessite l'autorisation préalable et expresse des auteurs ou de leurs ayants droit.



Elaboration of a positioning elbow orthosis for patients suffering from spasticity

Master thesis conducted by

Lou Gevaert

with the aim of obtaining the degree of Master in Biomedical Engineering

Under the supervision of

Florian De Boeck (Spentys) and Laurent Duchêne (ULiege)

University of Liege - Applied sciences

Academic year of 2020-2021

Contents

| | |
|---|-----------|
| Introduction | 6 |
| I Background and context | 6 |
| 1 Spasticity | 7 |
| 1.1 Introduction | 7 |
| 1.2 Physiology of spasticity | 7 |
| 1.2.1 Nervous system | 8 |
| 1.2.2 Description of the elbow's articulation | 8 |
| 1.2.3 Muscles group affected for the elbow spasticity | 8 |
| 1.3 Causes of spasticity | 10 |
| 1.3.1 Post-Stroke-Spasticity | 10 |
| 1.3.2 Multiple Sclerosis | 10 |
| 1.3.3 Cerebral Palsy | 11 |
| 1.4 Diagnosis | 11 |
| 1.4.1 Patterns observed | 11 |
| 1.4.2 Scales to assess the intensity of spasticity | 12 |
| 1.4.3 Other measurements to assess the severity of spasticity | 13 |
| 1.5 Treatment | 13 |
| 1.5.1 Non-surgical treatment | 13 |
| 1.5.2 Surgery | 14 |
| 1.6 Prognosis | 14 |
| 1.7 Population concerned | 14 |
| 1.8 Conclusion | 15 |
| 2 Current orthopedic solutions | 15 |
| 2.1 Solutions available on the market | 15 |
| 2.1.1 Prefabricated orthoses | 16 |
| 2.1.2 Custom devices | 17 |
| 3 3D modeling and printing | 18 |
| 3.1 All technologies available | 18 |
| 3.1.1 Material extrusion: Fused Deposition Modeling (FDM) | 18 |
| 3.1.2 Vat polymerization | 19 |
| 3.1.3 Power bed fusion: Selective Laser Sintering (SLS) | 20 |
| 3.1.4 Material jetting: Multi Jet Fusion (MJF) | 20 |
| 3.2 Materials available for 3D printing | 21 |
| 3.3 3D modeling software used | 21 |
| 4 Mechanical knowledge required | 22 |
| 4.1 Material properties | 22 |
| 4.2 Quantities of interest | 23 |
| 5 Spentys presentation | 24 |
| II Challenges and solution proposed | 25 |
| 1 Advantages of 3D printed orthoses | 26 |

| | | |
|------------|---|-----------|
| 2 | Needs to be fulfilled and solution initially proposed | 26 |
| 3 | Challenges faced | 27 |
| 3.1 | Problems faced during the design phase | 28 |
| 3.2 | Choices of material and printer | 30 |
| 3.2.1 | Material for the BOA design | 30 |
| 3.2.2 | Material for the blocking hinge design | 31 |
| 3.3 | Problems faced during the printing tests | 33 |
| 3.4 | Challenges due to interactions with external companies | 37 |
| 3.5 | Position of the limb during the scan | 38 |
| 4 | Resistance Analysis | 41 |
| 4.1 | Analytic analysis of the BOA design | 41 |
| 4.2 | Finite element analysis of the blocking hinge design | 44 |
| 4.2.1 | Introduction | 44 |
| 4.2.2 | Introduction to <i>Solidworks</i> | 45 |
| 4.2.2.1 | Requirements to run a simulation | 45 |
| 4.2.2.2 | Solvers and options used | 45 |
| 4.2.3 | Simulations done | 46 |
| 4.2.3.1 | Moment applied on the orthosis | 46 |
| 4.2.3.2 | Resistance of the teeth and comparison of materials | 48 |
| 4.2.3.2.1 | Initial geometry | 48 |
| 4.2.3.3 | Isotropic or orthotropic material | 53 |
| 4.2.3.4 | External part of the hinge | 54 |
| 4.3 | Forces applied on the assembly of the two parts | 56 |
| 4.3.1 | Results | 57 |
| 4.3.2 | Conclusion | 58 |
| III | Final solution specifications | 59 |
| 1 | Requirements and desired aspect | 59 |
| 1.1 | Overall design | 59 |
| 1.2 | Presentation of the different designs | 61 |
| 1.2.1 | BOA design | 61 |
| 1.2.2 | Blocking hinge design | 63 |
| 2 | Workflow from the patient consultation to the final orthosis | 65 |
| 2.1 | In the OT office | 65 |
| 2.2 | At Spentys, by the designer | 67 |
| 2.3 | At Spentys, by the production operator | 72 |
| 2.4 | Restitution to the patient | 73 |
| IV | Feedback from patients | 74 |
| 1 | Details of the trials | 74 |
| 2 | Results of the trials | 74 |
| 2.1 | First short trial | 74 |
| 2.2 | Longer trial period | 74 |
| 2.2.1 | Patient 1 | 75 |
| 2.2.2 | Patient 2 | 75 |

| | | |
|-----------|---|-----------|
| 2.3 | Conclusion of the trial | 76 |
| V | Conclusion | 77 |
| 1 | What has been done | 77 |
| 2 | Further improvements | 78 |
| 2.1 | Inclusion of the hand in the orthosis | 78 |
| 2.2 | Automation of the process | 79 |
| 2.3 | Long term tests | 79 |
| 2.4 | Adapt the splint for children | 80 |
| VI | Appendix | 80 |
| 1 | Technical drawings | 80 |
| 2 | Internship at Spentys | 81 |
| 2.1 | Help with the orders | 81 |
| 2.2 | New product | 82 |
| 3 | Production costs and reimbursement process | 83 |
| 4 | Inconclusive finite element simulations | 84 |
| 5 | Parameters used for the printing | 86 |

Abstract

Patients suffering from elbow spasticity, as a consequence of a stroke or a disease such as multiple sclerosis or cerebral palsy, see their quality of life decrease. Their spastic limb is constantly contracted and its regular elongation is needed to avoid further damages. Immobilization devices are commonly used to force the extension of the elbow. Several solutions are available on the market but they do not fully satisfy the needs of the patients. Static orthoses are described as uncomfortable, prefabricated positioning orthoses (the position of the arm can be changed) are usually bulky and lead to hygiene issues and custom positioning devices either deform easily and need regular adjustment or require a long and laborious production process.

This work presents two models of 3D printed orthoses made according to the patient anatomy and whose opening angle can be chosen and frequently changed. The anatomical data of the patient is captured using a 3D scanner. Two models are developed, one using a BOA dial, a small device able to shorten or lengthen a cable embedded in the splint. As the length of the cable changes, the splint's opening angle increases or decreases. The second model uses a blocking hinge that allows the splint to be blocked to a finite number of opening angles. Once the ideas were initially defined, both solutions were optimized by changing the design and the parameters according to the issues encountered. Resistance analysis are also conducted on both designs. The BOA model is shown sufficiently strong using an analytical analysis and the blocking hinge design is studied through *Solidworks* simulations and an analytical computations.

Finally, one patient tried the BOA design for 8 days and gave his feedback. The patient was satisfied and found the orthosis comfortable and easy to adjust (with external help). His physical therapist noticed a relaxation of the elbow joint but a larger study would be needed to assess the effects of the splint, independently of the other treatments of the patient. The blocking hinge design is available in two sizes (Small and Large). The Small model offers increments of 16.4° , is discrete, and allows many positions but it is less resistant than the Large one. The large model is advised for patients exerting a greater flexion force on the orthosis but it offers fewer positions (increments of 18°). The blocking hinge design has not been tested on patients yet.

Acknowledgments

This master thesis is the biggest project I ever did and many people helped me to make it possible.

First of all, I would like to thanks Laurent Duchêne, my academic supervisor. Thank you for supporting this project even though it was not only mechanically oriented. Thank you for your feedback and pieces of advice on the mechanical part.

I would also like to thank Florian De Boeck, my internship supervisor. Thank you for giving me the opportunity to work in your company, in a stimulating and welcoming team. The sanitary situation made me fear that it would be complicated to feel supported but our weekly meetings truly helped me to keep a constant rhythm and to be motivated. Of course, I would also like to thank Benoit Frisque and the rest of the Spentys team. All the employees were welcoming, ready to answer questions, and willing to exchange ideas and comments.

I would also like to thanks all the doctors, physical therapists, and orthopedist technicians who helped with the medical part of this work. A special thanks to Christophe Taens and Dr. Ueberham that answered many of my questions.

Thank you Anthony Sutura for your pieces of advice in the redaction of this work.

Finally, I am grateful for my family and friends who were great mental supports and who helped in many ways (including being a model/photograph for some images of this report and making this socially restricted period pleasant).

Part

Introduction

This project aims at improving the quality of life of patients suffering from elbow spasticity. Spasticity is a relatively common disorder resulting from accidents (such as strokes or spinal cord injuries) or diseases (such as multiple sclerosis or cerebral palsy) [1]. Patients experience involuntary muscles contractions due to damage in their neural pathways and have thus difficulties relaxing their limbs [2]. It is, however, very important that the limb does not stay in a contracted position for too long or the muscles' fibers might get permanently shorter [1][3].

Several types of treatments are prescribed and one of the less "intrusive" ones is the immobilization in extension using a cast or an orthosis [4]. The orthosis will help the patient elongate his arm during short periods without making any effort. The extension angle should be changed depending on the patient's evolution [5]. Such orthoses are already available on the market but they show some disadvantages that might be avoided. The orthoses can be prefabricated which means that it is not fully adapted to the anatomy of the patient. Those devices are usually bulky, they do not let the skin breathe and the arm's positions available are limited [6][7]. Other splints are custom made using thermo-formable plastic to be adjusted to the patient's anatomy but they are usually not comfortable, they have to be modified frequently and they do not let the skin breathe [8].

This work aims to propose an orthosis that can be regularly and easily adjusted to the position wanted by the health care provider. The orthosis must be comfortable, light, and resistant while letting the skin breathe.

To achieve that goal, it was decided to 3D print the splint and to develop two main designs. The first, and most promising one, uses the BOA technology [9]. The BOA dial¹ is made of a small *box* and a cable that can be released or tightened by turning the BOA wheel. The cable is passing through tubes embedded in the splint to force the arm extension as it is tightened. The other design is more similar to the orthoses already on the market as it uses a blocking hinge that can be adjusted to a finite number of extension angles.

After this short introduction, the report is divided into five chapters. The first one will give the medical knowledge required to understand the pathology and the solution proposed, the technical knowledge to understand the 3D printing technology, the mechanical knowledge to understand resistance analysis and the presentation of Spentys [10], the company in collaboration with which this project was done.

In the second chapter, the advantages of the 3D printing technology in the orthopedic field are developed and the initial solution is proposed. The multiple choices that had to be made and the various challenges that were encountered from the design phase to the production phase are then explained. The resistance analysis, both the analytical computations and the computed simulations are developed. The next chapter presents the final design solutions and the requirements to provide the desired products are listed. The entire workflow, from the first meeting with the patient to the orthosis delivery, is then detailed.

Finally, the BOA model was tried on two patients and their feedback are explained.

The conclusion includes a summary of the project and the future improvements that should be done to continue this work.

¹A dial is a small wheel ("une molette" in French).

Part I

Background and context

This first part provides the medical knowledge required to understand the pathology and the solution proposed, the technical knowledge to understand the 3D printing technology, the mechanical knowledge to understand resistance analysis and the presentation of the company in collaboration with which this project was done.

1 Spasticity

This section aims at giving the medical knowledge necessary to understand the rest of the project. After a short introduction, the physiology of the pathology is explained and the anatomical parts concerned are described. The main causes of spasticity are then developed, followed by the way it can be diagnosed, treated, and the prognosis of the patients.

1.1 Introduction

Spasticity is a muscle control disorder that is characterized by tight or stiff muscles and an inability to control them. In 1980, Lance defined it as *"a motor disorder characterized by a velocity-dependent increase in tonic stretch reflexes (muscle tone) with exaggerated tendon jerks, resulting from hyper-excitability of the stretch reflex, as one component of the upper motoneuron syndrome."* [11]. This definition of spasticity was contested by the scientific community and the SPASM definition (2005) : *"Disordered sensory-motor control, resulting from an upper motor neuron lesion, presenting as intermittent or sustained involuntary activation of muscles"* was preferred [43].

Spasticity appears when neural pathways within the brain or the spinal cord are damaged. It can be a symptom of multiple neurological conditions including spinal cord injury, multiple sclerosis, cerebral palsy, stroke, brain or head trauma, amyotrophic lateral sclerosis and hereditary spastic paraplegia [1].

Both the upper and the lower limbs can be impacted but this project focuses on the spasticity of the elbow. Various patterns can be observed as displayed in Figure 2 and for most of them, the elbow flexors are contracted. The muscles must be regularly elongated to avoid fibers' shortening, which would prevent the patient from moving his arm permanently [1].



Figure 2: Five typical arm spasticity patterns [39]

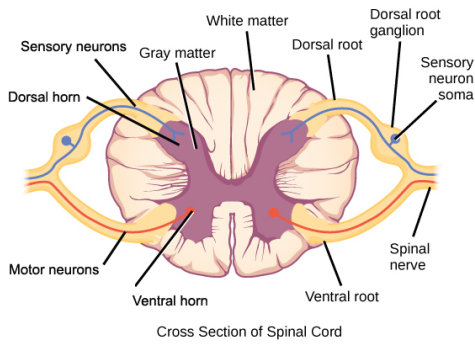
1.2 Physiology of spasticity

This section describes the underlining causes of spasticity at the nervous system scale and gives the anatomical knowledge needed to understand anatomical regions, muscles, and bones concerned.

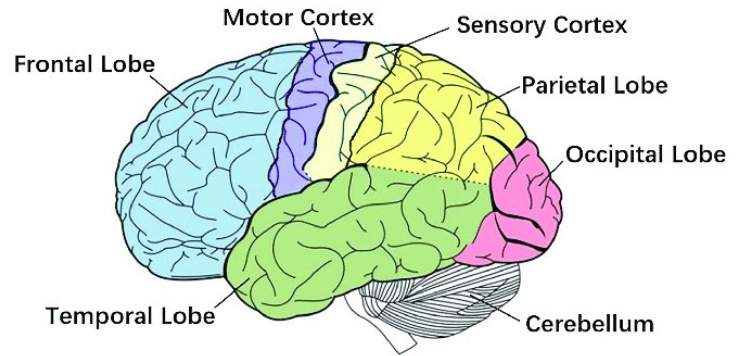
1.2.1 Nervous system

Spasticity is due to damages to the pyramidal tract, which is the network of corticospinal motor neurons transmitting the information from the cerebral cortex to the motoneurons and interneurons of the bone marrow [2]. In other words, spasticity is caused by an impairment of the link between the brain's requests and the muscles' movements. Indeed, they can create an imbalance between the inhibitory and the excitatory signals coming from those areas responsible for movements and stretch reflexes, which may lead to excessive velocity-dependent muscle contraction.

The cell body of these motor neurons is in the motor cortex and their axons reach the ventral horn of the spinal cord [13]. Those anatomical locations are displayed in Figure 3.



(a) Representation of the ventral horn of the spinal cord. This projections of gray matter (central region of the spinal cord, made of the neuroglia cells and neuron cells bodies) is located towards the frontal part of the spinal cord. Motor neurons exiting the ventral horn get out of the spinal cord through the ventral root to send the brain's requests to the muscles [12].



(b) Motor cortex in the frontal lobe of the brain and responsible for the execution of voluntary movements. A lesion in that area can lead to elbow spasticity as the request sent by the brain will not be received by the muscles [14].

Figure 3: Upper motor neurons locations

1.2.2 Description of the elbow's articulation

The elbow joint is composed of the distal end of the humerus and the proximal ends of the radius and the ulna [15] as displayed in Figure 4a. As a reminder, the distal part of a limb refers to the part further away from the center of the body while the proximal part of the limb is the closest to the center of the body.

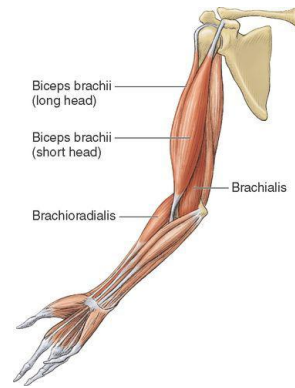
1.2.3 Muscles group affected for the elbow spasticity

The two main arm movements of interest are the flexion/extension of the elbow and the supination/pronation of the forearm, which are displayed in Figure 5. The elbow's flexor group [16] is responsible for bending the arm by decreasing the angle between the forearm and upper arm. The inverse of the flexion is the extension.

The arm supination, on the other hand, is a movement of rotation of the arm during which the radius crosses over the ulna so the forearm and the wrist can face upwards. The inverse of the supination is the pronation.



(a) Humerus, radius and ulna location. Those bones form the elbow articulation [44]. The radius is the bone in the extension of the thumb and the ulna is in line with the little finger.



(b) The brachialis, the biceps brachii and the brachioradialis, the muscles active during the flexion of the elbow [45].

Figure 4: Muscles and bones concerned by the elbow's flexion.

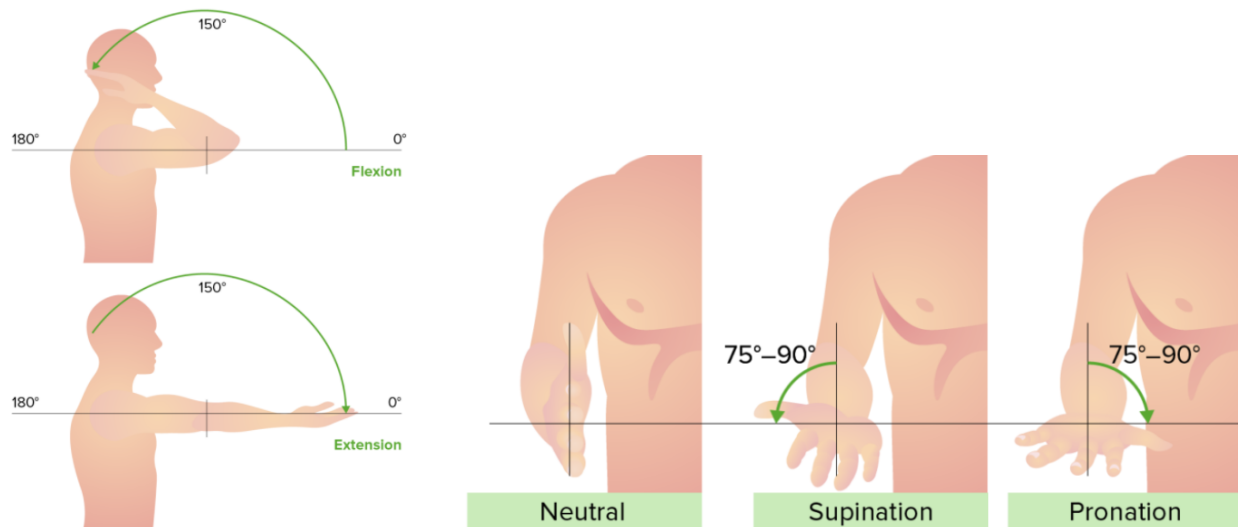


Figure 5: Flexion/extension of the elbow and supination/pronation of the forearm [17].

This group of muscles is displayed in Figure 4b and includes:

- The brachialis: primary flexor of the elbow, found mainly in the upper arm between the humerus and the ulna.
- The biceps brachii: superficial to the brachialis and runs anterior to the humerus from the scapula to the radius. This muscle is also able to supinate the forearm and turn the palm of the hand anteriorly.
- The brachioradialis: third flexor muscle of the elbow, running from the distal end of the humerus to the distal end of the radius.

1.3 Causes of spasticity

Numerous central nervous system diseases or incidents can lead to upper-limb spasticity but the attention is here focused on three major causes: strokes, multiple sclerosis, and cerebral palsy. Those causes were chosen to provide a solution to patients with chronic disease and not traumatic injuries. This choice was made due to the collaboration with Spentys, as it will be explained in Part I Section 5. Note that the solution proposed could also be considered for post-surgery or traumatic patients, which would highly increase the number of patients concerned.

1.3.1 Post-Stroke-Spasticity

Worldwide, strokes (cerebrovascular accidents) are the second leading cause of death and the third leading cause of disability [23]. During a stroke, the blood supply to the brain is disrupted which may lead to cells' death due to the lack of oxygen. If motor neurons are touched, the patient will suffer from some degree of spasticity.

According to a Belgian study [24], the yearly age-and-gender-adjusted stroke attack rates were estimated to 0.186% of the Belgian population. Similarly, the World Stroke Organization states that, in 2019, there were over 13.7 million new strokes (resulting in 0.179% of the world population) [25].

Zeng et al. [27] conducted a meta-analysis on the prevalence of Post Stroke Spasticity (PSS) and found that 25.3% of people suffering from a stroke developed some degree of spasticity. The proportion was even higher within patients after first-ever stroke with paresis (up to 39.5% and 9.4% of them reached the stage of severe or disabling spasticity). It has to be noted that PSS can appear a few months after the stroke.

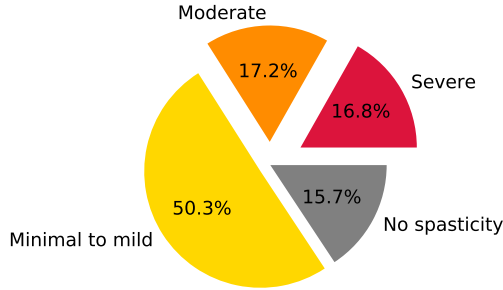
Also, younger patients are more likely to experience spasticity which might be explained by the fact that the reflex activity normally declines with age [28]. As they are younger, the need for treatment and devices (such as orthoses) will be repeated regularly for the rest of their life.

1.3.2 Multiple Sclerosis

Multiple sclerosis (MS) is a potentially disabling disease of the brain and spinal cord in which the immune system attacks the myelin sheath covering the nerve fibers. This sheath allows electrical impulses to transmit quickly and efficiently along the nerve cells. Hence, communication problems from the brain to the muscles may arise when this sheath is damaged.

In a worldwide study from Walton et al. [29], with 75 countries participating, the incidence rate was 2.1 per 100,000 persons/year. But regional variations in incidence are significant and usually follow the prevalence pattern, with Europe having the highest reported incidence (per 100,000 persons per year) at 6.8, followed by the Americas at 4.8. South East Asia and Africa have the lowest reported

incidence rates of 0.4.



A study [26] based on a cross-sectional database of 17,501 patients with MS taken from the NARCOMS Registry (project of the Consortium of Multiple Sclerosis Centers) showed that 15.7% of patients suffering from MS had no spasticity, 50.3% had minimal to mild spasticity, 17.2% had moderate spasticity and 16.8% had severe spasticity as seen in the Figure 6.

Figure 6: Spasticity levels in MS patients taken from the NARCOMS Registry [26].

Overall and considering that even minimal spasticity might require an orthosis, we can consider that 84.3% of 0.0068% of the population so 0.00573% of the population might need an orthosis because of MS, each year, in Europe.

1.3.3 Cerebral Palsy

Cerebral Palsy is a group of movement disorders that appear in early childhood and that are the most common cause of motor/movement disability in children (0.21% of children are touched worldwide [30]). According to several studies [31] conducted in the Centers for Disease Control and Prevention (CDC): Spastic Cerebral Palsy (when the cortex is the affected area) was the most common form, accounting for 76.9% of all cases. Overall, 0.16% of children are suffering from spastic cerebral palsy and since this disorder is non-progressive, a large adult population might still suffer from it.

1.4 Diagnosis

The diagnosis is based on a physical examination with neurological testing. The position of the arm and the intensity of the spasticity can be assessed using known classifications and scales described in the next section. The objective diagnosis of the patient can help to decide if the orthosis proposed is adequate to his/her condition. More information on the source and the extend of the damage caused can be assessed using imaging such as Magnetic Resonance Imaging (MRI) [4].

1.4.1 Patterns observed

Hefter et al. described the different patterns usually observed for upper-limb spastic patients [3]. They also computed the proportion of each of the patterns seen in the 665 patients participating to the study (only 5.6% of the patients could not be identified as one of the five patterns of Figure 2). As can be seen in Figure 7, the elbow is flexed in most of the patterns and even though the position of the elbow changes from one pattern to the next, more than 90% of the patients would need a device to keep their elbow elongated (as they present one of the patterns from I to IV).





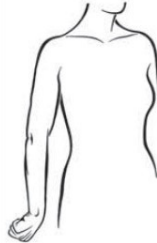
| | | | | | |
|-----------|---|---|---|---|---|
| | I | II | III | IV | V |
| |  |  |  |  |  |
| Shoulder | Internal rotation/ adduction | Internal rotation/ adduction | Internal rotation/ adduction | Internal rotation/ adduction | Internal rotation/ retroversion |
| Elbow | Flexion | Flexion | Flexion | Flexion | Extension |
| Forearm | Supination | Supination | Neutral | Pronation | Pronation |
| Wrist | Flexion | Extension | Neutral | Flexion | Flexion |
| Occurence | 24.8% | 5.3% | 41.8% | 18.9% | 3.6% |

Figure 7: Patterns of upper-limb spasticity as described by Hefter et al. [3].

1.4.2 Scales to assess the intensity of spasticity

Once the position of the arm is defined using the patterns described in the previous section, the intensity of the spasticity can be assessed using the Modified Ashworth Scale (MAS) [19]. Spasticity is diagnosed [28] for patients with $MAS \geq 1$ and severe spasticity is usually referred to $MAS \geq 3$ [27]. The entire scale is defined in Table 1

The Tardieu scale can also be used to assess spasticity [20]. This scale takes into account the angle formed by the articulation and the velocity at which the limb is moved since the health professional starts by slowly moving the limb to see the full range of motion and then moves it more quickly. This scale is said to adhere more to Lance's definition of spasticity (See Part I Section 1.1) [21]. The scale is displayed in Table 2.

| | |
|----|--|
| 0 | No increase in muscle tone |
| 1 | Slight increase in muscle tone, with a catch and release or minimal resistance at the end of the range of motion when an affected part(s) is moved in flexion or extension |
| 1+ | Slight increase in muscle tone, manifested as a catch, followed by minimal resistance through the remainder (less than half) of the range of motion |
| 2 | A marked increase in muscle tone throughout most of the range of motion, but affected part(s) are still easily moved |
| 3 | Considerable increase in muscle tone, passive movement difficult |
| 4 | Affected part(s) rigid in flexion or extension |

Table 1: Description of the Modified Ashworth Scale (MAS) [19]

| | |
|----|--|
| | Velocity to Stretch |
| V1 | As slow as possible |
| V2 | Speed of the limb segment falling (with gravitational pull) |
| V3 | At a fast rate (>gravitational pull) |
| | Quality of Muscle Reaction |
| 0 | No resistance throughout passive movement |
| 1 | Slight resistance throughout, with no clear catch at a precise angle. |
| 2 | Clear catch at a precise angle followed by release |
| 3 | Fatiguable Clonus (< 10s) occurring at a precise angle |
| 4 | Unfatiguable Clonus (> 10s) occurring at a precise angle |
| 5 | Joint immobile |
| | Spasticity Angle |
| R1 | Angle of catch seen at Velocity V2 or V3 |
| R2 | Full range of motion achieved when muscle is at rest and tested at V1 velocity |

Table 2: Description of the Tardieu scale [20]

Overall, it is important to keep in mind that spasticity is hard to assess for several reasons. First of all, the spasticity of a single patient changes over time, both in the long and the short terms. Moreover, the force exerted by the muscles as the limb is immobilized is not easy to measure since spasticity is a velocity-dependent disease. This explains why there is no clear measure of resistance force of patients at rest.

Note that the Lovett scale is also used by some physicians but it will not be described here as it is not specific to spasticity.

1.4.3 Other measurements to assess the severity of spasticity

The maximum range of motion, which gives the maximum angles both in extension and flexion, can be measured using a goniometer. Other tests can be carried out but they are usually used for study purposes rather than for classic diagnosis. The muscular activity can be measured using electromyography, the speed of the limb using opto-electronical material or electronic goniometer, the moment exerted by the arm using a dynamometer (or a motorized system that can compute the torque exerted) [43].

1.5 Treatment

Treating spasticity requires relevant medical guidance and depending on the medical case, different treatments may be prescribed [4]. Non-surgical treatments and surgery can be considered and both of those treatments need to be closely supervised by a health care professional, to ensure the good health and quality of life of the patient. Non-surgical treatments are usually preferred as they do not require the hospitalization of the patient, the inconveniences linked to it, and the possible post-surgery complications such as infections or sudden malfunctions. Patients should be treated to improve his/her mobility and dexterity, to reduce pain and muscle shortening but also to improve their posture and decrease the care burden (hygiene, positioning, and dressing) [18]. The following treatments will not repair the damaged neurons but they will prevent the constant contraction of the muscles to avoid fibers' shortening in the long term.

1.5.1 Non-surgical treatment

The non-surgical treatments are listed and briefly explained in this paragraph. The treatment administered depends on the clinical state and the will of the patient.

- Physical therapy: stretching and strengthening exercises of large muscle groups to improve mobility and movement range. This therapy is often encouraged but might require external assistance and/or equipment.
- Occupational therapy: exercises on smaller groups of muscles to improve coordination and strength. This therapy also requires external assistance and/or equipment.
- Immobilization in extension: using casts, splints, and braces, the flexibility, and range of motion can be maintained (or slightly improved) while involuntary spasms can be limited. Care must be taken to not exceed the maximal tolerable stress level to avoid tissue failure.
- Medical pharmacologic treatment: depending on the lesion's location, medications as baclofen [32], benzodiazepines, diazepam, dantrolene, or clonazepam may be effective. Those medications are skeletal muscle relaxants that will prevent the muscles from contracting.
- Botulinum Toxin injections: regular injections can paralyze muscles and thus prevent their contraction.
- Deep brain stimulation: this technique is currently being studied to compensate for the neural damage [33].
- Rehabilitation robotics: high volumes of passive or assisted movements can be provided, depending on the individual's requirements [34].

1.5.2 Surgery

In extreme cases, an Intrathecal Baclofen Pump can be placed in the patient's abdomen to deliver baclofen (preventing muscles from contracture) at a steady and controlled pace into the spinal canal for it to reach the Cerebro Spinal Fluid (CSF). As the drug is directly administered in the CFS, it does not need to pass the blood-brain barrier and the dose needed is thus smaller. This technique encourages the muscles' relaxation as the baclofen is a skeletal muscles relaxant and lowers the side effects compared to oral administration. However, this surgery is only performed on patients suffering from generalized spasticity as it is not possible to target a single muscle.

To target specific muscles, several localized surgical solutions can be considered. One of them is selective peripheral neurotomy: a procedure in which some nerves are cut to reduce the unwanted signal, asking for muscle contraction, while maintaining enough nerves to not paralyze the limb [35].

1.6 Prognosis

The prognosis of patients highly depends both on the cause and the severity of the spasticity. Most patients with a significant motor neuron lesion will have an ongoing impairment, but, progress is possible for some of them. Reorganization of the neurons in the cortex can help recover certain functions [40] but this requires for the muscles to be able to contract and relax properly. To gain back mobility and functionality, it is thus important that the muscles' fibers did not shorten due to prolonged contraction. If not treated, spasticity can lead, not only to shortening of the muscles fibers but also to other secondary defects such as joint dislocation or bone deformation [43]. For patients whose neurons do not reorganize, it is still important to avoid shortening of the muscles fibers to allow passive movements (limb elongated by a care provider to get dress, to get clean, etc).

1.7 Population concerned

In this section, the number of patients suffering from elbow spasticity is estimated. No clear and well-documented data were found to estimate the number of people concerned by this disorder. Some approximations are thus made to have a rough estimation of the market size.

Considering 11.46 million (2019) inhabitants in Belgium and 746.4 million (2018) inhabitants in Europe, we can consider the following statistics:

- 0.047% of the population has a stroke leading to spasticity each year. This would mean 5,386 new cases each year in Belgium and 350,808 in Europe.
- Taking into account patients suffering from spasticity due to MS, we can add 657 new cases each year in Belgium and 43,342 in Europe.
- 0.16% of children might suffer from cerebral palsy. Based on an average of 115,565 babies born in Belgium each year we expect 185 new cases per year in Belgium. Considering an average of 4.2 million babies born in the EU per year we can approximate to 6,720 new cases per year in Europe.

By adding those statistics, we obtain, each year, 6,228 new cases in Belgium and 400,870 new cases in Europe.

Those statistics do not consider the area of the body affected. In this work, only the upper limb spasticity is concerned. However, the upper limbs seem to be subjected to spasticity more commonly than the lower limbs and it has been shown that spasticity is more severe in the upper than the lower limbs [28]. After discussions with several orthopedists and occupational therapists, the observations are that an orthosis is needed for a majority, but not all patients. Indeed, doctors will not prescribe an orthosis to patients suffering from very light spasticity as the implementation will be quite heavy for only small improvements. In the same way, extremely severe cases will not be suitable as the hope of recovery is null. In conclusion, the targeted patients are the ones suffering from spasticity between 1+ and 3 on the Ashworth Scale (see Part I Section 1.4.2).

These proportions are given as estimates due to the disparity of the population and areas studied. However, it gives us an idea of the population targeted. As a reminder, only the chronic patients are taken into account in those statistics but the developed orthoses could also suit traumatic cases.

1.8 Conclusion

To conclude this chapter, spasticity is a common disorder that can be the consequence of various diseases and traumatic injuries. Due to the death of some motor neurons, there is an imbalance between the inhibitory and the excitatory signals coming from the areas responsible for movements and stretch reflexes, which leads to excessive velocity-dependent muscle contraction. Most patients suffering from elbow spasticity flex their arm involuntarily and are unable to relax it. There is no perfect treatment at the moment and the full recovery of the patient is usually not possible. However, patients can prevent further damage and see some improvements in their daily life by keeping their limbs active, by regularly and gently extending them.

2 Current orthopedic solutions

As stated in the list of possible treatments for spasticity, the immobilization device is one of the least intrusive methods to prevent the shortening of the muscle's fibers and thus guarantee a better range of motion of the patient's arm. In this section, solutions already available on the market are cited and explained. It is crucial to understand the number of patients impacted, the solutions offered, and the limitations that they have to develop a solution that addresses those remaining issues.

2.1 Solutions available on the market

Several immobilization devices are already available on the market to support for the limb to keep it elongated and avoid shortening of the muscles' fibers. Different types of orthoses can be used. Static

and fixed splints block the limb in an extended position but this position cannot be changed regularly, leading to problems to tolerate the orthoses for long periods. Moreover, the level of spasticity can change during daytime and it would be interesting to be able to adapt the splint's position to the current level of spasticity [5]. Positioning orthoses immobilizes the limb in a position that can be changed. Current positioning orthoses are either "off-the-shelf" or custom-made devices using thermo-formable plastics. Note that these splints' aims are not to get rid of spasticity but to avoid the patient's state worsening.

2.1.1 Prefabricated orthoses

Here are some examples of prefabricated orthoses:

- *Innovator X* by Össur [6] and *X-ACT rom elbow* by Donjoy® [7] displayed in Figure 8: Both allow a range of motion to be chosen by blocking the minimum and the maximum angles of flexion and extension. The mechanisms are made of aluminum but the range of possibilities are different for the two brands.

The flexion and extension limits of the Innovator X device can be independently chosen with 10° increments for small angles (from 0 to 30°) and 15° increments for bigger angles (from 30 to 120). Supination and pronation of the forearm can be prohibited by adding an optional arm bar kit.

The X-act rom design also allows a range of motion to be chosen with 10° increments but it also provides a "quick lock" at a specific angle (0, 15, 30, 45, 60, 75, or 90°).

Both designs are quite heavy and bulky. The straps are adjustable but concentrate the stress on small areas. The skin can breathe where there is no strap but the fabric of the orthosis will quickly get dirty due to the accumulation of sweat. If the tissue is wet, it should be dried before being worn again.

- ELB0-ELBOW by Symmetric Designs [36] shown in Figure 9a: A stainless-steel shaft connects the two parts of the orthosis. One extremity is fixed to the forearm's cuff while the other one is fixed to the cuff near the shoulder. Straps are joining the elbow pad and the shaft. Their length is reduced or increased to choose the extension angle. As the straps are shortened, the shaft gets closer to the elbow and the arm is forced to extend. This splint is available for children but there is no possibility of wearing a sweater or a coat over it. There is also a non-negligible risk of injury due to violent movement if the rod is hooked. This splint should not be wet either and the tissue of the cuffs can also accumulate sweat resulting in hygiene issues.

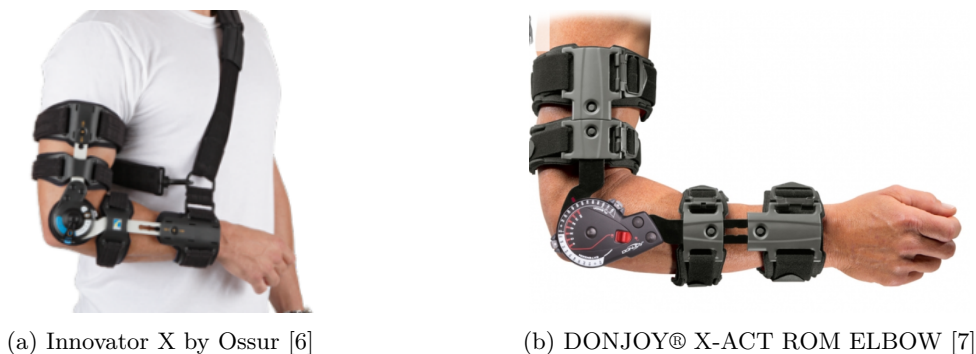


Figure 8: Össur and Donjoy orthoses



(a) ELB0-ELBOW by SYMMETRIC DESIGNS [36] (b) Hinge to be fixed to thermo-formable parts [59]

Figure 9: ELB0-ELBOW, a prefabricated orthosis and a hinge that can be fixed to a splint made of thermo-formable plastic.

2.1.2 Custom devices

Custom devices already available on the market are made of thermo-formable parts (one on the forearm and one on the upper arm) that are connected by a hinge that is fixed after the molding. An example of an aluminum hinge is shown in Figure 9b. This hinge is blocked with hex screws and the range of motion is chosen with increments of 15° .

The orthosis can be made of low or high-temperature plastics.

- **High-temperature:** A thermoplastic orthosis is created through a long process displayed in Figure 10. A negative impression of the limb is created to get the anatomy of the patient. This negative impression is then filled with plaster to create a positive model. The thermoplastic sheet is then heated and molded onto this plaster mold. This process is dirty and uncomfortable for the patient and the practitioner. If the positive is not perfect, it will only be noticed once the splint is finished and this heavy process will have to be done again from the beginning. The process will also have to be entirely repeated if the splint is broken or lost since the anatomical data of the patient cannot be stored [37].

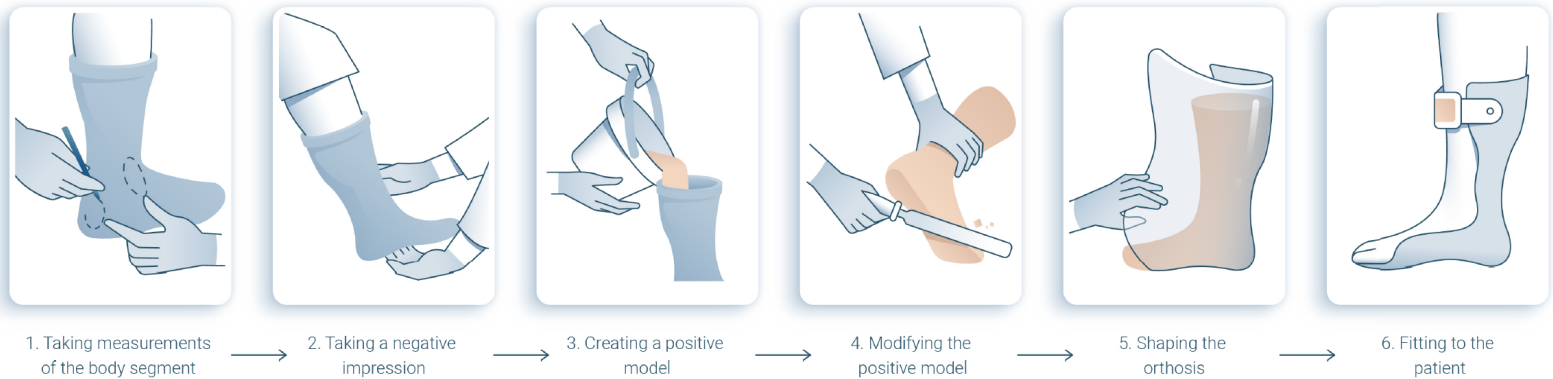


Figure 10: High-temperature thermo-formable splint process [10]

- **Low-temperature:** The material deforms at 60°C , it can thus be directly molded on the patient's limb without damaging the skin. This process is cleaner, faster and easier but the splint requires regular adjustments since it gets easily deformed. Moreover, the plastics used may show insufficient strength².

²The thermo-formable plastic has an Elastic modulus of 145 MPa and a tensile strength of 10 MPa [38]. In compar-

For both methods, it might be complicated to immobilize the limb of the patient for a long period (time to create the plaster mold or for the plastic to cool down in the good position). These orthoses regularly cause discomfort, have poor ventilation and can be detrimental to the patient [8]. Thanks to new technologies, it is now possible to think about innovative devices using 3D printing.

3 3D modeling and printing

The technical background to understand 3D printing is given in this section. The main 3D printing technologies are explained and both their advantages and disadvantages are given. The technologies developed are the ones that can print plastic materials. The materials available are then listed and the software used for the 3D modeling and printing are presented. The choice of technology and material for this project is developed in Part III, Section 3.2.

3.1 All technologies available

Several techniques are currently used to 3D print pieces. The main technologies available are cited and explained in this section [47]. All of them use the same principles, in this order:

1. A numerical model of the object is created using any modeling software such as *Maya*, *Rhino3D*, *3D builder* or *Solidworks* (all of which will be described in Section 3.3).
2. The object is virtually sliced (the thickness of the slices depends on the technique used).
3. Layer by layer, the object is built by adding material in a solid, liquid or putty state and consolidated only in selected regions to form the shape wanted.
4. This last step is repeated for each layer until the object is finished.

3.1.1 Material extrusion: Fused Deposition Modeling (FDM)

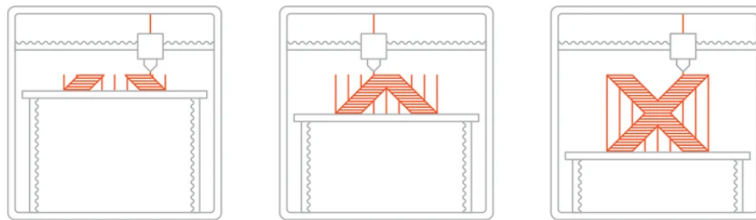


Figure 11: Fused Deposition Modeling (FDM) [47]

Also called FFF (Fused Filament Fabrication), this technique is the most popular, according to the number of machines sold, thanks to its affordability. Solid thermoplastic filaments are pushed through a moving head that heats, between 170 and 260 °C, and melts the plastic to extrude it on top of the growing work. The head deposits the material on the horizontal plane, where it cools down and solidifies, before moving vertically by a small increment to start printing the next layer. The printer plate should be heated to avoid thermal shocks that would cause unwanted deformations. Indeed, if the plate is not heated, the first layer will not stick to it as it would quickly cool down and shrink. Moreover, it is important to keep a small temperature gradient between layers for them to adhere to each other. A slow and homogeneous cooling prevents unwanted deformations.

ison, the Polypropylen used for 3D printing that is used in this project has a Elastic modulus of 470 to 554MPa and a tensile strength between 27 and 36MPa [76][78].

If there are overhanging parts, it might be necessary to add 3D-printed temporary supports, as there will be no material at the previous layer to deposit the new layer on.

The movements of the printer head are controlled through a G-code file created by *Cura*. *Cura* is an open-source software that slices the user's model file (STL or OBJ for example) into horizontal layers and generates a printer-specific G-code. The printer knows how to move, along which path and at what speed to create the exact model thanks to the instructions provided by the G-code. The software is now related to Ultimaker [60] but also works with other printers. A wide range of materials can be used with FDM such as Transparent Polypropylene (PP), Fortis (another type of Polypropylene), Polyethylene terephthalate (PET), PET reinforced with 15% of carbon fiber, Polylactic acid (PLA), Thermoplastic polyurethane (TPU) and Resin ST45 (medium-viscous, highly reactive photo-polymer). Those materials are sold as filaments' bobbins.

| Advantages | Disadvantages |
|--|---------------------------------------|
| Cost of the materials (usually between 18 and 79€/kg, see Section 3.2) | Unreliability of the printer |
| Possibility of multi-materials in different areas of one piece | Relatively low precision ^a |
| Cheap maintenance ^b | Anisotropy of the material properties |
| Customization of the printing parameters | Post-processing needed |
| Weight reduction is possible | Relatively small productivity |
| Material waste (supports...) can be recycled | |
| Very wide material choice (metals, wood...) | |

Table 3: Advantages and disadvantages of FDM

^aThe layer thickness is usually between 0.1 and 0.3mm and can be changed depending on the finishing quality needed and time available to print the piece. The width of the filament deposited is fixed by the printer head size which is usually 0.4mm wide but can be tuned to be smaller.

^bUltimaker, selling the FDM printers available at Spentys, advises to clean the printer and lubricate the axis every 125 hours of printing. A bigger maintenance is advised after 375 hours (check for play on axles, check the tension of short belts check for residue in front fan of print head...) [48]. Technicians working with 3D printers advised to do it less regularly as it takes time and is usually not necessary to do it as often.

3.1.2 Vat polymerization

This technique is displayed in Figure 12 and uses a photopolymer resin which is stored in a vat and selectively cured by a light source. Two forms are usually used:

1. Stereolithography (SLA): Known to be the first 3D printing technology, it has been developed in 1986, and it uses two galvanometers (mirrors), one in the X-axis and one in the Y-axis. Those mirrors are used to guide a laser beam that will hit the surface of the liquid resin at the location of the object's cross-section. The vat then goes down so a new layer of resin can be illuminated to build the object layer by layer.
2. Digital Light Process (DLP): It works with the same principle as the SLA but is faster as a digital light projector is used to selectively flash the entire cross-section at once, unlike the SLA that has to illuminate each point, one after another. An array of micro-mirrors controls where the light (coming from light-emitting diodes or a UV light source) is projected.

This technique creates very precise but fragile models (low flexibility so the pieces can undergo less deformation before failure) [50]. After printing, it is necessary to rinse the rest of the resin and to solidify the object in an oven which makes the overall process quite long.

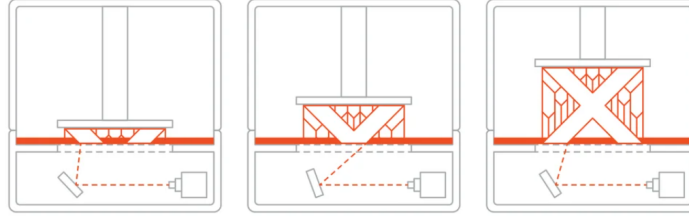


Figure 12: Digital Light Process (DLP) [47]

| Advantages | Disadvantages |
|---|---|
| Excellent precision (μm) | Fragile models (also because they are usually smaller/more detailed) |
| Nice finishing | Need to be printed in a room with low luminosity |
| Quick printing | Long post-processing |
| No supports needed | Relatively expensive (90€/L for the one available at Spentys) |
| The layers are not visible on the final piece | Lacking in Strength and Durability |
| | The resin is toxic so working with gloves is necessary |
| | Can still be affected by UV light after printing if not well post-printed |

Table 4: Advantages and disadvantages of vat polymerization [49]

3.1.3 Power bed fusion: Selective Laser Sintering (SLS)

A thermal energy source induces selective fusion between powder particles inside a build area to create a solid object. This process is displayed in Figure 13. The polymer powder is heated at a temperature just below its melting point into a bin and a thin layer (0.1mm) is then deposited by a wiper on the platform. Galvanometers then focus a CO2 laser beam on the cross-section of the object. Once the cross-section is cured, the platform moves down and a new and fresh layer of powder is then laid down on top of the previous one. The powder that has not been sintered supports the piece, there is thus no need for additional supports. This powder can partly be recycled by mixing it with fresh one.

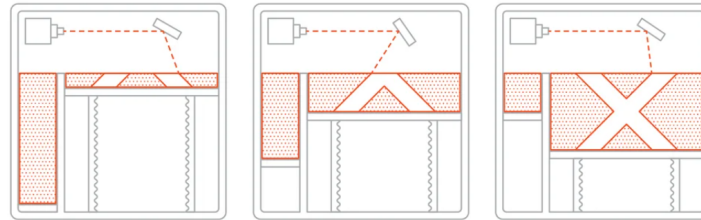


Figure 13: Selective Laser Sintering (SLS) [47]

This technique can use very interesting and pure materials such as glass, metals, ceramics or plastics but is very expensive even though it is getting cheaper as the technology evolves.

3.1.4 Material jetting: Multi Jet Fusion (MJF)

As shown in Figure 14, droplets are selectively deposited on the build plate and by using photopolymers or wax droplets, the object is built up one layer at a time. After the deposition of the fresh powder, a fusing agent is released where the particles should molten and a detailing agent is added around the contours to improve the quality and the resolution of the surface finishing. The piece is then heated

| Advantages | Disadvantages |
|--------------------------------------|--------------------------------|
| Pure materials (such as pure metals) | Expensive technology |
| No need for support structures | Porous and brittle |
| Fast | Prone to shrinkage and warping |
| Excellent layer adhesion | Produces a lot of waste |

Table 5: Advantages and disadvantages of SLS [50]

where the material should be cured, using ultraviolet light exposure. After removing the powder that was not cured, the part is ready and there is no risk of having marks due to supports [51].

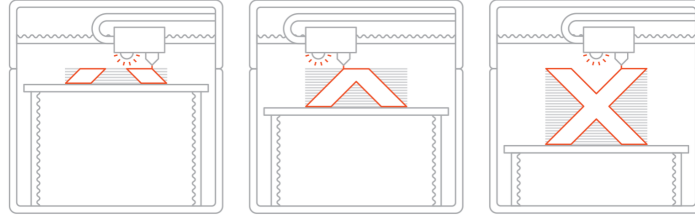


Figure 14: Multi Jet Fusion (MJF) [52]

| Advantages | Disadvantages |
|-----------------------|------------------------------|
| No need for supports | Very expensive 3D printers |
| Cheap cost per part | Limited material options |
| Fast printing process | Ability to print color parts |

Table 6: Advantages and disadvantages of MJF [52]

3.2 Materials available for 3D printing

Due to the growing interest for 3D printing, a lot of materials are already available on the market to meet various types of needs. The most commonly used material is plastic thanks to its affordability, flexibility, smoothness, and firmness. Powders such as Nylon and Alumide are very popular for their strength and precision while resins can be preferred for their aesthetic and their ability to give highly detailed pieces. Several metals such as stainless-steel, bronze, gold, nickel, aluminum and titanium can also be 3D printed to obtain superior strength and to reduce the number of parts needed in comparison to conventional parts. Carbon fibers can also be mixed with plastic to make it stiffer.

Working in the bio-medical industry, only bio-compatible materials, certified by ISO norms are considered to avoid potential issues.

3.3 3D modeling software used

Several programs are used for the modeling of the various parts depending on the specifications needed. The final workflow describing the interactions between the software is displayed in the Part III Section 2.

- *Maya* [53] is a 3D computer graphics application owned by Autodesk and mostly used for visual effects with powerful character creation, rigging, animation, and simulation tools. This software gives very good results for smooth and organic designs.

- *Solidworks* [54] is a solid modeling CAD (computer-aided design) and computer-aided engineering software developed by Dassault Systèmes. Being more engineering oriented, the software is very powerful but does not allow flexible mesh modeling. Indeed, the parts are designed by the user but *Solidworks* decides how to create the mesh to export the file that will be 3D printed. This is not really a problem if the pieces are drawn as they should be printed but it is an issue if they have to interact with another mesh or if more advanced modifications need to be made. This software is commonly used to design precise pieces and allows the creation of technical drawings very easily. Those drawings are usually used in the industry as they contain all the information needed to perfectly reproduce the design. Moreover, this software enables to run finite elements simulations to see how the pieces react to external forces and pressures. Stresses distribution and displacements generated can be displayed.
- *3D builder* [55] is a free Microsoft software that allows to view, create, and personalize 3D objects. The options and functions are quite limited but the software is very simple and intuitive to use, which is why it is chosen for simple applications.
- *Meshmixer* [56], is an Autodesk software to work with triangular meshes. This software is particularly useful to easily clean or smooth meshes.
- *Rhino3D* [57] is developed by Robert McNeel & Associate is a commercial 3D computer graphics and CAD application software that can be used with *GrassHopper* to manage rhino functions with a visual algorithm [58]. It allows the creation of scripts to automate the modeling of the orthosis, as explained in Section 2.2.

4 Mechanical knowledge required

A small reminder of some mechanical notions is given to understand the resistance analysis done in Part II Section 4. The most commonly used properties to describe a material and the results that the simulation gives us are detailed.

4.1 Material properties

Each material has its own properties and knowing them allows us to choose the most adequate material for the specific need but also to simulate its behaviour under external loads.

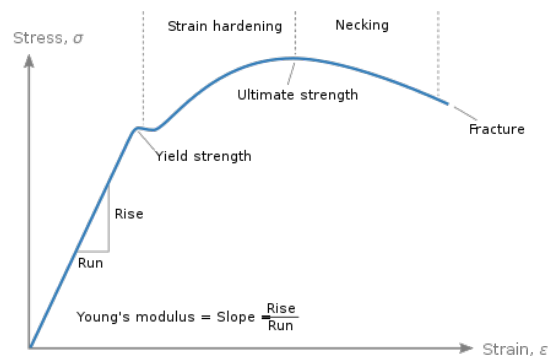


Figure 15: Typical stress-strain curve

The Figure 15 shows the strain observed as a stress is applied, the stress is proportional to the load applied (if the area of the cross-section is considered constant) since $\sigma = \frac{F}{A}$ with F the force in

Newtons and A the area of the cross-section in m^2 or mm^2 . It was decided to express all the stresses in N/m^2 ($1 N/m^2 = 1 Pa$) as it is the unit used in *Solidworks* and to be consistent through the report.

The graph of Figure 15 is separated in two main parts, the first one, as the stress is lower than the yield strength, is the linear elastic domain in which Hook's law can be applied: $\sigma = E\epsilon$ (in 1D). This means that the deformation is proportional to the stress by a factor E, the Elastic modulus (also called Young's modulus), can be expressed in N/m^2 (but is commonly given in MPa). The second part is the plastic domain in which the relationship is no longer linear and spreads from the yield strength to the fracture point. While the yield strength describes the maximum stress after which the deformations are plastics (permanent deformations remain once the load is removed), the ultimate strength (also called the tensile strength) is the maximal stress that can be sustained. The yield and ultimate strengths are also given in N/m^2 (or in MPa).

Another important parameter is the Poisson's ratio, ν_{ij} , that describes the contraction (for most materials) in one direction j when a traction is applied in another direction i. This parameter is unitless.

The Shear modulus characterizes the elastic shear stiffness. It characterizes the deformation of a solid when it experiences a force parallel to one of its surfaces while its opposite face experiences an opposing force (such as friction). It may not be given in the data sheet of the material but, for isotropic materials, the shear modulus can be expressed in terms of the Elastic modulus and the Poisson's ratio such as

$$G = \frac{E}{2(1 + \nu)} \quad (1)$$

4.2 Quantities of interest

The results that will be compared are the von Mises stress, the resultant displacements and the equivalent strain and each of them is explained in this section.

- Von Mises stress (N/m^2): As the piece is subjected to complex loading (in several directions), it is necessary to combine the three principal and the three shear stresses (σ and τ respectively) into a single resolved stress value. Von Mises defined an equation that combined those values to give the von Mises stress value that can be compared to the yield strength of the material to see if plastic strain is going to happen or not [75]. The von Mises equation is:

$$\sigma = \sqrt{\frac{1}{2} [(\sigma_x - \sigma_y)^2 + (\sigma_y - \sigma_z)^2 + (\sigma_z - \sigma_x)^2] + 3(\tau_{xy}^2 + \tau_{yz}^2 + \tau_{zx}^2)} \quad (2)$$

In some situations it might be interesting to see the principal and the shear stresses separately but in this study, the goal is to see if the pieces will fail, no matter if it is due to shear or principal stresses.

- Resultant displacement (mm): Distance measured between the initial location of a point and the final location of that point after the simulation is completed. It can also be used to notice unrealistic results.
- Equivalent strain (no unit, N/A): Defines the state of strain in solids and can be computed using several equations and the one used by *Solidworks* is [73]

$$2\sqrt{\frac{\epsilon_1 + \epsilon_2}{3}} \quad (3)$$

with

$$\begin{aligned}
\epsilon_1 &= \frac{(EPSX - \epsilon^*)^2 + (EPSY - \epsilon^*)^2 + (EPSZ - \epsilon^*)^2}{2} \\
\epsilon_2 &= \frac{GMXY^2 + GMXZ^2 + GMYZ^2}{4} \\
\epsilon^* &= \frac{EPSX + EPSY + EPSZ}{3}
\end{aligned} \tag{4}$$

and

| | |
|-------|--|
| ESTRN | Equivalent strain |
| EPSX | Normal strain in the X-direction of the selected reference geometry |
| EPSY | Normal strain in the Y-direction of the selected reference geometry |
| EPSZ | Normal strain in the Z-direction of the selected reference geometry |
| GMXY | Shear strain in the Y direction in the YZ-plane of the selected reference geometry |
| GMXZ | Shear strain in the Z direction in the YZ-plane of the selected reference geometry |
| GMYZ | Shear strain in the Z direction in the XZ-plane of the selected reference geometry |

Table 7: Parameters from the formula used to compute the equivalent strain in *Solidworks* [73].

5 Spentys presentation

This master’s thesis was done in coupling with an industrial internship at Spentys. As stated on their website, *“Spentys offers a complete, efficient and clinically-validated 3D scanning, modeling and printing platform that enables healthcare providers to create high-quality, patient-specific orthosis faster and at lower costs.”* [10]

The company is a start-up founded in 2017 by Louis-Philippe Broze and Florian De Boeck in Brussels, Belgium. Spentys’ goal is to implement 3D technologies into the hospital environment enabling customization of orthopedic medical devices through a web platform. This solution will improve the quality of life of a large number of people suffering from orthopedic disabilities.

Spentys is active in several fields but we will focus here only on the solution they provide for chronic pathologies. A deeper analysis of the company is provided separately, in the “Spentys: Internship’s report” document. This choice was made as they are more present in the “chronic pathologies” market than the “traumatic injuries” one. At the moment, their expertise in that field is better and most of their consumers are orthopedists with patients suffering from longer-term diseases. Another non-negligible argument is the difference in the reimbursement process. Indeed, as the patient will use the orthosis for a longer period, the reimbursement, and thus the budget to make the orthosis were higher as shown in Section 2. Moreover, the number of patients suffering from chronic pathologies constantly increases due to the population’s aging. Finally, as the health care system is under great pressure to reduce its costs, the digitization/automation of the orthoses’ production will be highly encouraged to allow greater accessibility to these devices.

Spentys proposes a 3-step solution, displayed in Figure 16, to create a custom-made orthopedic immobilization device in the orthopaedist’s clinic. The aim is to propose a large range of orthoses (arm, leg, foot, neck, etc) whose dimensions could be adjusted to perfectly fit the patient’s anatomy.

The first step is the scanning of the patient’s limb using the Spentys iOS App on an iPad, directly in the OT’s office, without the help of any external, trained technician. Beforehand, external hardware, called a structure sensor (a 3D scanner), is added to the iPad to obtain the 3D scan on

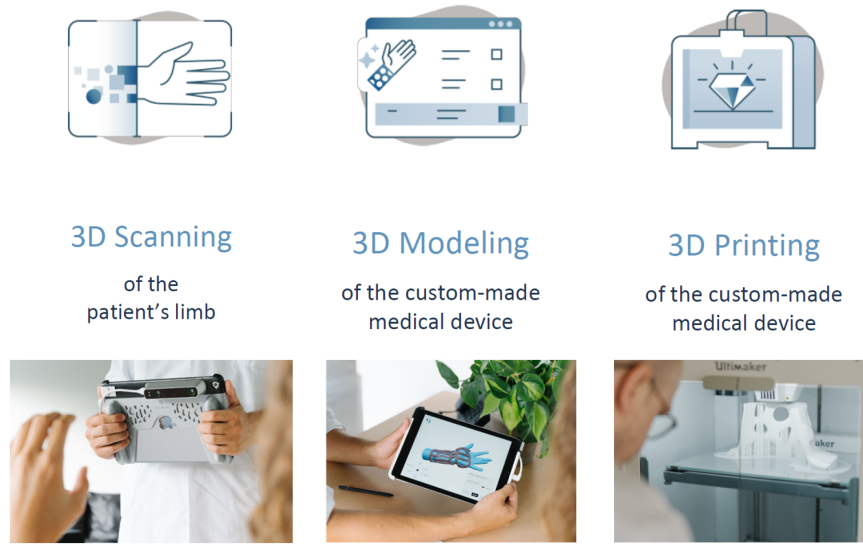


Figure 16: Spentys' process steps [10]

which the designer will work. This sensor is easily fixed to the back of the iPad following a simple and detailed procedure. This sensor allows depth data to be captured to create the 3D scan by using the distortion between the pattern sent and the one measured. First, an IR (infrared) projector casts a specific pattern of dots on the object. Thanks to the different focal lengths of the multiple micro-lenses, the pattern will depend on the depth of each dot and will thus be non-uniform. Two cameras are then used. The IR camera measures the intensity of the reflected infrared light on the 2D plane of the camera, and the RGB iOS camera gives the timing at which the reflected light was received. Those data are sent to a System On a Chip that uses triangulation to reconstruct the 3D scene.

The second step is the modeling of the brace adapted to the measurements taken from the scans. The OT³ chooses the part of the body he wishes to immobilize and the platform suggests the different models available for that limb. He/She can add pictures and, comments and all the needed clinical information so that the designer can perform the design of the needed orthopedic immobilization device for his/her patient.

The last step is 3D printing, which can either be done in the OT's office⁴ or in Spentys' office.

This solution is already implanted in twelve countries and before the end of 2021, clinical studies will be carried out to prove the advantages of this technique compared to the actual standard.

Part II

Challenges and solution proposed

Having identified the need for an elbow orthosis that can be regularly adjusted in many positions but that is also light, hygienic, resistant and, elegant, and having seen that the 3D printing technology can be used to offer new ideas of design, as done at Spentys, it was decided to create a 3D printed

³The abbreviation OT refers to the orthopedic technician and will be used in the rest of the report.

⁴The OT can have his/her own 3D printer or he/she can rent a 3D printer from Spentys

positioning orthosis.

1 Advantages of 3D printed orthoses

3D printed orthoses can meet the patient's and the practitioner's expectations by providing a custom solution that fits perfectly and avoids many issues encountered with traditional methods. Some of the main advantages are listed below.

- This splint is adapted to the patient's anatomy and to his/her needs. Scars or sensitive areas can be taken into account during the modeling to avoid pain and injuries.
- The 3D shape of the patient's limb is stored and can be used for device renewal or repair as well as for reimbursement justification.
- The alveoli ensure skin ventilation to avoid hygiene issues due to the accumulation of sweat and the lack of fresh air.
- Not having to fix an external hinge to thermo-formable splints is a big advantage for the OT. Indeed, the time needed for the production and the costs will be reduced.
- The scan can be modified on a modelling software if the arm cannot be immobilized in a good position. It is even possible to scan the opposite limb and to mirror it, which cannot be done with a classical cast. This can be very convenient for inaccessible limbs. This is already done at Spentys, when it is required.
- The splint is waterproof thanks to the water-resistant and non-porous material used.
- The overall orthosis is very light. A classical forearm orthosis weights approximately 50g. The ones developed during this project will be heavier as they are bigger and contain external pieces but the weight will not exceed 400g, which is still lighter than a classical cast (approximately 1kg for a forearm cast made of plaster [10]).
- The orthosis can be directly printed in the orthopedist lab if he has a 3D printer.
- The 1mm accuracy and the AI-based scan software limits the potential human errors or imprecision.
- Changes of designs can be made before the printing of the splint as the OT can give his/her feedback after receiving a link to the orthosis preview.
- The materials are recyclable and can be used for the manufacturing of new medical devices after having special treatment. It is thus more environmentally friendly than the traditional methods.

2 Needs to be fulfilled and solution initially proposed

Spasticity characteristics are very patient-dependant but, as seen in Part II, Section 1.1, the flexion of the arm should be prohibited for most patients, while the extension of the arm could be allowed or restricted depending on the patient's needs. This positioning device should be worn as the patient rests or during periods of non-physical activities such as watching TV or reading. It needs to be comfortable for the patient to accept to wear it. According to specialists, it is more efficient to wear the splint several times a day during short periods (approximately one hour) than only one time during a long period (during the night for example) [85].

The pressure applied by patients on the splint is difficult to measure as it changes over time (in the long, but also short term). Spasticity is a complex condition and the patients' behavior cannot

always be predicted. For example, a stronger contraction will happen if they sneeze or if something is hitching or tickling them. The amplitude of the contraction can change if the treatment does, for example, muscle relaxants can reduce the contracture. But the contraction of the muscles can even change throughout the day or depending on the tiredness or stress of the patient. As explained in Section 1.7, the solutions offered in this work focuses on patients having a MAS between 1+ and 3 (see Part I Section 1.4.2).

After having thought of several possibilities, two designs were chosen to be implemented. In this section, the initial ideas are presented. In Part II Section 3, all the issues and choices will be explained to justify the final design presented in Part III.

Both models are maintained on the arm using Velcro straps [46]. The first design is shown in Figure 17b and prevents elbow flexion above a chosen angle by using a BOA (see Figure 17a) [9]. Free hinges keep the two parts of the splint together and the range of motion allowed is defined by the BOA. The BOA is a system that allows a cable to be either tighten or loosen. Since the cables go through tubes embedded in the splint, reducing the length of the cable will force the brace to open and the arm to extend. The tubes are shown in Figure 17c. There should be an extrusion at the elbow for the cables to not touch the skin.

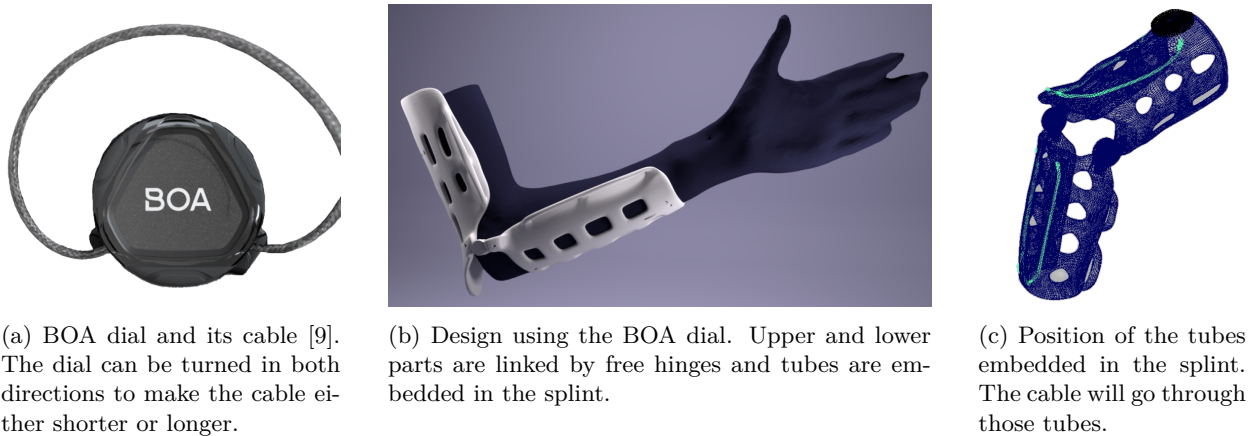


Figure 17: Important features of the design using the BOA.

The second design uses a blocking hinge that prevents both the extension and the flexion by being locked at a certain angle (see Figure 18). The overall design is similar to the first one but the BOA and the tubes are not needed. The internal hinge linking both parts of the splint moves freely while the external articulation's position can be changed regularly according to the patient need (that can vary throughout the day). The increments' size and the diameter have to be chosen.

Both final designs will be developed in detail in Part III, Section 1.2.

3 Challenges faced

Many challenges were faced at each phase of the development and the final designs are influenced by the changes made to counteract these issues.

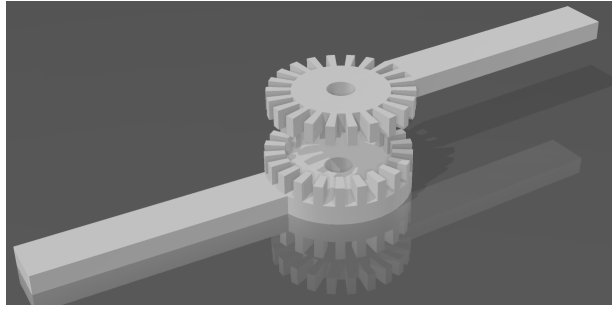


Figure 18: Blocking hinge

3.1 Problems faced during the design phase

Interactions between the different software

Several computer programs are used for the modeling of the various parts. Importing and exporting parts from a software to another is sometimes problematic due to the different ways the meshes are created and interpreted by the other software. As an example, the blocking hinge was created in *Solidworks* and was imported in *Maya* to be embedded in the orthosis designed there (note that the final design does not require the parts to be embedded). For *Maya* to export a printable part, the two meshes have to be combined into one by sewing vertex by vertex. Indeed, if there is a hole in the mesh, the model is non-manifold and can thus not be printed. Sewing vertex is long and difficult as *Solidworks* exports the pieces by creating a complex mesh as shown in Figure 19a.

This method can be considered for prototypes and simple parts but it quickly becomes unrealistic for complex parts or for the production's scale. To cope with that issue, it has been decided to use *3D builder* to merge the parts created in *Maya* (the upper and forearm parts of the orthosis), the ones created in *Solidworks* (blocking hinges) and the one already done in *3D builder* (free hinges).

This problem was encountered for the hinges designed in *Solidworks* but not for the one designed in *Fusion360* (complex hinges, created by a previous intern) and the mesh seems compatible with the one in *Maya* which allows to directly combine them using a simple command.

Tubes embedded in the orthosis for the BOA design

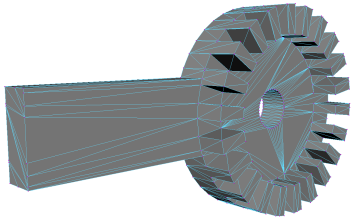
The angles of the tubes should be very smooth to be able to get the cable through without problems. Placing the tubes exactly halfway through the thickness of the splint is difficult and due to the imperfections of the printing, some tubes that were fully embedded but not perfectly centered were badly printed. As can be seen in Figure 19b, the tubes were letting the cable out. This issue was tackled by changing the thickness of the orthosis.

Thickness of the orthosis

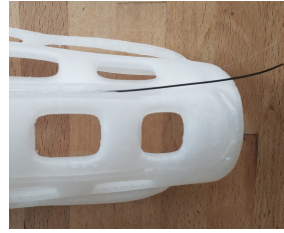
To reduce the risk of the tubes being open, the thickness of the BOA model is increased to 5mm (instead of 4mm for common orthoses). To be sure not to have any problem, where the tubes pass, the faces can be slightly pulled to increase the local thickness of the splint. To avoid confusion and improve strength, the blocking hinge design is also 5mm thick.

Hanging soft tissue of older patients

Some tissues tend to relax as people age and lose muscle mass. As the arm is raised to make the scan, the soft tissues will hang and will be seen on the scan as displayed in Figure 20a. However, the orthosis



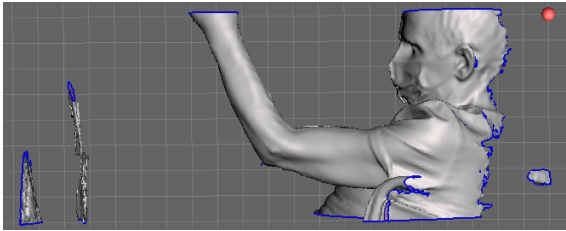
(a) Piece designed in *Solidworks* and imported in *Maya*. The numerous vertexes are visible. Sewing vertexes per vertexes this piece would be long and laborious.



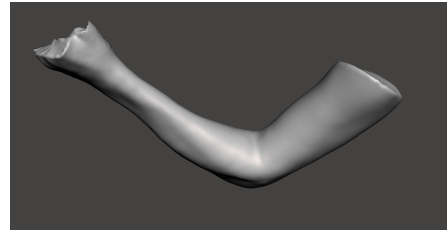
(b) The tubes are badly printed so the cable can go out of it. This happens when the tube is not exactly in the middle of the orthosis thickness.

Figure 19: Problems during the design phase.

should not be modeled on this surface as it does not represent the anatomy of the limb that should be supported. Indeed, the soft tissue should be flattened in the splint. Several solutions are possible. The scan can be modified afterward to lift the soft tissue (as displayed in Figure 20b) or the patient can wear a tight sleeve, only covering his/her upper arm, during the scan. If the scan is modified, the designer should add a small overall offset (the value depends on the volume of the hanging skin) to take into account the space the soft tissue will take as it is flattened.



(a) Original scan where the hanging soft tissues can be seen.



(b) Cleaned up scan with the soft tissues being lifted.

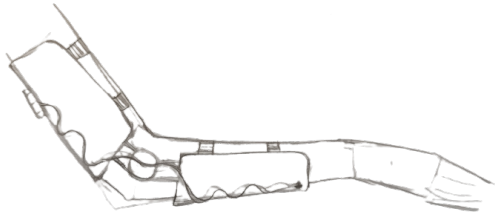
Figure 20: Scans of a patient with hanging soft tissues.

Extrusion for the BOA design

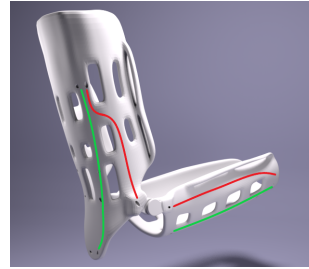
To make the design more simple, a trial was done with the tubes for the BOA cable passing near the free hinges, as displayed in Figure 21. Indeed, if the cable passes near the hinges, the extrusion at the elbow is not needed and the design is simplified. To reduce the number of printing tests, both the usual tubes and the ones near the hinges are embedded in the same model. The cables did not touch the skin but the lever arm was not sufficient to force the extension of the arm so this idea was not investigated any further.

Simplification of the design

Trials were carried out to simplify the design by reducing the number of hinges. Indeed, the first hinges considered were bulky and deleting them would have been an advantage. An orthosis was printed without any hinges to link its two parts. The idea was that the Velcro straps might be sufficient to keep both parts into place. However, the force exerted is too high for the straps to not slip on the skin. Another splint was printed with only one hinge, as displayed in Figure 22. Even though the two parts could not slip to get closer to each other, the orthosis closed in a bent direction and the resistance of the overall model was impacted. In conclusion, two hinges are needed and their design should be elegant and smooth to not bother the patient.



(a) Design using the BOA technology without the elbow extrusion. The tubes for the BOA cables are on the side of the splint, near the free hinges.



(b) 3D model of the printed prototype. The tubes passing near the free hinges are highlighted in red and the tubes in their original position are shown in green.

Figure 21: Trial to get rid of the extrusion at the elbow by placing the tubes near the free hinges.



Figure 22: Trial of design simplification using only one hinge. Note that the hinge design is the initial one and is thus very bulky.

3.2 Choices of material and printer

The materials available at Spentys are compared in Table 8. Indeed, the range of possibilities was sufficient to not look for other materials, especially since the orthosis developed has similar requirements as the ones proposed by Spentys.

| Material | Transparent PP | Fortis | PET | PET with Carbon | PLA | TPU | Resin ST45 |
|----------------------|----------------|---------------|-----------|-----------------|--------|-----------|-------------|
| Flexibility | Semi-flexible | Semi-flexible | Rigid | Rigid | Rigid | Flexible | Rigid |
| Solidity | Resistant | Resistant | Resistant | Resistant | Medium | Resistant | Resistant |
| Density (kg/m^3) | 890 | 930 | 1,329 | 1,050 | 1,220 | 1,220 | 1,200 |
| Price (€/kg) | 34.97 | 62.81 | 18.02 | 47.67 | 53.27 | 79.33 | 90 (€/L) |
| Technology used | FDM | FDM | FDM | FDM | FDM | FDM/SLS | DLP/MJF/SLA |

Table 8: Comparison of materials available at Spentys: Transparent Polypropylene (PP), Fortis (another type of Polypropylene), Polyethylene terephthalate (PET), PET reinforced with 15% of carbon fiber, Polylactic acid (PLA), Thermoplastic polyurethane (TPU) and Resin ST45 (medium-viscous, highly reactive photo-polymer).

3.2.1 Material for the BOA design

The material used for the BOA design is transparent polypropylene (PP) which is semi-flexible, fatigue-resistant (retain shape after deformation), chemical-resistant (maintain its original properties after being exposed to an indicated chemical agent) and lightweight (low density: $890kg/m^3$). This material seems optimal as the splint should be resistant (unlike the PLA), light, comfortable and thus relatively

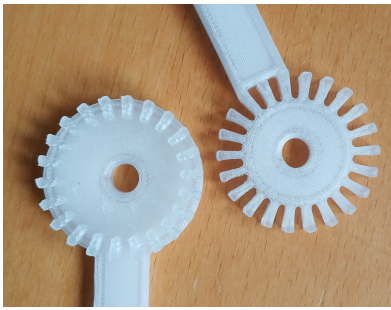
flexible (the carbon will not be sufficiently soft and the TPU could bend under the force exerted by the patient).

The printer chosen is the Ultimaker 3 extended due to reasons developed in Part II Section 3.3.

3.2.2 Material for the blocking hinge design

The blocking hinge design was initially printed in PP as well. When printed horizontally, the results were very satisfying (see Figure 23a) but once the hinge was embedded in the splint, the hinge was no longer horizontal and the quality dramatically dropped.

Several possibilities were considered: printing without any supports or printing with manual supports such as displayed in Figure 23b. The next idea was to print in PET with PLA supports. Indeed, the precision and printing quality of pieces printed in PET are better. This material was not initially chosen as it is less flexible and is thus not as comfortable⁵. The supports are made of PLA and not PET to be taken off more easily. Even with PLA supports, it was not easy to post-process the splint and two teeth were broken during the process. Overall, the precision is better, as can be seen in Figure 24b, but still not good enough. Indeed, it was still difficult to make the two parts fit and even more difficult to detach them without breaking any other tooth. As the splint needs to be comfortable and easy to readjust, this solution is not validated.



(a) Blocking hinge printed horizontally in PP, no supports were needed. Very good result, the parts are precise and fit perfectly



(b) Blocking hinges printed vertically in PP. Supports in PP were added on the hinge on the left but they cannot be easily removed and the quality is mediocre. The hinge on the right was printed without any supports, some teeth are missing and the quality is also very poor. Both parts are unsatisfying.

Figure 23: Blocking hinges printing tests using PP.

⁵Moreover, under large forces, the PET would break rather than deform, which can be more harmful for the patients.



(a) Blocking hinge printed vertically in PET, supports in PLA were added.



(b) Blocking hinges printed vertically in PET. Supports in PLA were removed. The missing teeth are noticeable and the two parts do not fit easily.

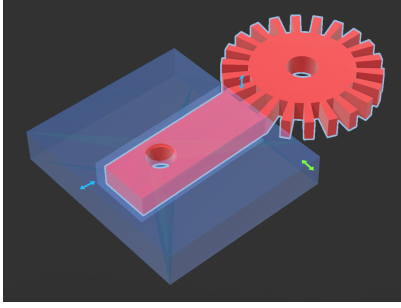
Figure 24: Blocking hinge printing tests using PET.

The printing quality of the PP, printed laid down is very good and the hinge seems resistant but if it is embedded in the splint during the printing, the quality tremendously deteriorates. The idea was thus to print the blocking hinge separately from the rest of the orthosis so the splint can be printed vertically and the hinges can be printed horizontally to optimize the printing quality of both parts. The hinge could be fixed to the splint in two ways, shown in Figure 26. For the tests, only small boxes are printed to represent the splints (to reduce the printing time).

1. The first idea is to create a rectangular hole in the splint in which the hinge can slide. The part is then fixed by screwing a binding screw in a perpendicular hole made both in the hinge and in the splint. This solution is displayed in Figure 25a and is easy but requires four screws. One binding screw is used for the free hinge, one to fix the internal part of the blocking hinge to the forearm splint, one to fix the external part of the blocking hinge to the upper arm splint and the last one to join the two parts of the blocking hinge (see Picture 25b).
2. The second idea, and the preferred one, is to design the arm of the hinge to be clipped inside the orthosis. The hinge is displayed in Figure 26a. A counterpart, whose shape should be discussed, is designed to be subtracted from the splint. The most intuitive idea would have been to subtract a T shape as displayed at the left in Figure 26a to be sure that the clip part would not get out of the splint once it is clipped, if an external force is applied by the patient. However, supports would have been needed for the overhanging parts and it would have been impossible to take them off easily in post-printing. The angles of the counterpart are thus chosen to be sharp enough to not let the clip go but to not require supports (as displayed to the right of Figure 26a). The first trial worked but the gaps, in the 3 directions, were too big so the piece could move. The parameters were changed two times and the final ones worked well, with only very small and acceptable movements and the result is displayed in Figure 26b⁶.

The solution was tried and validated on a complete orthosis (see Figure 26b). Both the BOA and the blocking hinge designs are thus printed in PP.

⁶Note that the gaps of the second trial seemed small enough when clipped in a small box as displayed in Figure 26a but, once clipped in an entire orthosis, due to the lever arm, the movements allowed by the gaps were too big. A third trial was done by reducing the gaps to 1mm in each direction and was successful.

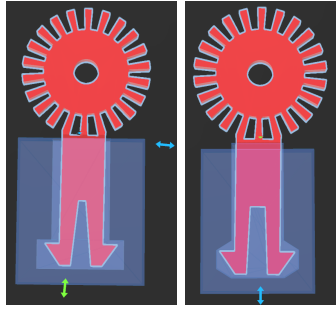


(a) Blocking hinge to slide in the splint and then to fix with a binding screw.



(b) Two binding screws are visible and the two additional screws would be placed on the red points to fix the sliding hinge in the splint.

Figure 25: First idea. A rectangular hole is made in the splint in which the hinge can slide. The parts are then fixed by screwing a binding screw in a perpendicular hole made both in the hinge and in the splint.



(a) Blocking hinges clipped in the splint. T-shape to the left and final shape to the right.



(b) Prototype using hinges clipped into the splint.

Figure 26: Second idea. A rectangular hole is made in the splint in which the hinge can slide. The part is then fixed by screwing a binding screw in a perpendicular hole made both in the hinge and in the splint.

3.3 Problems faced during the printing tests

Supports in the tubes

Using the FDM technique, the model is first sliced in the *Cura* software into thin (usually 0.1 to 0.3mm ⁷) horizontal layers. Then, at each height, the printer looks at the G-file created by *Cura* to put plastic at the coordinates of the object's cross-section. When an extrusion is modelled, if there is no material under it (from a previous layer) and that the angle of extrusion is high, supports will be needed. Otherwise, the material would drop or leak on the plate. Those supports can either be added automatically or manually. The automated supports will change depending on the parameters chosen during the slicing such as the type of support, the cantilever angle ⁸, the density (high and thin

⁷The thickness of the layers can be chosen in *Cura*. Thinner layers give a slightly better finishing but the quality does not tremendously change as the thickness is increased. On the other hand, the printing time is proportional to the thickness, so, most prototypes were printed with a 0.2mm thickness but some small tests were done with a 0.3mm thickness.

⁸Note that the cantilever angle is chosen by the technician and depends on the model and the material used. It is usually 70 °C for the PLA (polylactic acid) and 55 to 60 °C for the PP since the PP cools down less quickly and might thus leak more easily which would reduce the printing quality.

supports should be denser), etc. R&D research needs to be carried out to choose adequate parameters but once those parameters are known, the automatic supports are quicker to use than the manual ones.

However, for the BOA design, it is recommended to put the supports manually as they would fill the tubes and block the articulation if placed automatically. It is also possible to place boxes where supports are forbidden but it takes the same amount of time and is not as visual as placing manually the supports as wanted.

The initial parameters chosen were the ones found by the R&D team for the forearm model (A1) of the Spentys' catalog [10] as the material is the same and that the overall design is the closest to the orthoses developed. Those parameters could have been changed, but it was not needed.

Layer shifting

It happened that one (or several) layer of the 3D printed parts does not align with the others even though the rest of the model is well-printed (see Figure 27). It may be because the speed requested is too high for the engine so the printer head is not quick enough to be in a good position at the good time. It can also be due to lack of maintenance of the 3D printer (the screws that fix the pulleys are not tight enough for example), due to collision with the printed piece, due to electronics over-heating, or due to software bug [64]. The maintenance of the machines is done regularly and the parameters are almost never changed so the speed of the printer head is constant and reasonable. The problem usually disappears when the printing is launched a second time (no time for the electronics to cool down) so the issue probably comes from a software bug. Even though it is not very common, it is still troubling as it cannot be predicted and that the piece has to be printed again from scratch (which takes time). Due to that kind of unpredictable issue, FDM is usually more used for prototyping than for producing.



Figure 27: Piece with shifted layers. Note that on this model the shift is small does not impact too much the quality of the piece, at least for prototyping.

Printer used

Spentys has different printers depending on the technology and the material used. To print with PP using the FDM technology, the possible printers are the Ultimaker S5, the Ultimaker extended 3 [60], the Raise [61] and the Wasp [62] printers.

The Wasp printer was not fully calibrated and was thus unusable at that time. Some problems were also occurring on the Raise printer (the layers did not fuse together anymore) so the Ultimaker printers were preferred. As the quality is better when the model is printed as vertical as possible, the Ultimaker 5 was first chosen due to its bigger dimensions (330 x 240 x 300 mm). Unfortunately, the quality of the printing was very bad. Inside the feeder, there is a cogwheel that moves the filaments back and forth and it is reinforced in this model, to be able to work with abrasive materials such as carbon or fiberglass. The hypothesis is that the rapid retraction with this reinforced cogwheel damages the filament which leads to bad printing quality. The filaments are fragile due to their humidity, it

is thus necessary to dehumidify the bobbins for at least 16 hours before printing PP on this model. To avoid this problem, printing tests were carried out on the Ultimaker 3 extended. Although smaller (215 x 215 x 300 mm), it gave better results and was thus chosen.

Size of the printer

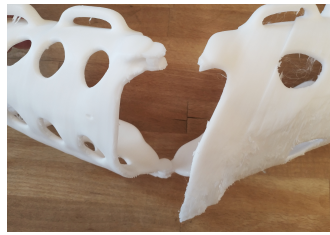
Initially the BOA design was modeled to be printed in one piece. As the Ultimaker 3 was chosen to guarantee a good quality, the size of the orthosis was limited. It was necessary to check, during the modeling, that the orthosis fits in a box of 215 x 215 x 300 mm and reduce the lengths on the forearm and the upper arm if it was not the case. For the orthosis to fit in the printer, it would either be printed in an open position or in a V shape as shown in Figure 30a and 30b.

The problems faced were the following:

1. As the splint was not vertical, supports were needed on the external surface, which gave really bad finishing quality, as can be seen in Figure 28a.
2. As the splint was slightly tilted, supports were added on the free hinges and one hinge broke as they were removed (shown in Figure 28b).
3. The two parts of the splint, printed in a V shape, were too close (even though not touching in the 3D model). The parts merged during the printing and could not be detached in post-printing as displayed in Figure 28c.



(a) Bad finishing quality due to supports on the outer surface of the splint.



(b) Broken free hinge due to a fragile design and the need to put supports on the hinge.



(c) Merged parts due to insufficient gap between the upper arm and the forearm parts when printed in a V-shape.

Figure 28: Problems due to the size of the printer when the BOA design is printed in one piece.

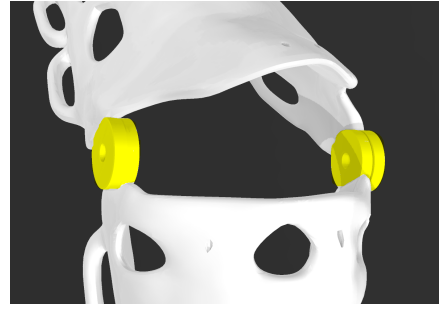
It was thus decided to print the BOA design as the blocking hinge design, in two pieces, with bigger and more resistant hinges, that are to be fixed with a binding screw. For the final BOA design and the blocking hinge design, there will be no problem as the orthosis will be printed in two parts and then joined using a metallic piece. Both parts are printed as vertical as possible to avoid having many supports (see Figure 30c).

Post-processing of the BOA design

Most pieces produced at Spentys are post-processed using the "through vibrator Rosler" [63] which is a polishing machine made of a big vibrating tray filled with small ceramic stones and water. As the tray vibrates, a rotating motion is induced and the ceramics polish the piece. The problem encountered was that small stones could enter and block the tubes. It is thus better to post-process the splint by rubbing the blade of a scalpel to get rid of the asperities.



(a) Initial free hinge used in the BOA design. To be embedded in both parts of the splint and to print in one piece. The gaps inside the hinge were made to avoid merging of the articulation. No external piece is needed but the piece is more fragile.



(b) Final free hinge used in the BOA design. To be embedded in each part of the splint that are printed separately. A binding screw keeps the two parts together.

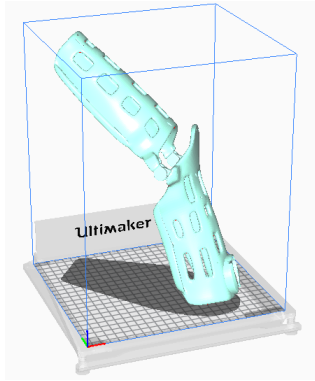
Figure 29: Comparison of the free hinges that could be used for the BOA design. The free hinges are highlighted in yellow.

Deformation after printing

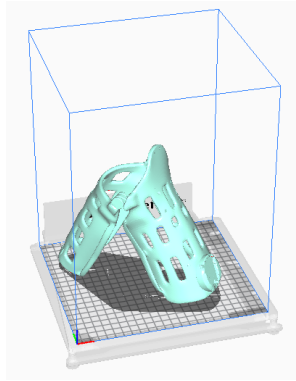
As the PP gets colder, the geometry of the piece could change and parts that were designed to fit together could not be interlocked. Indeed, small deformations lead to very slightly bent parts. For the pieces that should fit together, such as the blocking hinges, an offset should be added to take into account the unpredictable small deformations of the PP.

Shrinkage of PP

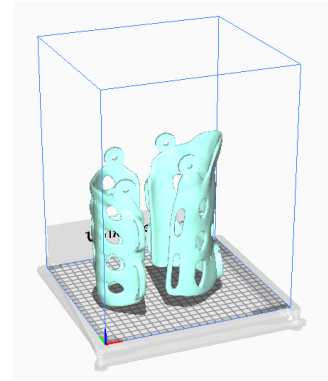
Due to the PP retraction as it cools down, the piece does not stick to the bed and the printing quality is highly impacted as shown in Figure 31a. To avoid that problem, a brim should be added while printing. The brim is a thin layer of PP that is deposited after having spread a special glue on the printer bed. The glue used at Spentys is the "Magigoo Pro PP" [65] adhesive for polypropylene. It is not efficient under 80 °C but it works here as the bed of the printer is heated at 90 °C. The brim is one layer thick (0.2-0.3mm) but should be as wide as possible to increase the sticking area and thus the stability and the quality of the model printed. If wrapping does occur, the brim will be impacted instead of the piece. An example is displayed in Figure 31b. During the printing, the temperature is around 50 °C in the printer (thanks to the heated bed and the "closed" environment) but once the piece is printed, the temperature goes down and it gets easier to take the piece off the plate.



(a) The splint is printed in an open and tilted position to fit in the printer.

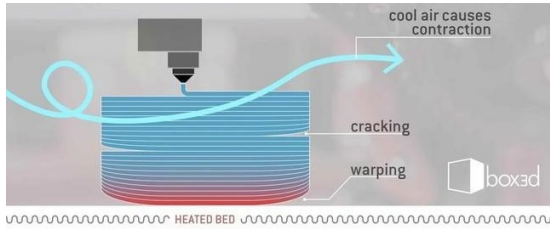


(b) The splint is folded to fit in the printer, with the hinges upwards.

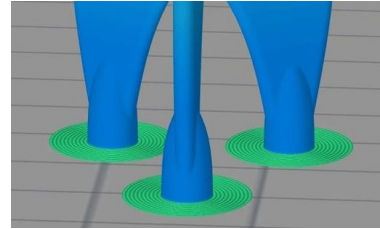


(c) The two parts are printed vertically with the hinges upwards. They can be printed in the same printer or simultaneously in two different printers to gain time.

Figure 30: Printing positions considered for the BOA design.



(a) PP printing problem due to the temperature difference [66]



(b) Example of a brim to improve the stability of the printed piece.

Figure 31: Shrinkage of the PP: problem faced and solution found.

3.4 Challenges due to interactions with external companies

Choice of the BOA model

Different BOA models are presented on the manufacturer website [9] so several dials were initially considered for this project. The models are classified into the following categories:

1. H, M, and L-SERIES: Push in to engage, turn to tighten, pull up for fast release. The H series are very robust but are voluminous. The M series combine strength and durability but are also quite bulky. The L series are light-weighted and precise.
2. L-SERIES 2: Push in to engage, turn to tighten, turn to loosen, pull up for fast release.
3. S-SERIES: Turn to tighten, turn to loosen. Low-profile and light-weighted, these dials are usually the ones chosen for medical applications.

The dial should be resistant but should not be too large so both the H and M series were not considered. The cable should be strong and long enough to go through the entire splint. This was initially an issue as the supplier could not provide small dials with long cables but it is possible to open the BOA and change the cable. This allows the cable's length and material to be chosen.

The "quick release" option, which completely releases the cable as the dial is pulled up, is not desired as the loosening should be slow and controlled. Indeed, quick movements of the elbow and thus possible muscle contractions should be avoided. On the other hand, the security system that requires pushing for the dial to be engaged would have been useful to secure the cable position. Considering all those aspects, the L-series BOA were initially chosen. Even if the "quick release" option is not desired, the "push in to engage" is advantageous. But, due to the unreliability of the stock and the delivery of the distributor of the brand, it was impossible to obtain the model wanted. The S-series BOA were thus used as the choice of the BOA had to be adapted to those external constraints.

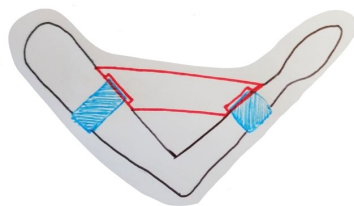
Financial aspects

As explained in Part VII, Section 2, this orthosis was initially designed to be included in Spentys' catalog [10]. The financial aspect is thus important so both the production's cost and the reimbursement procedures are considered. As Spentys was interested in finding a solution for chronic patients, custom devices can be reimbursed by the state, which allows the design not to suffer from this constraint since the final production cost is reasonable. Indeed, the raw material (Polypropylene) is not expensive and the biggest costs are the BOA dial and the salary of the designer. The precise analysis is developed in Part VII, Section 3.

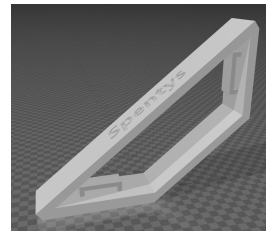
3.5 Position of the limb during the scan

To guarantee a scan of good quality, the iPad should be able to move around the limb at a distance between 50 and 70cm (ideally 60cm). This is necessary to get a good scan's quality⁹ but it means that the arm of the patient should be visible from all sides, the patient thus has to extend his/her arm in front of him/her. Even though the time needed to scan the limb of the patient is very short (1-2min) compared to the traditional methods (30min to form a spastic thermoplastic splint), it can be challenging for some patients to hold a pose. A possible solution was thus to create a support for the arm during the scan.

The first idea was to design a set square (see Figure 32) to immobilize the relative positions of the two parts of the arm. The following model was designed to keep a 90° angle but this could be adapted to the desires of the OT (a more extended position would probably be preferred).



(a) Position on the arm



(b) 3D model

Figure 32: Set square used as a support for the arm. Both parts of the limb are maintained at a certain distance from each other.

Unfortunately, this solution could not be used for spastic patients. Even though the angle would be fixed and maintained, patients might not be able to hold their arm in front of them as required. Several ideas were investigated to find a solution in which the hand was supported.

1. "Crane design", displayed in Figure 33. A handle is fixed to a vertical pole stabilized by a base and both the height and the inclination of the handle can be modified depending on the position

⁹If the quality of the scan is not sufficient, the orthosis might not fit the limb perfectly.

wanted by the OT. The structure would be built using aluminum profiles that are light and resistant. The patient will be sited in a comfortable position with the relevant arm extended to catch the handle and the opposite arm relaxed on the lap or on the side in order not to block the view. The size of the base should be tested to be sure the structure does not fall as the patient holds the handle.

2. Plexiglas table

- Small table placed on top of a normal table as displayed in Figure 34. The height of the top plate of the table is adjusted so that the upper arm completely rests on it. The patient holds a handle that is fixed to the table so the arm is in an open position. The Plexiglas part is invisible on the scan, the elbow is thus visible but the arm anatomy might change as it will be pressed on the surface. It might be difficult to scan around the arm as the normal table might get in the way.
 - An entire table made of Plexiglas would allow the iPad to scan the limb with a distance of 60cm but the structure will be bulky and it would be hard to carry around if the OT wants to put it away when he does not have a patient to scan. Moreover, as the table will have to be rather high (if the patient is sited and even higher if the patient is standing up), the stability of the structure will not be easy to maintain.
3. Handle hanging from a bar fixed in the door-frame, as displayed in Figure 35. Pull-up bars are easily found in sports shops and can easily be fixed or removed from the door frame. The height can be adjusted so the handle hanging from it is at the appropriate height for the arm to be in a good position. The patient can sit or stand.

The problem with those solutions is that spastic patients are very different from one another and they might be unable to control their force and muscles' contraction. As the clenched fist is one of the main features of the upper-limb spasticity, it was thought that the patient would close his hand around the handle and press it but this approach is not reflecting reality. Indeed, the contraction of the hand changes over time and depends also on the environment and external distractions (a sound, a sneeze, an itch...) and the arm might be a dead weight with the incapability to hold the handle. All these solutions might thus be interesting for patients able to hold a handle but not for all patients. The preferred solution for those patients would be the crane as the door-frame and the small Plexiglas table do not allow the scan to be done at 60cm and that the entire table is too heavy and reduces scan quality.

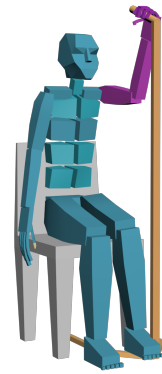
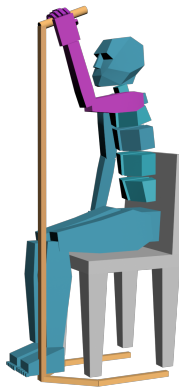


Figure 33: Crane arm support

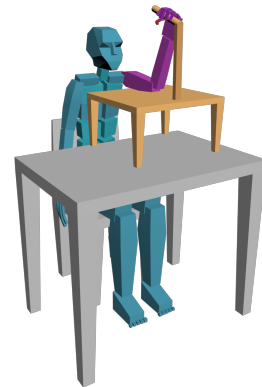
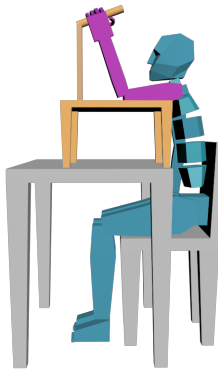


Figure 34: Plexiglas table support

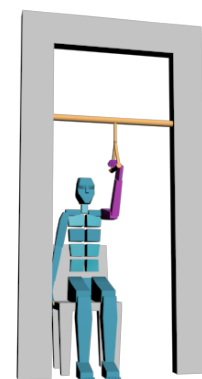


Figure 35: Handle in the door frame support

4 Resistance Analysis

Several analysis are done to evaluate the resistance of the potential designs. Indeed, some features might be adapted if the tests show insufficient strength. The BOA design resistance is assessed with an analytical analysis of the stresses experienced in the BOA cables. The blocking hinge design, on the other hand, is both tested using analytical analysis and *Solidworks* simulations.

4.1 Analytic analysis of the BOA design

To measure the stresses in the BOA cables, an analytic analysis was conducted. The following assumptions were made:

1. The two parts of the arm can be modelled as beams.
2. The movement is in 2D, entirely in the sagittal plane.
3. The upper part of the arm will not move. Indeed, the analysed movement is the elbow flexion so only the relative movement between the two parts is of interest.
4. The shoulder is considered embedded.
5. The moment equilibrium will be done around the hinge point. The hinge and the rotation point of the elbow might be slightly different but they will be assumed coincident since only a negligible difference is acceptable for the orthosis to be worn.
6. The angle between the upper arm and the forearm is considered in the 30° to 130° range, which is described as the functional range of motion to perform activities of daily living by Sardelli, et al. [68].

The first step is to assess the force exerted by the patient's muscles on the orthosis. A first moment equilibrium will be computed, without the orthosis but with an external force to measure the maximum force the muscles can develop. A second moment equilibrium will then be computed as the muscles force is applied on the orthosis.

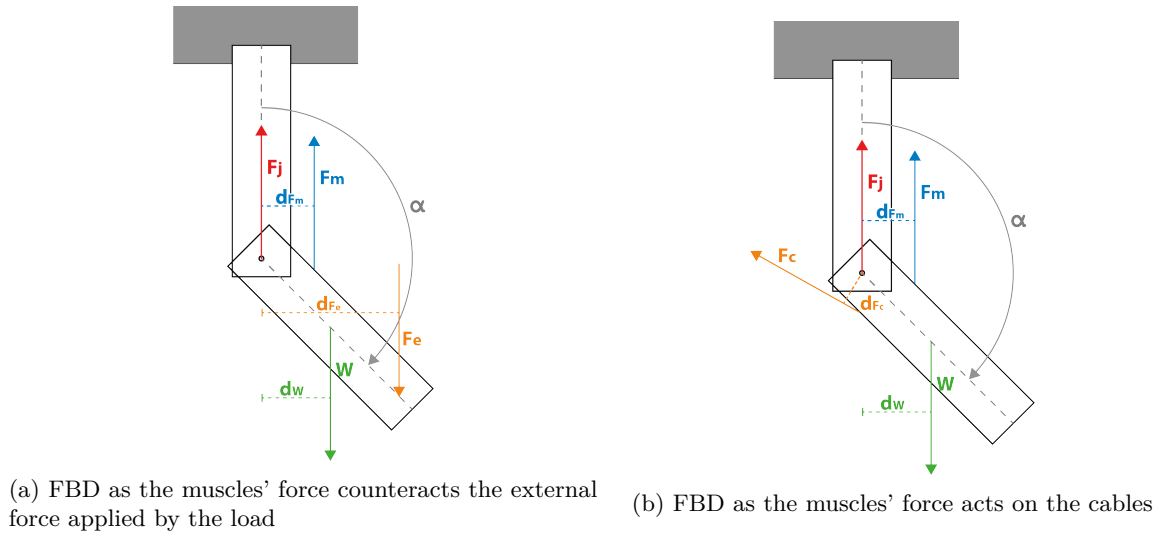


Figure 36: Free body diagrams (FBD) considered for the moment equilibria

We consider the following parameters:

- F_e (N): External force applied. This force is computed as the product of the maximum load (kg) that the patient can sustain at the opening angle α and the gravitational constant $g = 9.81m/s^2$. The assumption is that the force applied by the muscles on the orthosis will be, at maximum, the force that the patient can apply to hold the load. Due to the complexity of spasticity, it is not certain that all patients will be able to test their maximum muscles' force by holding a load. Moreover, the reflex and the voluntary forces might be different. As the force depends on velocity, environmental and unknown factors, assumptions have to be made. However, the point of this analysis is to establish the equations and get an order of magnitude of the stresses in the cable but the values of the parameters can be refined later to be more precise.
- d_{Fe} (m): Lever arm of the external force. With l the length of the forearm and hand, the lever arm's length is equal to

$$d_{Fe} = l \cos(\alpha - 90^\circ) = l \sin(\alpha) \quad (5)$$

- α : angle between the two parts of the arm
- l (m): is the patient-dependant length between the hinge and the location on the hand where the force is applied
- F_j (N): Joint reaction force. Being applied at the center of rotation, it will not impact the moment equilibrium
- W (N): Self weight of the forearm-hand segment, applied at the center of mass
- d_W (m): Lever arm of the self weight
- F_m (N): Force exerted by the muscles active for the flexion of the elbow: the Biceps Brachii, the Brachial and the Brachioradial
- d_{F_m} (m): Lever arm of the muscles' force. This distance is difficult to assess but Loss et al. [69] estimated the mean of the tree muscles moment arms according to the opening angle of the arm. This length varies between 0.02 and 0.03m but as will be seen, this length will be cancelled out, its exact measure is thus not needed.

Using the moment equilibrium we can state that

$$\sum T = I\eta = 0 \quad (6)$$

with

- $\sum T$: Sum of all the torques created by the forces acting on the forearm-hand segment
- I : Inertial moment of the forearm-hand segment
- η : Angular acceleration of the forearm-hand segment which is null at equilibrium. It is difficult to immobilize human beings, especially while holding a heavy load but movements induced will be very small and the acceleration might thus be considered negligible.

By computing the moment equilibrium at the hinge point (see Figure 36a), we get the following equation:

$$F_m d_{F_m} = F_e d_{Fe} + W d_W \quad (7)$$

The same equilibrium can now be done without the external load and with the orthosis (see Figure 36b), considering that the muscles exert the same force and we obtain:

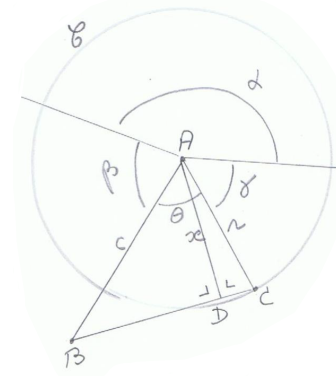
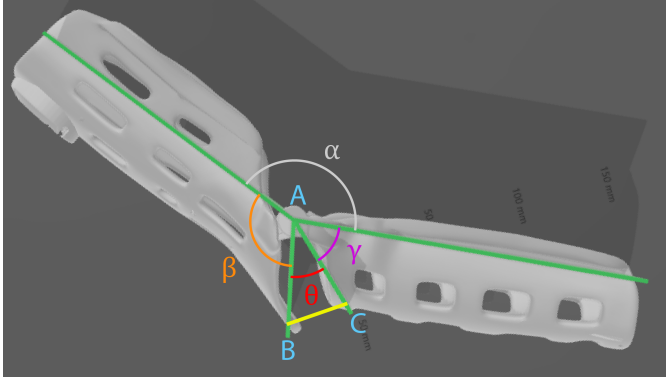
$$F_m d_{F_m} = F_c d_{Fc} \sin \phi + W d_W \quad (8)$$

with

- F_c (N): Force in the cables
- d_{F_c} (m): Distance between the hinge point and the cable line (in yellow in the following schematic). The cable line is the line joining the point B where the cables exit the upper-part of the orthosis and the point C where the cables exit the forearm part of the orthosis. A geometric construction has to be made to obtain this distance according to the angle α .

Side note for the computation of the parameter d_{F_c} .

The equations needed to find the expression of d_{F_c} will be developed in this section. Let's define a circle C of center A (center of rotation) and radius r . A fixed point B and a point C describing the circle C as α changes. We want the length of the segment [AD].



The point D is the orthogonal projection of A on BC. Let's simplify by establishing $|AD| = x$, $|AB| = c$ and $|AC| = r$. The area of the triangle $\triangle ABC$ is $S = \frac{|BC|x}{2}$ and $S = \frac{1}{2}cr|\sin\theta|$ with $\theta = \widehat{CAB}$.

We thus get $|BC|x = cr|\sin\theta|$ with $x = \frac{cr|\sin\theta|}{|BC|}$ ($B \neq C$ since A, B and C are not aligned). Moreover, $|BC|^2 = c^2 + r^2 - 2crcos\theta$.

Overall, $x = \frac{cr|\sin\theta|}{\sqrt{c^2 + r^2 - 2crcos\theta}}$ with β and γ , two angles fixed and centered in A, we get, $\theta = 2\pi - (\alpha + \beta + \gamma)$ and we finally get

$$x = \frac{cr|\sin(\alpha + \beta + \gamma)|}{\sqrt{c^2 + r^2 - 2crcos(\alpha + \beta + \gamma)}} = |AD| = d_{F_c} \quad (9)$$

- ϕ is the angle between F_c and the direction in which d_{F_c} is measured. This angle is equal to $\pi/2$ since the lever arm is taken perpendicular to the direction of F_c . The factor $\sin\phi$ is thus equal to 1.

By combining Equations 7 and 8 we get:

$$F_c = F_e \frac{d_{F_e}}{d_{F_c}} \quad (10)$$

This force is going through the two cables so the stress in each cross-section is, using Equations 9 and

10:

$$\begin{aligned}
\sigma &= \frac{F_c}{2\pi R^2} = \frac{Xg}{2\pi R^2} \frac{l \sin(\alpha)}{\frac{cr |\sin(\alpha+\beta+\gamma)|}{\sqrt{c^2+r^2-2crcos(\alpha+\beta+\gamma)}}} \\
&= \frac{Xgl}{2\pi R^2 cr} \frac{\sin(\alpha) \sqrt{c^2+r^2-2crcos(\alpha+\beta+\gamma)}}{|\sin(\alpha+\beta+\gamma)|} \\
&= \frac{Xgl}{2\pi R^2 cr} \frac{\sin(\alpha) \sqrt{c^2+r^2-2crcos(\alpha+\beta+\gamma)}}{|\sin(\alpha+\beta+\gamma)| \sin\left(\arccos\left(\frac{ccos\beta - rcos(\gamma+\alpha)}{\sqrt{c^2+r^2-2crcos(\alpha+\beta+\gamma)}}\right)\right)}
\end{aligned} \tag{11}$$

To see if those results are feasible, we can take a numerical example: the patient is a female, with $l = 0.3m$. For her orthosis, $r = 5cm$, $c = 5.5cm$, $\beta = 123^\circ$ and $\gamma = 50^\circ$. The radius of the steel cable can be measured and was estimated. The current cable radius is 0.3mm but it could be changed for a larger cable (0.4mm of radius). The influence of the cable's radius, as well as the load and the angle α can be seen in Table 9.

| Cable radius, R (mm) | Load hold, F_e/g (kg) | Angle, $\alpha(^\circ)$ | Stress, σ (MPa) |
|----------------------|-------------------------|-------------------------|------------------------|
| 0.8 | 5 | 90 | 424 |
| | | 110 | 338 |
| | 2 | 90 | 169 |
| | | 110 | 135 |
| 0.6 | 5 | 90 | 754 |
| | | 110 | 602 |
| | 2 | 90 | 301 |
| | | 110 | 241 |

Table 9: Estimations of the stress in the cables depending on the cables' radius, the maximum load hold by the patient and the angle of extension of the arm α . As other parameters change depending on the size of the arm, and thus the splint, those values are taken as an example for the orthosis shown in Figure 47.

As can be seen in Equation 11, the stress is directly proportional to the load the patient can carry and inversely proportional to the square of the radius of the cable section. Typical values of ultimate tensile strength of the steel range from 295 - 2400 MPa. The range is wide as the steel composition and heat treatment have a big impact on the properties. Yield strength varies as ultimate tensile strength values, from 200 - 2100 MPa [70]. These results thus indicate that the type of steel used in the cable is important to ensure that the maximum stress does not exceed the Yield stress. If a sufficiently strong cable is taken, the orthosis should resist the force exerted by the patient.

4.2 Finite element analysis of the blocking hinge design

4.2.1 Introduction

Finite Element Analysis are carried out in this section using the simulation tool of *Solidworks*. This is done to compute and show the displacement field as well as the von Mises stress map (see Section 4.2) as the object is subjected to an external force or pressure. These analysis show the critical points and help to make the model stronger. This Finite Element Method is used for the blocking hinge design as the BOA design has been analysed using an analytic approach (see Section 4.1).

4.2.2 Introduction to *Solidworks*

4.2.2.1 Requirements to run a simulation The parameters that must be chosen to run a simulation are listed:

- **Material:** The material used can either be selected in the library offered by *Solidworks* or it can be created by the user as long as the required properties are given. To define an isotropic material, which means that the behavior of the material is the same in all directions, only the Elastic modulus, the Poisson's ratio, and the density are needed. Other parameters such as the shear modulus, the yield, tensile and compressive strengths, and thermal parameters can be added but are not necessary. As we will not study the influence of temperature, the thermal expansion coefficient, the thermal conductivity, and the specific heat are left undefined. To simulate orthotropic materials (whose behavior differs along three mutually orthogonal axes), additional parameters are required.
- **Fixtures:** A part of the geometry has to be fixed in order for the model to experience stresses as a load is applied or the part would simply move without being deformed.
- **Create a contact:** When several parts interact to form an assembly, creating and defining the contact will be necessary. The options available are: bonded, penetration or no penetration. The bonded option considers the parts as if they were welded.
- **Mesh:** The part(s) previously design is subdivided into small pieces of simple shapes, called elements, that are connected at their vertex, called nodes. The mesh definition (size of the elements) is chosen by the user. A compromise has to be made as a thinner mesh is more precise but increases the time needed to run a simulation. The mesh created is a solid mesh with tetrahedral elements. For all the simulations performed, it has been checked that the aspect ratio is less than 5 for most of its elements (90% and above) since the quality of the mesh is guaranteed if this condition is respected. A perfect mesh would have only uniform and perfectly tetrahedral elements (aspect ratio = 1) but complex geometries make it impossible so this ratio is used to describe the deviation from this perfect shape.
- **Results:** The results that are displayed in the report can be chosen. Von Mises stress, displacement and equivalent strain maps were chosen.

4.2.2.2 Solvers and options used *Solidworks* simulations use the finite element method to represent problems as sets of algebraic equations that must be solved simultaneously. There are several ways to solve the sets of equations and different solvers can be used. Two solvers were used in this work [79]:

- **FFEPlus:** Iterative solver used for large problems, that uses advanced matrix reordering techniques. At each iteration, a solution is assumed and the errors are computed until they are small enough.
- **Intel Direct Sparse:** Direct solver that uses exact numerical techniques to solve the equations. When the simulations become too complex (non-linear, working on an assembly with the no penetration condition between the pieces, etc), and that the FFEPlus solver fails at solving the constraint equations, *Solidworks* can voluntarily switch to this solver. However, trials were done with this solver but none of the simulations shown in this Section used it.

Solidworks can also work with the *Large* or *Small displacement* options. The *Large Displacement* option computes the displacements of the next iteration by taking into account of the variation of the geometry at the previous iteration while the *Small Displacement* option assumes the geometry to remain unchanged. The *Large Displacement* option is thus preferred but if the incremental elastic strain is too big ($> 25\%$), the *Small Displacement* option should be chosen or *Solidworks* cannot finish the analysis.

4.2.3 Simulations done

Several simulations are carried out to test different parameters. For all simulations, the moment applied by the muscles on the orthosis is the same. This moment is computed in Section 4.2.3.1 and is used in the following simulations. Once this moment is computed, the effects of considering an orthotropic material (rather than an isotropic one) are studied. Then, the influence of the properties of different materials is analysed and the resistance of the teeth is assessed. As the initial geometry did not satisfy our requirements, a new geometry was designed and the resistance of the teeth is assessed again. To confirm the results (stresses and displacements) obtained with the simulation, an analytical analysis is performed.

4.2.3.1 Moment applied on the orthosis We can reuse the free body diagram of the resistance analytic analysis of the BOA system, which is displayed in Figure 37.

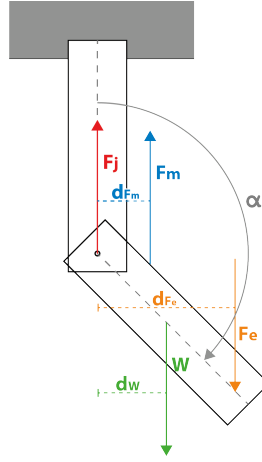


Figure 37: FBD as the muscles' force counteracts the external force applied by the load

By computing the moment equilibrium at the rotation center, the moment applied on the orthosis is equal to

$$M = F_m d_{F_m} = F_e d_{F_e} + W d_W \quad (12)$$

with

- M (Nm): The moment the muscles are exerting on the orthosis.
- F_m (N): Force exerted by the muscles active for the flexion of the elbow: the Biceps Brachii, the Brachial and the Brachioradial
- d_{F_m} (m): Lever arm of the muscles' force. This distance is difficult to assess but Loss et al. [69] estimated the mean of the three muscles moment arms according to the opening angle of the arm. This length varies between 0.02 and 0.03m but as will be seen, this length will be cancelled out, its exact measure is thus not needed.
- F_e (N): External force applied. This force is computed as the product of the maximum load (kg) that the patient can sustain at the opening angle α and the gravitational constant $g = 9.81m/s^2$. The assumption made is explained in the Section 4.1. For the analysis on the blocking hinge design, we will consider the maximum load to be 5kg. The moment computed will thus probably larger than the one that will be applied in reality but this is done to compute the most critical scenario.

- d_{Fe} (m): Lever arm of the external force. With l the length of the forearm and hand, the lever arm's length is equal to

$$d_{Fe} = l \cos(\alpha - 90^\circ) = l \sin(\alpha) \quad (13)$$

- W (N): Self weight of the forearm-hand segment, applied at the center of mass. Deleva et al. [80] estimated the mass and the position of the center of mass of the hand and the forearm both for male and female subjects and gave the data displayed in Table 10.

| | Female | Male |
|--|--------|--------|
| Forearm mass relative to body mass (%) | 1.38 | 1.62 |
| Hand mass relative to body mass (%) | 0.56 | 0.61 |
| Total body mass (kg) | 61.9 | 73 |
| Computed forearm mass (kg), $m_{forearm}$ | 0.854 | 1.183 |
| Computed hand mass (kg) m_{hand} | 0.347 | 0.445 |
| Computed total weight of the forearm/hand segment (N), W | 11.781 | 15.971 |

Table 10: Averaged anatomical data provided by Deleva et al. [80]. The relative body masses are given as a percentage of the total body weight. The last three rows were computed using the given data. The weight was computed by multiplying the gravitational constant ($g = 9.81m/s^2$) by the sum of the forearm mass and the hand mass.

- d_W (m): Lever arm of the self weight. Data provided by Deleva et al. [80] are also used and displayed in Table 11.

| | Female | Male |
|--|--------|-------|
| Longitudinal length of the forearm (m) | 0.264 | 0.268 |
| Longitudinal length of the hand (m) | 0.078 | 0.086 |
| Longitudinal CM position of the forearm (%) | 45.59 | 45.74 |
| Longitudinal CM position of the hand (%) | 74.74 | 79 |
| Longitudinal CM position of the forearm (m), from the elbow, $L_{forearm}$ | 0.12 | 0.126 |
| Longitudinal CM position of the hand (m), from the hand | 0.058 | 0.068 |
| Longitudinal CM position of the hand (m), from the elbow, L_{hand} | 0.178 | 0.194 |

Table 11: The longitudinal CM position are given as a proportion of the segment length and are taken from the proximal endpoint (the elbow for the forearm and the wrist for the hand). [80] The last three rows were computed using the given data.

The weight of the hand and the weight of the forearm are not applied at the same location so an average was taken to get the weighted longitudinal CM position of the forearm/hand segment (m) such as

$$L_{CM} = \frac{m_{forearm} * L_{forearm} + m_{hand} * L_{hand}}{m_{forearm} + m_{hand}} \quad (14)$$

which gave 0.137m for the women and 0.144m for the men. This length should be multiplied by $\sin(\alpha)$ to take into account the direction of the lever arm such as $d_W = L_{CM} \sin(\alpha)$

The moment, for a man at $\alpha = 90^\circ$ is thus

$$M = (F_e l + W L_{CM}) \sin \alpha = 15.445 Nm \quad (15)$$

The moment chosen for the following simulations is the one for a man, as it is the most critical scenario. Indeed, the moment of a woman is 14.563Nm. This moment is used in the rest of the analysis.

4.2.3.2 Resistance of the teeth and comparison of materials The first analysis was done on both parts (internal and external parts) separately. The pressure was equally distributed on each of the tooth of the hinge to analyze their resistance and to see the influence of the material chosen. This analysis focuses only on the teeth and is not representative of the entire problem. Since the simulation only looks at a single piece under external loads, the solver (different solvers are explained in Section 4.2.2.2) handles linear equations and is thus very quick which is a big advantage to test a lot of different parameters (material, load applied, size of the mesh).

Some tests were made (not described here) to choose the mesh size, giving a final mesh size of 0.5mm of element size with a tolerance of 0.025mm. This very high quality was possible without having a long simulation time as the problem is very simple (only one part, simple load, no interactions).

As a reminder, to make the following example of analysis, the parameters were the one of one male patient: load sustained = 5kg, length of hand and forearm (l) = 0.268m, $\alpha = 90^\circ$ (to compute the biggest pressure possible), lever arm $L_{CM} = 0.144m$, and weight of the hand-forearm segment $W = 15.971$. These parameters give the moment $M = 15.445Nm$ as stated in the previous paragraph.

4.2.3.2.1 Initial geometry The pressure that should be applied on each tooth has to be computed according to the moment computed in Section 4.2.3.1. Indeed, the moment to which the orthosis is subjected creates a pressure on each tooth which is equal to that moment divided by the lever arm (between the center of rotation and the surface the pressure is applied on) and the area of that surface:

$$p = \frac{M}{22aR} \quad (16)$$

with

- p (N/m^2): Pressure applied on each tooth
- a (m^2): Area of a single tooth. The teeth of the inside part, have an area of 6mm x 5mm so $3e-5m^2$. For the teeth of the outside part, the area is equal to 5mm x 5mm so $2.5e-5m^2$. Not that there is 22 teeth in the design studied.
- R (m): Distance between the center of rotation and the middle of the teeth internal face. Due to the symmetry of the geometry, this distance is the same for all the teeth. For the internal part of the hinge, this length is equal to 15mm and for the external part, this length is equal to 15.5mm.

The pressure is computed and we get $p = 1,560,123N/m^2$ for the internal part and $p = 1,811,756N/m^2$ for the external one. By the action-reaction principle, both pressures should be equal since the area to be considered in the surface of contact between the two pieces. The two areas considered are different since a part of the surface of the teeth of the internal part is not in contact with the external teeth. The surface that should be considered is thus the area of the teeth of the external part (the smallest). However, applying the pressure on only a portion of the teeth is complicated in *Solidworks* (especially as we do not know exactly where the teeth will be in contact). An assumption is thus made by applying the pressure in the entire surface of the teeth. Different pressures are thus exerted on the internal and the external parts.

Two materials are compared, the Polypropylene (PP) and the Polyethylene Terephthalate (PET), as there were the possible materials for the blocking hinge. The properties given in the data sheet of the supplier and the ones given by *Solidworks* differ and they are compared in this analysis. As there were no value for the Poisson's ratios in the data sheets of the supplier, the ones from the *Solidworks* data were taken.

The value of the elastic modulus is given as a range since the data sheet gives values that depend on the printing direction. For this isotropic analysis, the maximum value of this range is taken and

| Properties | PP (<i>Solidworks</i>) | PP (Data sheet) | PET (<i>Solidworks</i>) | PET (Data sheet) |
|-----------------------------|--------------------------|-----------------|---------------------------|---------------------|
| Elastic Modulus (N/m^2) | 896e+6 | [470; 554]e+6 | 2,960e+6 | [1, 665; 1, 993]e+6 |
| Poisson ratio (N/A) | 0.4103 | 0.4103 | 0.37 | 0.37 |
| Density (kg/m^3) | 890 | 900 | 1420 | 1329 |

Table 12: PP and PET properties that were used for the simulations. Both the *Solidworks* properties and the properties found in the data sheet of the supplier are tested [76][77]

the effect of the printing direction is studied in Section 4.2.3.3.

Results of the analysis: Materials

We can compare the results obtain with PP and PET by taking both the *Solidworks* values and the ones found in the data sheets, those values are displayed in Table 12. The properties given in the data sheet are weaker as the material gets more fragile when 3D printed. Moreover, material properties vary depending on the composition and the process of production which is specific to each supplier. This analysis is done using simulations of the internal part of the hinge as we want to consider the most critical piece. This assumption is checked in the Section 4.2.3.4. The results are shown in Table 13.

For all of them, the minimum resultant displacement is null since the surface of the internal cylinder is fixed.

| | PP (<i>Solidworks</i>) | PP (Data sheet) | PET (<i>Solidworks</i>) | PET (Data sheet) |
|----------------------------------|--------------------------|-----------------|---------------------------|------------------|
| Min von Mises Stress (N/m^2) | 3.837e+4 | 5.216e+4 | 2.415e+4 | 2.595e+4 |
| Max von Mises Stress (N/m^2) | 8.606e+7 | 8.761e+7 | 8.335e+7 | 8.415e+7 |
| Max resultant displacement (mm) | 2.339 | 3.783 | 0.6909 | 1.032 |
| Min equivalent strain | 8.102e-5 | 9.944e-5 | 1.649e-5 | 2.587e-5 |
| Max equivalent strain | 7.843e-2 | 1.349e-1 | 2.266e-2 | 3.376e-2 |

Table 13: Comparison of the results obtained using PP or PET (both with the *Solidworks* and the data sheet properties)

The conclusions that can be drawn are that the maximum displacements and the von Mises stresses are smaller for the pieces in PET than for the pieces in PP (both with *Solidworks* data and the data from the supplier). This makes sense as the Elastic modulus and the density of the PET are higher than the ones of the PP. As explained in Section 4, the elastic modulus links the stress applied and the strain measured such as $\sigma = E\epsilon$ so for the same pressure applied, the strain will be smaller if the Elastic modulus is greater. The von Mises stresses are not dramatically different and the displacements and equivalent strain are reasonable so both materials could be considered. As explained in Part II Section 3, the material chosen is the PP due to the printing quality and the flexibility of the material.

Results of the analysis: Teeth resistance

The von Mises stresses, the displacements and the equivalent strain maps can be compared for the four materials tested above. Even tough the values change, the distributions are similar (the maximums and minimum are always in the same locations) so only the maps of the analysis run with PP (parameters from the data sheet) are shown in Figure 38 and 39. This analysis was chosen as the PP is chosen as the final material and the properties from the data sheet are taken since it gives more critical results than with the *Solidworks* proprieties (the most critical scenario should be considered).

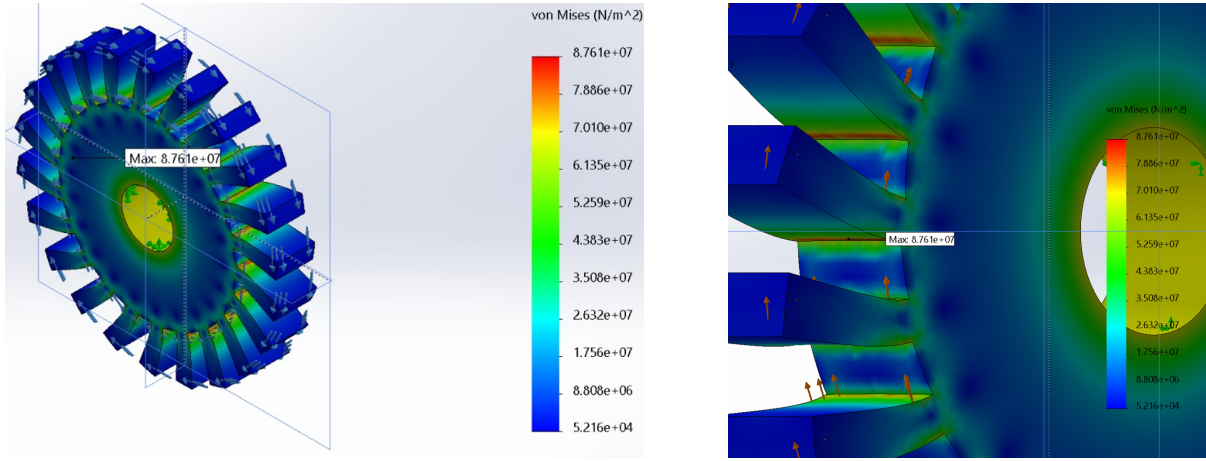
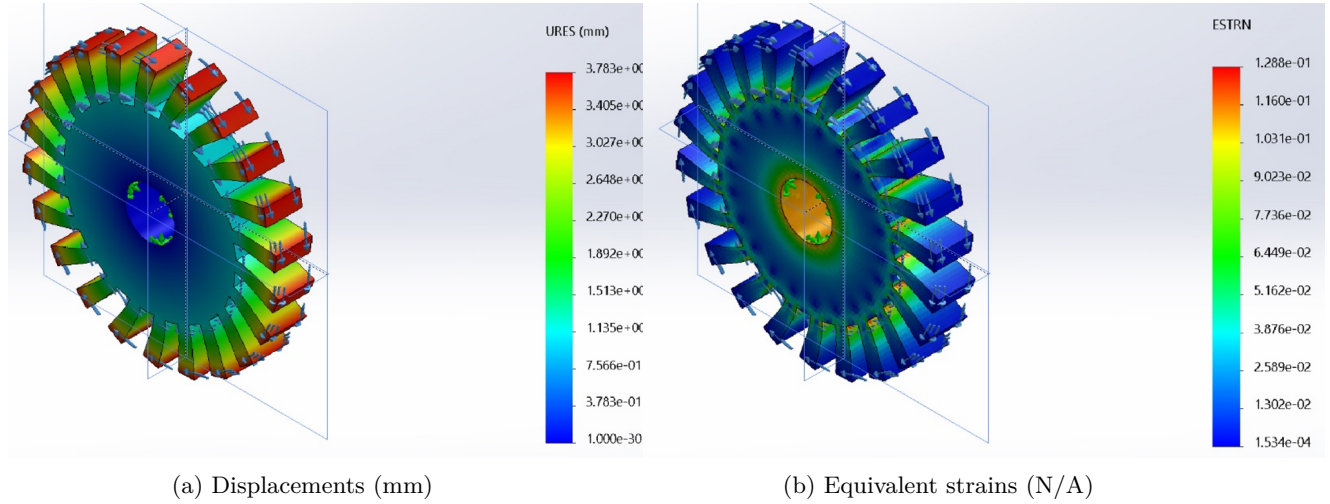


Figure 38: Color map of the von Mises stresses (N/m^2) resulting from the analysis done with the properties of the PP given in the data sheet [76].



(a) Displacements (mm)

(b) Equivalent strains (N/A)

Figure 39: Color maps of the analysis done with the properties of the PP given in the data sheet [76].

This analysis is done to see the resistance of the teeth but does not reflect the entire problem. Indeed, the boundary conditions are not correct since the internal cylinder is taken as a fixed geometry as if the hinge could not rotate around the binding screw. The high von Mises stresses and equivalent strains around the internal cylinder should not be taken into account. The conclusions that should be drawn are that the maximal stresses are situated at the basis of the teeth, which is thus the most critical zone that could be reinforced, if needed. The maximum displacements are at the extremities of the teeth as it is the zone the farthest from the mounting in the core of the part.

However, Woern et al. [78] state that 3-D printed PP tensile strength ranges from 27 to 36 MPa, which is lower than the stresses obtained for the PP simulation with the data sheet properties. The geometry of the pieces should thus be modified to reduce the stresses experienced.

Improved geometry To increase the resistance of the pieces, it was decided to decrease the number of teeth (from 22 to 20), and increase both the thickness (from 5 to 6mm) and the diameter

(36 to 46mm)¹⁰.

The value of the pressure applied changes, as the geometry does:

$$p' = \frac{M}{20a'R'} \quad (17)$$

with

- p' (N/m^2): Pressure applied on each tooth
- a' (m^2): Area of a single tooth. For the teeth of the inside part, it is 6mm x 6mm so $3.6e-5m^2$. For the teeth of the outside part, it is 6mm x 5mm so $3e-5m^2$. Note that there is 20 teeth in the design studied.
- R' (m): Distance between the center of rotation and the middle of the teeth internal face. Due to the symmetry of the geometry, this distance is the same for all the teeth. For the internal part of the hinge, this length is equal to 20mm and for the external part, this length is equal to 20.5mm.

For the inside part we get $p = 1,072,569N/m^2$ and for the outside part we get $p = 1,255,691N/m^2$ ¹¹.

Results of the analysis: Teeth resistance

The results obtained with the new geometry are compared to the ones from the initial geometry in Table 14. The maximal von Mises stress is taken as $2.505e+07 N/m^2$ and the maximum equivalent strain is taken as $3.352e-2$. Indeed, the overall maximal stress is equal to $5.876e+07 N/m^2$ and the overall maximal equivalent strain is equal to $9.513e-02 N/m^2$ but they are located on the surface of the internal cylinder. As explained, this part of the geometry should not be taken into account as the boundary conditions do not reflect the reality. The *probe* tool is thus used to find the maximal stress and strain on the teeth.

| | Initial geometry | Improved geometry |
|----------------------------------|------------------|-------------------|
| Min von Mises Stress (N/m^2) | 5.216e+4 | 7.705e+3 |
| Max von Mises Stress (N/m^2) | 8.761e+7 | 2.505e+07 |
| Max resultant displacement (mm) | 3.783 | 2.29 |
| Min equivalent strain | 9.944e-5 | 1.939 e-5 |
| Max equivalent strain | 1.349e-1 | 3.352e-2 |

Table 14: Comparison of the results obtained using PP (data sheet properties), for the initial and the improved geometries

The maximal displacement decreased by 39.47% and the maximal stress by 71.4%. The maximum stress experienced is now lower than the range of possible tensile stresses given by Woern et al. [78] ($[2.7 ; 3.6] e+7 N/m^2$). Even though less positions are possible (increments of 18° and not 16.36°), those changes seem reasonable to decrease the stresses experienced and are thus kept for the rest of the analysis. Note that the analysis done for the different materials does not have to be done again as the results obtained allow the comparison of the different materials. Note that the maximal displacement is still quite high but this is due to the material properties. Indeed, the PP is semi-flexible and can bend a lot before breaking. This particularity is appreciated as we would prefer the splint to bend (and even get deformed under heavy loads) than to break and hurt the patient.

¹⁰Note that to keep a binding screw of 10mm while increasing the thickness of the teeth from 5mm to 6mm, the flat part of the external hinge (from which the teeth emerge) is decreased to 4mm.

¹¹The same assumption as the one done in Section 4.2.3.2.1 is made which explains why the two pressures are not the same.

Analytical analysis To check that the values obtained with the *Solidworks* simulation, an analytical analysis can be done by making multiple assumptions. This analysis will not be as precise since approximations are made but it gives an idea of the order of the stresses experienced at the teeth base and the displacements of the teeth extremities.

Each tooth can be represented as a beam clamped into a fixed structure if we consider the cylindrical part of the hinge to be rigid. The Navier equation can be used as the plane of bending corresponds to the one of the principal axes of the cross section [72]. This equation describes the linear distribution of the stress, $\sigma(N/m^2)$, along the beam as:

$$\sigma = \frac{M_{beam}y}{I} \quad (18)$$

with

- M_{beam} (Nm): Moment at the clamping that depends on the force at the center of the tooth. The force is equal to the product of the pressure calculated for each tooth by the area of a tooth. The moment is the product of that force and the lever arm of the force (distance between the base and the center of the tooth ($l_{tooth}/2$)) such as

$$M_{beam} = p'a' \frac{l_{tooth}}{2} = \frac{M}{20R'} \frac{l_{tooth}}{2} = 0.1158 \quad (19)$$

- y (m): Position along the cross-section of the beam. Equal to zero the neutral axis of the beam and varies between -1.25mm and 1.25mm.
- I (m^4): Second moment of inertia that describe how the points of an area are distributed with regard to an axis. For a rectangular beam, this moment of inertia is equal to $\frac{bH^3}{12}$ with b the width of the beam (6mm) and H the height of the beam (2.5mm). For this problem, it is equal to $7.81e-12 m^4$.
- R (m): Distance between the center of rotation and the middle of the teeth. Due to the symmetry of the geometry, this distance is the same for all the teeth. For the internal part of the hinge, with the new geometry, this length is equal to 20mm.

Still considering the same parameters as the previous calculations and computing the maximum stress (for $y = 0.00125m$)

$$\sigma = \frac{M_{beam}y}{\frac{bH^3}{12}} = 1.8534e + 7N/m^2 \quad (20)$$

The values obtained are 26% lower than the ones obtained with the *Solidworks* simulation. Approximations are made in the analytical analysis so having small differences is acceptable as long as the results are in the same order of magnitude. The simulation software computes the maximum von Mises stress, which is computed by considering the stresses in the 3 directions as well as the shear stresses. In this analytical analysis, only the stress in one direction (the one of the application of the pressure) was considered. This could partly explain why the value is lower than for the *Solidworks* simulations. On the other hand, the analytical analysis does not take into account the stresses concentrations. Both analysis consider that the stresses decrease as the lever arm increases but the analytical analysis is simplified and does not consider the abrupt changes of stress concentrations that *Solidworks* does.

To compute the maximal displacement of the teeth extremities, the equation of the maximum displacement of a cantilever beam (f) can be used [72]:

$$f = \frac{p'L^4}{8EI} \quad (21)$$

with¹²

¹²The other parameters are defined in Section 4.2.3.2.1.

- L (m): The total length of the beam, which is here the tooth, equal to 6e-3 m for the teeth of the internal part of the hinge.
- E (N/m^2): Elastic modulus of the material, equal to 554e+6 N/m^2 for the PP used.

The displacement computed is equal to 5.12 mm, which in the same order of magnitude as the displacement obtained with the *Solidworks* simulations. The analytical value is 2.23 times higher than the one from the simulation. The gap could come from simplifications made in the analytical analysis or due to the parameters chosen for the simulations. However, since the results are of the same order of magnitude, further tests are not needed.

In conclusion, some small differences are noticed between the results of the simulations and the one analytically computed but the orders of magnitude are similar, which confirms that the simulations are realistic.

4.2.3.3 Isotropic or orthotropic material As the piece is printed layer by layer, problems might occur due to the non-perfect adhesion between filaments belonging to the same layer (due to a lack of pressure). The direction in which the part is printed can have a non-negligible impact. The material is thus anisotropic and it can eventually be considered orthotropic. Indeed, its behavior changes along three mutually orthogonal axes.

To efficiently avoid tensile forces, the deposition direction of the filaments should be the one of the force applied. Unfortunately, the printing quality is strongly influenced by the direction of printing. The printing direction is thus not chosen to optimize the material properties but to obtain a good printing quality. The best results are obtained by printing the piece horizontally as explained in Section 3.

A new material is defined to take into account the effect of the orthotropy. By comparing the results with the isotropic and the orthotropic material, we can see if it was reasonable to assume it to be isotropic in the previous analysis. Note that this analysis was performed both on the initial and the improved geometry and gave similar results so only the ones of the initial geometry are displayed.

When an orthotropic material is defined, the elastic modulus in the three directions, the three Poisson's ratios and the material density must be given. Unfortunately, few data are available for the Poisson's ratio of 3D printed PP so the one given by *Solidworks* was kept for the three directions. The direction of the 3D printed fibers, as well as the order in which they are deposited on top of each other, would probably give three different Poisson's ratios. It is thus a big approximation to assume the three ratios equal to 0.4103. The properties considered are displayed in Table 15 and the results of the analysis are given in Table 16.

| Properties | Orthotropic PP | Units |
|-----------------------|----------------|---------|
| Elastic Modulus in X | $470 * 10^6$ | N/m^2 |
| Elastic Modulus in Y | $470 * 10^6$ | N/m^2 |
| Elastic Modulus in Z | $554 * 10^6$ | N/m^2 |
| Poisson's ratio in XY | 0.4103 | N/A |
| Poisson's ratio in YZ | 0.4103 | N/A |
| Poisson's ratio in XZ | 0.4103 | N/A |
| Density | 900 | N/m^2 |

| Properties | Isotropic PP | Units |
|-----------------------------|--------------|--------------|
| Elastic Modulus (N/m^2) | 554e+6 | N/m^2 |
| Poisson ratio (N/A) | 0.4103 | N/A |
| Density | 900 | (kg/m^3) |

Table 15: PP properties that were used in *Solidworks* to compare the results obtained with an isotropic or an orthotropic material.

| | PP isotropic | PP orthotropic |
|----------------------------------|--------------|----------------|
| Min von Mises Stress (N/m^2) | 8.911e+3 | 6.303e+3 |
| Max von Mises Stress (N/m^2) | 8.545e+7 | 8.553e+7 |
| Max resultant displacement (mm) | 3.342 | 3.937 |
| Min equivalent strain | 2.667e-5 | 3.528e-4 |
| Max equivalent strain | 1.383e-1 | 1.630e-1 |

Table 16: Comparison of the results obtained using isotropic and orthotropic PP.

The maximum von Mises stress, the maximum displacement, and the maximum equivalent strain are lower for the isotropic material. This was expected as the elastic modulus chosen for the isotropic material was the equal to the maximum of the three different elastic moduli chosen for the orthotropic material. However, the maximum stresses obtained are the one in the internal cylinder, which are not representative. The maximum stresses experienced by the teeth are situated at the base of it and are equal to approximately $2.6e+7 N/m^2$.

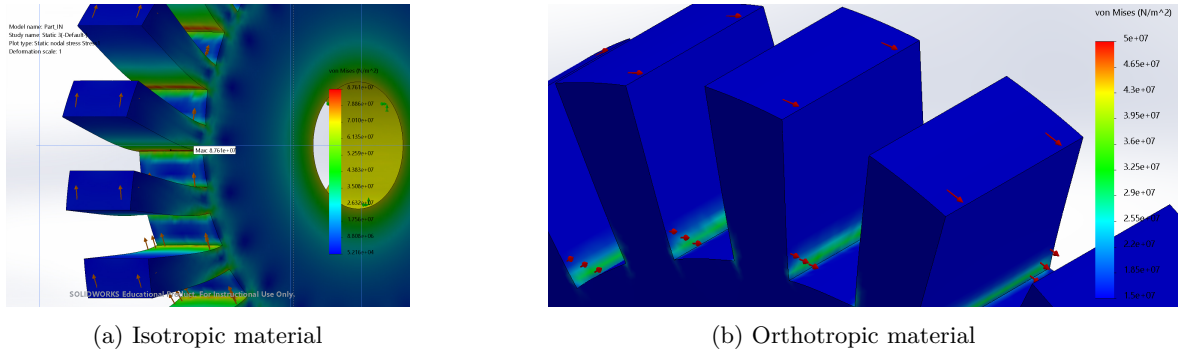


Figure 40: Color map of the von Mises stresses (N/m^2).

As displayed in Figure 40, the location of the maximum von Mises stress can be considered the same for the isotropic and the orthotropic material. The maximum is achieved near the edge of the base of each tooth. Overall, the results are close so the material can be considered isotropic for the other analysis.

4.2.3.4 External part of the hinge The goal is to consider the most critical scenario to keep a safety margin. The analysis were thus done on the internal part of the hinge as it is expected to be weaker. To confirm that the external part is more resistant than the internal part, the simulation was also done for the external part of the hinge with PP (with the properties of the data sheet).

Initial geometry The results of the internal and the external parts of the initial geometry are compared in Table 17¹³.

As can be seen, the inner part will be subjected to higher von Mises stresses, strains and displacements. The maximum von Mises stresses of the external part are located at the base of the teeth, as can be seen in Figure 41a. As for the internal part, the maximal displacement is experienced by the extremities of the teeth, as displayed in Figure 41b. This is expected as these points are the farthest from the embedded base of the teeth.

¹³The highest von Mises stress of the external part is equal to $7.02e + 7 N/m^2$ but is experienced in this internal cylinder, which is not to take into account. Using the *probe* tool, the maximum von Mises stress experienced by the teeth is estimated to $3.615e + 07 N/m^2$.

| | Internal part | External part |
|----------------------------------|---------------|---------------|
| Min von Mises Stress (N/m^2) | 5.216e+4 | 4.921e+4 |
| Max von Mises Stress (N/m^2) | 8.761e+7 | 3.615e+07 |
| Max resultant displacement (mm) | 3.783 | 2.425 |
| Min equivalent strain | 9.944e-5 | 4.662e-5 |
| Max equivalent strain | 1.349e-1 | 1.147e-1 |

Table 17: Comparison of the results obtained using PP (data sheet properties) for the internal and external parts of the initial geometry.

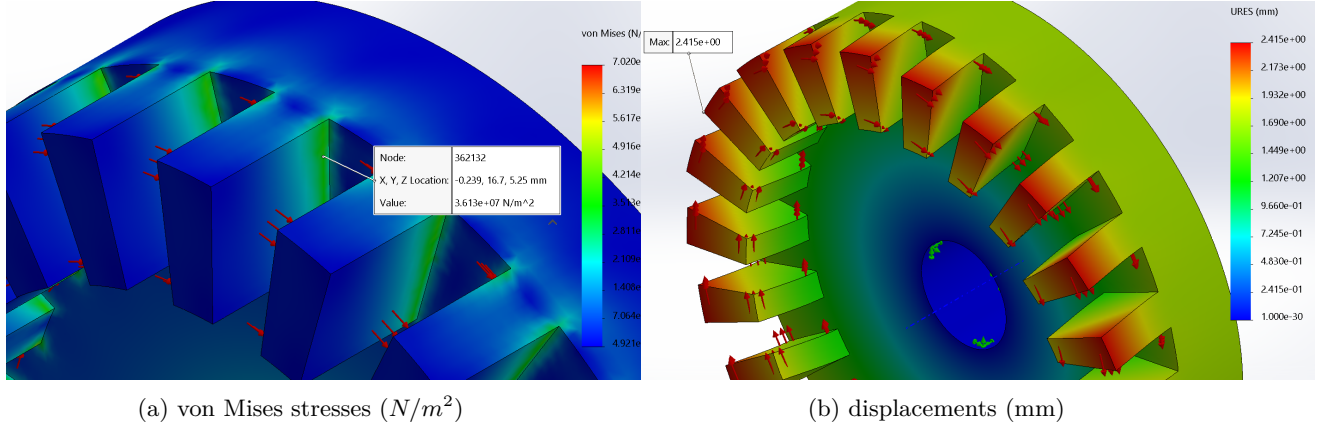


Figure 41: Color maps of the analysis done on the external part of the hinge with the properties of the PP given in the data sheet [76].

Improved geometry In this paragraph, the external and the internal parts of the new geometry are compared and the results are displayed in Table 18.

| | Internal part | External part |
|----------------------------------|---------------|---------------|
| Min von Mises Stress (N/m^2) | 7.705e+3 | 1.305e+4 |
| Max von Mises Stress (N/m^2) | 2.505e+7 | 3.196e+7 |
| Max resultant displacement (mm) | 2.29 | 3.248 |
| Min equivalent strain | 1.939e-5 | 1.213e-5 |
| Max equivalent strain | 3.352e-2 | 4.065e-2 |

Table 18: Comparison of the results obtained using PP (data sheet properties) for the internal and external parts, for the improved geometry.

In this case, the external part will be subjected to higher von Mises stresses, strains and displacements. By changing the geometry of the internal part, its resistance strongly improved but the one of the external part slightly decreased. Indeed, for both pieces to fit together, the size of the teeth of the external part could not be increased as much as the ones of the internal part. Overall, this new geometry is still acceptable as the stresses experienced by both parts are lower than for the initial geometry. Considering the internal part of the hinge in the previous analysis is acceptable as the differences between the results is small.

4.3 Forces applied on the assembly of the two parts

Both pieces of the hinge were designed independently (as parts) and were then uploaded to form an assembly. The pieces chosen are the ones of the new geometry, described in Section 4.2.3.2.1. As can be seen in Figure 42, the pieces are interlocked to create an opening angle equal to 90° . Indeed, the moment M was computed using $\alpha = 90^\circ$ to consider the most critical scenario. The relative position of both parts was adjusted manually and to check that the gap was sufficient, the *clearance verification tool* was used. This tool checks if there is a location where the parts are closer to each other than a threshold specified and gives the distance at that location. An alloy steel cylinder was added to mimic the binding screw that will keep both pieces together.

The condition for the contact between the pieces is taken as "no penetration" to avoid unrealistic overlapping of the teeth. The two pieces of the hinge are simulated in PP using the data sheet properties, as they are probably the closest to the printed parts' real properties. The size of the mesh elements was initially taken as 1.3mm to reduce the simulation time required. However, the size is later reduced (to 1mm) to improve the quality of the simulations' results¹⁴. Note that the time taken by the solver to run the simulations strongly increased compared to the tooth-by-tooth simulations (from less than 10 minutes to a minimum of two hours) due to the solving of the contact constraints between the pieces. It should also be highlighted that, for these simulations, the *Large displacements* option could not be chosen or the solver would systematically fail. The *Small displacements* option is thus chosen even though it is less precise, as explained in Section 4.2.2.2.

In this case, the arm of the external part is fixed and the force is applied on the extremity of the internal part. To apply the moment computed in Section 4.2.3.2, the force applied should be

$$F_x = \frac{M}{x_1} = 245.158N \quad (22)$$

with

- x_1 (m): Lever arm between the rotational point and the point where the force is applied. The lever arm is taken perpendicularly to the direction of the force applied. As the force is chosen perpendicularly to the arm of the articulation, it is not needed to project it in another direction. The length of the arm is 0.04m and the radius of the internal part is 0.023 m so the distance x is equal to 0.063 m for the piece designed for the test. The length of the articulation arm could have been chosen differently and the results would have been similar as the computation of the moment takes into account the lever arm.

The results obtained showed unrealistically big displacements at the extremity of the lever arm. This does not represent how the load will be applied on the hinge so it was decided to apply a pressure distributed uniformly on the lever arm.

$$p_x = \frac{M}{x_2 A} = 1,496,608N/m^2 \quad (23)$$

with

- x_2 (m): Lever arm between the center of rotation and the point of application of the resultant force of the pressure applied. It is equal to the sum of the radius and half of the arm of the hinge. It is thus equal to 0.043 m.
- A (m^2): Area on which the pressure is applied. It is the bottom surface of the arm, equal to $40mm \times 6mm = 2.4e-4 m^2$.

¹⁴Since the simulation time increases with the mesh quality, the first simulations are done with elements of bigger dimensions to have preliminary results to check the feasibility of the parameters chosen (load, fixtures, boundary conditions, etc). One simulation was done with the size of the elements of the mesh equal to 0.5mm but the results were not good, as explained in Appendix 4.

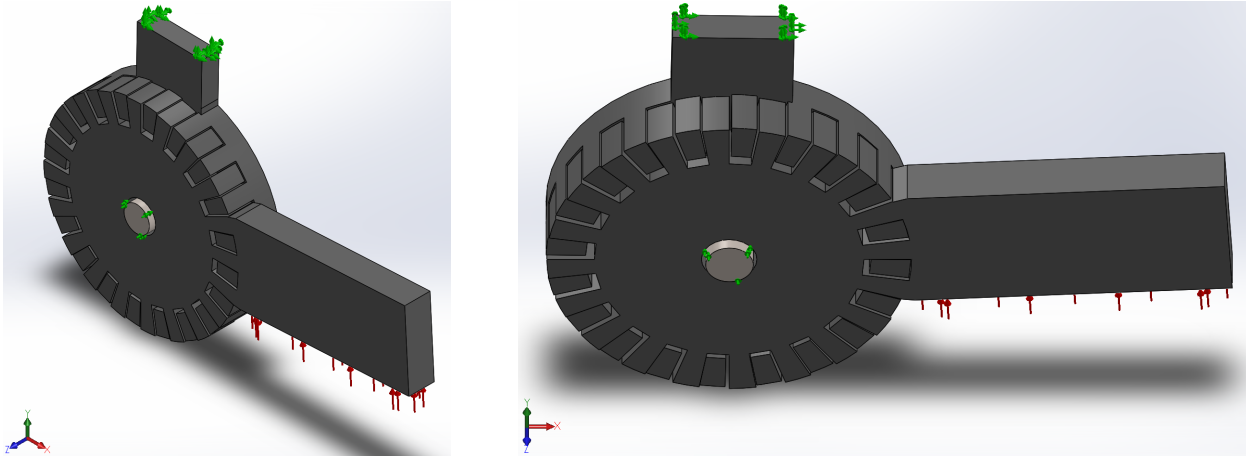


Figure 42: Assembly of the internal and external hinge as well as the cylinder mimicking the binding screw. The pressure is applied on the bottom surface of the internal hinge.

4.3.1 Results

Several trials were made to model the interactions between the parts. The most realistic one is explained in this paragraph while the inconclusive trials are briefly explained in the Appendix 4. For this simulation, a small cylinder (whose diameter is the one of the real binding screw) is added in the holes of the two pieces, and its movements in the axial direction (perpendicular to the flat surface of the hinge) are forbidden. The faces of the internal cylinders of both the external and the internal parts are also forbidden to move in that direction (see Appendix 4 for further explanations of this choice). Indeed, the goal is to mimic the action of the binding screw linking the two parts.

As can be seen in Figure 43, the simulation is not perfect as the stresses form strange patterns. This is probably due to the size of the mesh elements (1mm) that is too large. The quality of the mesh is said to be high by *Solidworks* but the spotted aspect would probably disappear if an extremely fine mesh was used¹⁵. However, even though the simulation gives imperfect results, they are sufficiently good to drive some conclusions. For better visualization, several plots are done by changing the threshold of the stresses displayed (see Figure 44). As can be seen, the highest stresses are experienced near the internal cylinders and in the arm of the external part. These zones are the ones where the fixtures are defined and these high stresses might thus not reflect the reality.

On the other hand, high stresses (around $7e + 7N/m^2$) are noticed on the teeth near the arm of the internal part. The values of these stresses are in the same order of magnitude as the one measured in the tooth-by-tooth analysis (equal to $2.505e + 7N/m^2$). Intuitively, the location of these high stresses is expected as this part of the geometry is in compression when the arm is pushed upward. In the tooth-by-tooth simulations, the pressure was assumed to be equally distributed on all the teeth. This analysis allows us to see that this assumption, even though useful to test materials and other parameters, does not represent the real behavior of the hinge¹⁶.

Simulating the interactions between the parts is interesting to see the regions of the hinge that could be reinforced. Indeed, the base of both arms could be widen¹⁷ and it could be possible to locally

¹⁵Due to the contact interactions the simulations are long and increasing the resolution of the mesh increases the simulation time.

¹⁶The stresses measured for the assembly are higher than the one obtained with the tooth-by-tooth simulations as the pressure is not equally distributed on all the teeth and is thus concentrated in specific areas.

¹⁷The arm of the internal part could include three and not only two teeth. The arm of the external part could be

increase the thickness of the internal hinge near the base of its arm (these ideas are displayed in Figure 45).

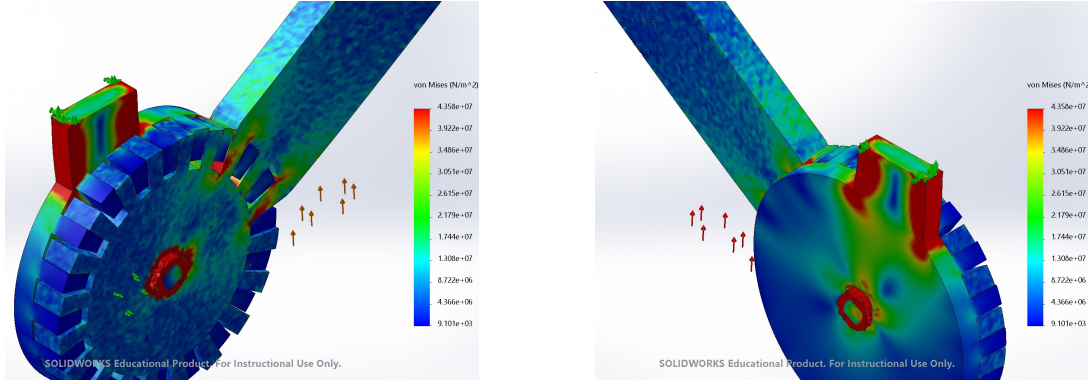


Figure 43: Two views of the simulation done on the assembly.

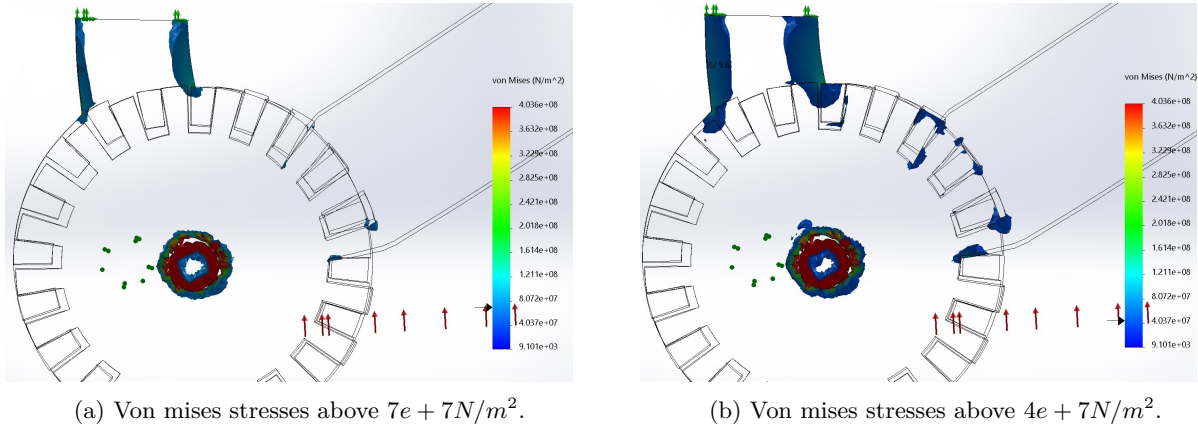


Figure 44: Simulation of the assembly with thresholds on the stresses to only see the most critical points.

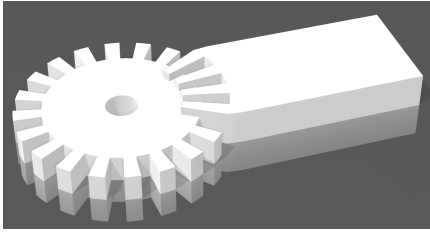
4.3.2 Conclusion

In conclusion, two models of the blocking hinge are offered. The Small one, that allows increments of 16.36° but that is not able to resist high loads, and the Large one, with increments of 18° that supports higher loads¹⁸. Even though the PET showed better simulations results, both materials are resistant enough to be considered and the PP was chosen as explained in Section 3.2. Considering the material to be isotropic and running the simulations on the internal part of the hinge are shown to be acceptable.

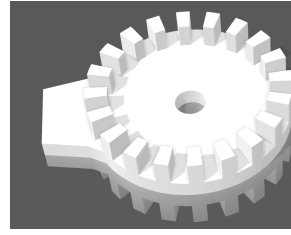
The simulations of the assembly of the two parts show that the pressure is not equally distributed on all the teeth and that the bases of the arms could be reinforced to increase the resistance of the models.

wider and the angle between the arm and the hinge would be smoother.

¹⁸The Large model resists to the moment tested. This moment is computed considering that the force applied by the patient's muscles is equal to the one developed to hold 5kg with the elbow at 90° . This force is probably greater than the maximum force the orthosis will be subjected to.



(a) Internal part



(b) External part

Figure 45: Possible improvements to reinforce the arms of the blocking hinges.

Part III

Final solution specifications

This chapter precisely describes the final designs. Once the requirements are clearly stated, the entire process to create the model desired is explained.

1 Requirements and desired aspect

In the first part of this section, the requirements valid for both designs are given. In the second part, both designs are described separately.

1.1 Overall design

The design should be elegant and discrete. Several design features are common to both designs and should be highlighted:

- The alveoli that will provide aeration for the skin and will allow the orthosis to be lighter. The shape of the alveoli can be chosen by the designer but elongated droplets would be preferred to limit the supports needed while printing.
- Belt loops will be added to attach the Velcro straps. belt loops are bridges designed on the edge of the orthosis and parallel to the opening, as displayed in Figure 46. On the forearm part, there are two Velcros and four belt loops while the upper-arm side only has two belt loops at the external side of the orthosis. Indeed, the alveoli on the internal side are designed closer to the edge and with dimensions corresponding to the velcro so they can be used as belt loops. This is done to avoid friction between the splint and the side of the patient's torso. The belt loops

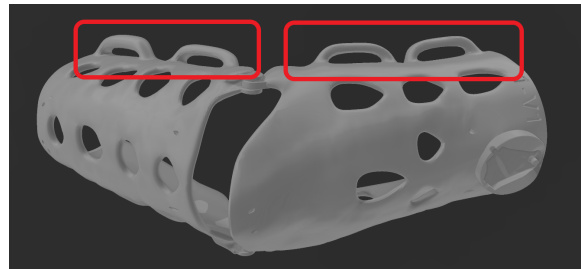


Figure 46: Belt loops on the edges of the splint to attach the Velcro straps around the patient's limb.

should be at least 35mm long for the velcro to fit in, 5mm high and 8mm wide to be resistant.

- Two thirds of the forearm and two thirds of the upper arm should be covered to maximize the surface that will support the load while keeping the sensitive areas free (styloid, wrist articulation, elbow crease and armpit). It is also important for the splint to be small enough to be printed in the desired printer.
- For both designs, it is needed to identify and position the axis of rotation to center the hinges. The OT will place extrusions on the bony bumps at the end of the humerus called the epicondyles. The rotation points should be a little bit lower (+/- 1cm towards the hand) than the epicondyles. The designer can then draw a cylinder passing through those rotation points to mimic the rotation axis to have a reference to place the hinges.

This definition of the rotation axis is not as precise as the one found in the literature for elbow surgery. Graham et al. [41] defined a protocol to find the precise rotation points but orthopedists never use it as such a high level of precision is not required. Indeed, Brinckmann et al. [83] showed that an error in the order of 1cm can be considered negligible while placing the hinge of the elbow's splints.

- The two parts of the splint should be printed vertically, with the hinges upwards. They can be printed in the same printer or in two printers so the impression time is reduced ¹⁹.

The requirements to be taken into account by the designer are described in Table 19 and are valid for both designs. The rest of the requirements depends on the model chosen.

¹⁹The prototypes for the patients (see Section IV) took 30 and 37 hours to be printed. Each prototype was printed using only one printer. By printing the upper arm part and the forearm part simultaneously in two different printers, the printing time is reduced to 17 and 20 hours.

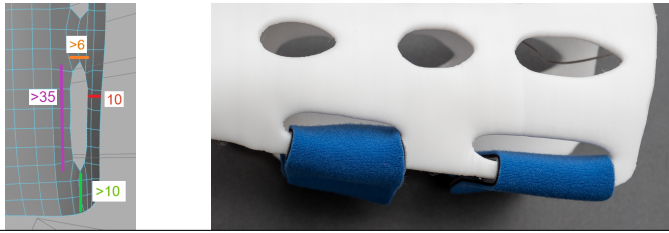
| | |
|----------------------------|---|
| Size on the forearm | 2/3 of the forearm (elbow crease and wrist articulation remain free) |
| Size on the upper arm | 2/3 of the upper arm (elbow crease remains free and no friction near the armpit) |
| Overall thickness | 5mm |
| Offset for padding | Only if asked by the client. Uniform or could be added during the scan to have an offset only in the exact areas wanted by the OT |
| Opening location forearm | The radius is free, as the arm is in a natural position along the body, as seen in picture 47 and 49. 50 to 60% coverage |
| Opening location upper arm | The triceps is covered while the biceps is free. 50 to 60% coverage |
| Elbow protection | The upper part should get wider towards the elbow so that there is no discomfort as the elbow is flexed or extended. It should be wide enough for the lateral and medial epicondyle (bony bumps at the bottom of the humerus) to not touch the splint |
| Closure system | 4 Velcro straps to close the brace |
| Fasteners | Forearm: 2x2 belt loops Upper arm: 2 belt loops on the internal edge of the splint but no belt loops on the external edge |
| Belt loops size | Minimum 35mm wide, 8mm depth and 5mm height |
| Alveoli shape | Elongated droplets, following the shape of the lateral branches in parallel. Two bigger (dimensions shown on the picture) alveoli should be designed along the internal edge of the upper part to pass the velcro.  |
| Branch thickness | 10mm minimum inside the brace 15mm minimum for the lateral branches |
| Articulation points | A little bit lower (+/- 1cm) than the epicondyles highlighted by the OT with extrusions |
| Hinge placement | Axis of rotation is highlighted by drawing a cylinder passing through the articulation points |

Table 19: Main design requirements that are applicable to both designs.

1.2 Presentation of the different designs

As stated, two designs will be implemented. One using a BOA and the other one using a blocking hinge.

1.2.1 BOA design

Free hinges keep the two parts of the splint together and allow both extension and flexion of the arm. Each hinge (internal and external) is made of two parts, one embedded in each part of the splint (upper arm and forearm) as displayed in Figure 48b. The two parts of the hinge should be maintained together using a binding screw with a length of 10mm and 5mm of diameter. To calibrate the range of motion allowed, a BOA is used. The BOA is a system that allows a cable to be either tighten or loosen (by turning the wheel in one direction or the other). The BOA is placed on the upper-arm part, near the shoulder.

The cables go through tubes embedded in the splint so that they can guide the movement of the

splint, without being in contact with the skin or being caught. As the cable length is reduced, the brace is forced to open and the arm to extend.



(a) The splint is fixed in a position close to 90° . This means that the cable of the BOA is relaxed.



(b) The splint is fixed in an open position, close to 180° . The BOA was turned to shorten the cable and extend the arm.



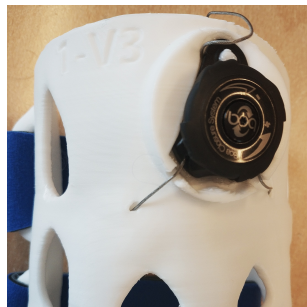
Figure 47: Final prototype of the BOA model.

The exact angle at which the orthosis is blocked is not precisely known. Each patient is very different and each of them will be treated very differently. There is thus not a universal protocol with the order and the duration of each elongation period. It is thus not a problem to choose the angle in an organic way. This orthosis thus prevents the flexion of the arm (the minimum angle allowed is fixed by the BOA) but the extension is always allowed up to 180° .

The BOA uses a nylon-coated steel lace to provide high strength while maintaining low friction. Several BOA models can be chosen and, as explained in Section 3, the model chosen is one of the S-series. The BOA is glued with an epoxy glue [67] to the splint in a counterpart especially designed to fit the model chosen (displayed in Figure 48a). This counterpart is an OBJ file that can be imported and merged into the splint.



(a) To the right, counterpart created to fix the BOA. The counterpart is oval (46x41mm). To the left, BOA dial glued in its counterpart.



(b) Free hinge. One part is embedded in the upper part of the splint and the other one is embedded in the forearm part. They are secured by a binding screw.

To avoid contact between the cables and the elbow, the upper-part is enlarged and extruded towards the elbow as can be seen in Figure 47. Table 20 sums up the additional requirements for the BOA design.




| | |
|----------------------|--|
| Elbow protection | <p>It should be long enough for the cables to never touch the skin. Approximately 40 to 55mm between the articulation and the point where the cables leave the orthosis</p>  |
| BOA model | S-series, turn to adjust |
| BOA counter piece | The OBJ file can be downloaded and integrated in the splint. Centered, near the shoulder (proximal side) on the upper-part |
| Tubes for BOA cables | <p>Embedded in the splint so the cables are as covered as possible. Cylinders of diameter 2.5mm Angles formed by the cables going out of the BOA and in the tubes should not be too sharp</p>   |
| Free hinges | On both the internal and the external parts. The OBJ file can be downloaded and the hinge can be integrated to the splint |

Table 20: Main design requirements for the BOA design.

1.2.2 Blocking hinge design

The overall design is similar to the BOA design but the extrusion at the elbow, the counterpart, and the tubes are not needed. This design is displayed in Figure 49 The free hinges are replaced by one free and one blocking hinge. The blocking hinge is similar to cogwheels and as the orthosis, it is made of PP. The two parts of the blocking hinge are printed separately from the splint and are clipped in it during post-processing.

The free hinge used for this model is the same as the ones used in the BOA design. The splint is thus printed in two parts with a free hinge to be secured with a binding screw. An OBJ file has been made to easily import and embed it in the splint.

This design allows only the orthopedist to modify the opening angle ²⁰, which might be good for troubling patients. On the other hand, it might be restrictive for the more independent patients that could be involved in their treatment and that would want to change it by themselves. Only one angle is allowed and not a range of motion as in the BOA design and only a few angles are possible. Blocking movements in both directions would also be an advantage for patients suffering from hypertonia in extension (due to a spinal cord injury for example).

The size of the hinge and the amplitude of the increments had to be chosen according to tests and simulations. First, the parameters are tested with printing trials. The different parameters tested are listed in Table 21.

²⁰The binding screw is secured with a screwdriver. It is thus not impossible for the patient to change the opening angle but it is less intuitive than with the BOA model.



(a) The blocking hinge is fixed in a position close to 90°.



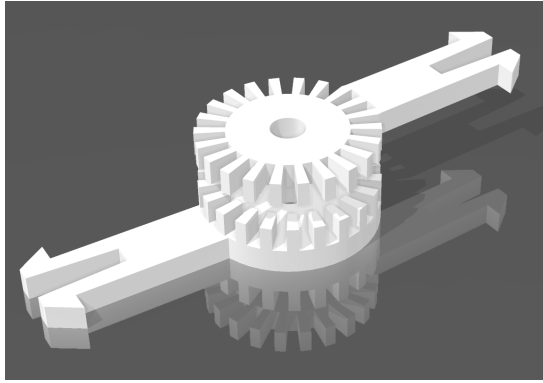
(b) The blocking hinge is fixed in an open position, close to 180°.

Figure 49: Final prototype of the blocking hinge model (small).

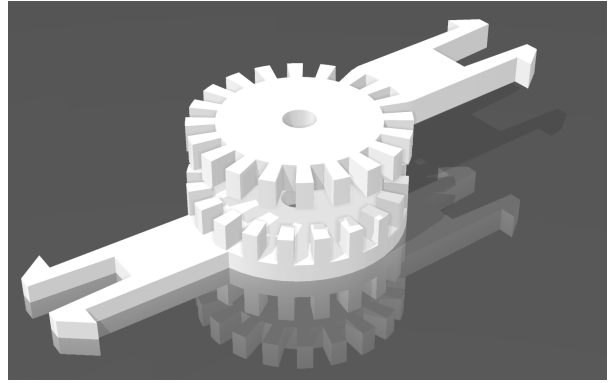
| Increments' amplitude | Number of teeth | Diameter of the hinge | Opinion |
|-----------------------|-----------------|-----------------------|---------------------------------|
| 30° | 12 | 40mm | Too big increments and diameter |
| 20° | 18 | 40mm | Too big diameter |
| 30° | 12 | 30mm | Too big increments |
| 20° | 18 | 30mm | Good but could be more optimal |
| 16, 4° | 22 | 40mm | Good but could smaller |
| 16, 4° | 22 | 36mm | Validated |

Table 21: Blocking hinge parameters that were tested with printing trials.

A compromise has to be made to have an elegant design (small articulation) and a wide range of possible positions while maintaining a good printing quality and having a strong hinge that will not break under pressure. As can be seen in Table 21, the chosen design has 16, 4° of increments and 36mm of diameter and is displayed in Figure 50a. However, as the simulations done in *Solidworks*(see Section 4.2) showed, this hinge could be too weak if the patient applies an important force. A more resistant hinge is thus proposed. However, the new hinge is bigger (46mm of diameter) and less positions are available (18° of increments). The two models can be kept so the OT can chose, depending on the patient, to focus on the resistance or the number of positions wanted. The technical drawings of both models are available in the Appendix 1.



(a) Small model with 16, 4° of increments and a 36mm diameter.



(b) Large model with 18° of increments and a 46mm diameter.

Figure 50: Final designs of the blocking hinge.

| | |
|---------------------|--|
| Blocking hinge | The OBJ files can be downloaded and both parts should be printed horizontally, laying down |
| Holes in the splint | The OBJ files of the hinge-counterpart can be imported to be placed and subtracted for both parts of the splint |
| Free hinge | The OBJ file can be downloaded and the free hinges can be integrated to the internal part of the splint |
| Overall shape | No need of an extrusion. Both parts of the splint should get wider towards the elbow to not touch the bones. No tubes or counterpart embedded in the splint. |

Table 22: Main design requirements for the blocking hinge design.

2 Workflow from the patient consultation to the final orthosis

Each step of the production, from the OT office to the final orthosis, is developed in this section. It is important to provide the OT a list of the information he/she should mention to have the wanted design but also a list of the criteria he/she should pay attention to as he does the scan. The design requirements are also cited to ensure that the designer respects the model proposed. Finally, the important points for the production step are detailed.

2.1 In the OT office

First, the requirements that need to be taken into account by the OT as he/she meets the patient are listed then the workflow is described, step by step.

Steps to follow to take the order:

1. The patient arrives with his/her prescription.
2. The OT decides if the positioning orthosis corresponds to the patient's needs and choose between the two designs proposed. For the blocking hinge design, the model (small or large) should be chosen depending on the patient.
3. The patient is comfortably installed on a chair.
4. If the OT desires padding, he/she can stick it to the patient's limb where it is needed.

| | |
|----------------------|---|
| Padding | Padding should be added on the sensitive areas during the scan (both in the case where the OT will want to place padding on those areas or to be sure the splint will not touch the skin on those areas). This is not necessary if a uniform padding over the entire brace is wanted but it should be mentioned. |
| Epicondyles location | The lateral and medial epicondyles should be highlighted by the OT by sticking small extrusions or putting a thick creme on the skin (or the padding if it covers that area). |
| Arm position | The arm should be placed in front of the body for all sides to be properly seen by the scanner. An external help can hold the hand of the patient to guide him into the correct position. The position should be the one in which the orthosis will be most of the time (more or less extended arm depending on the patient). The forearm should be in a neutral position (between pro and supination). |
| Choice of design | Depending on the patient's needs, the OT should choose between the BOA and the blocking hinge design |

Table 23: Summary of the main information to think about as the OT scans the patient.

- Two anatomical points have first to be found and extrusions are stuck on the skin to show them in the scan: the lateral and medial epicondyles. These points are the salient part of the humerus and depending on the patient. Depending on the patient body type and weight, they can be more or less easy to find. The extrusions can either be voluminous stickers or a thick creme, as long as the thickness is sufficient to be seen on the scan.
- The patient is prepared for the scan with his bare elbow in the appropriate position (the position in which the orthosis should be most of the time) and is kept in that position by the OT or an assistant that holds his hand, and eventually holds the arm with two fingers.

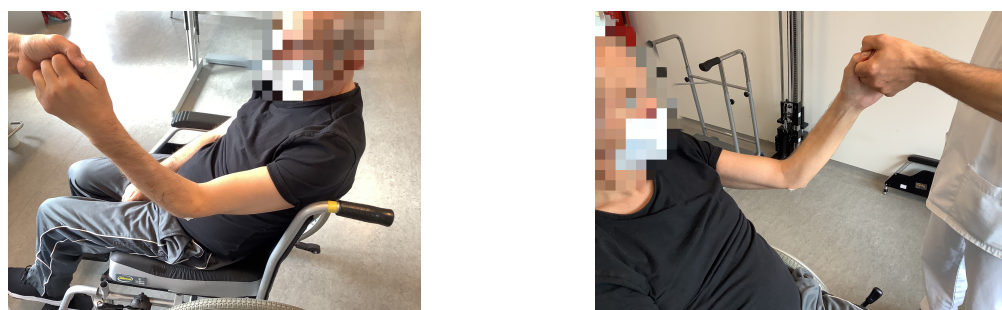


Figure 51: The patient is sited comfortably, his arm is bare and in front of him. The epicondyles are shown by applying a thick creme.

- The OT/helper scans the patient's limb (in the right position and with the extrusions). The size of the scanning area can be chosen by clicking on the rectangle and changing the parameters. Once it is chosen, the scan is started and a red/orange/green circle indicates if the distance is right.



Figure 52: The patient is sited comfortably, the OT or the helper holds the hand of the patient so that the limb is in the correct position will the other person scan the limb by turning around it at an adequate distance

8. The OT/helper turns around the patient's limb to capture it from all sides in order for the scan to be complete.
9. The OT sends all the information about the patient via the Spentys Application (iOS or Web) as well as the choice of design and special requirements (sensitive parts, maximum length...).

2.2 At Spentys, by the designer

The workflow followed by the designer at Spentys is described in this paragraph. The entire workflow describing all the interactions between the software is displayed in Figure 53. However, the workflow

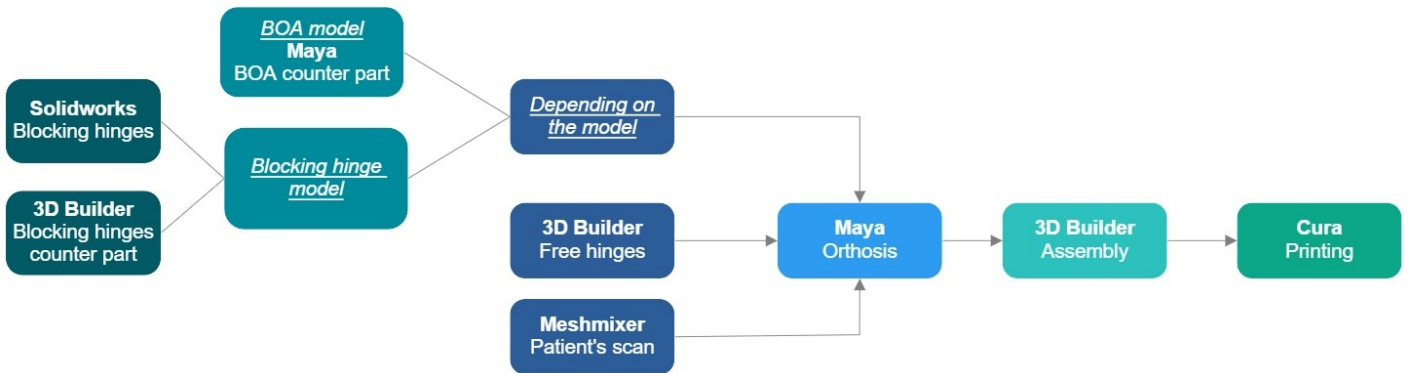


Figure 53: Interactions between the software used during the modeling. Several parts have previously been designed/modified in *Solidworks*, *Maya*, *3D Builder* and *Meshmixer* (respectively the blocking hinges, the BOA counter part, the free hinges and the blocking counter part and the patient's scan) and are then imported and positioned in *Maya* to create the whole orthosis. *3D builder* is then used to subtract some parts (tubes or hinges counter parts) and merge others (free hinges and BOA counter part). The model is then printed using *Cura*.

described in this paragraph does not consider the creation of the parts that are designed only once. As the OT could have chosen either the BOA or the blocking hinge design, both are developed in parallel. Most steps are the same and for the ones that differs, the two possibilities are listed, a) for the BOA model and b) for the blocking hinge model. The workflow to follow at each order is :

1. Spentys receives the new order and validates the scan quality

2. The designer corrects the scan on *Meshmixer*: remove holes, artifacts and unwanted anatomical parts and smooths (with the *RobustSmooth* tool) the scan as displayed in Figure 54.

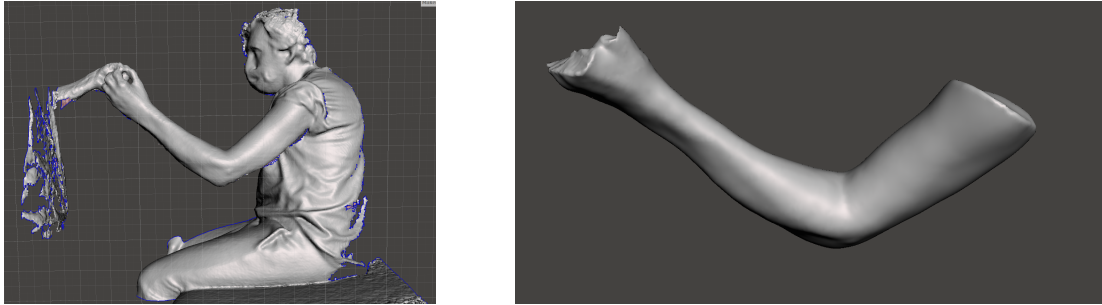


Figure 54: Comparison of the raw scan uploaded on the platform (left) and the clean scan (right). The clean scan is smooth and all the anatomical parts that are not necessary for the orthosis are removed. Note that the raw scan usually includes the arm, the hand of the OT and the chest or chin of the patient but this one was particularly large.

3. The designer imports the scan in *Maya* and draws a small cylinder of 5mm of diameter that goes through both points highlighted by the OT (polygon cylinder, radius 3mm, height 150mm). The cylinder is then translated parallel to the original orientation and towards the forearm/hand to be a lower (1cm approximately) lower.
4. The designer carefully corrects the position of the forearm if needed. This could be needed if the patient was not able to elongate his arm at all or that the pronation/supination of the forearm is not the one desired by the OT.
5. Using the "Quad Draw" tool, the shape of the orthosis is drawn on both parts of the limb, using the "make live" tool that make the polygons stick to the arm. The vertexes of the polygons are drawn (LMB) and polygons are created (shift+LMB). The big polygons are then divided (Ctrl+LMB) and relaxed (shift+LMB) as displayed in Figure 55. The splints should take 2/3 of the forearm and of the upper arm.

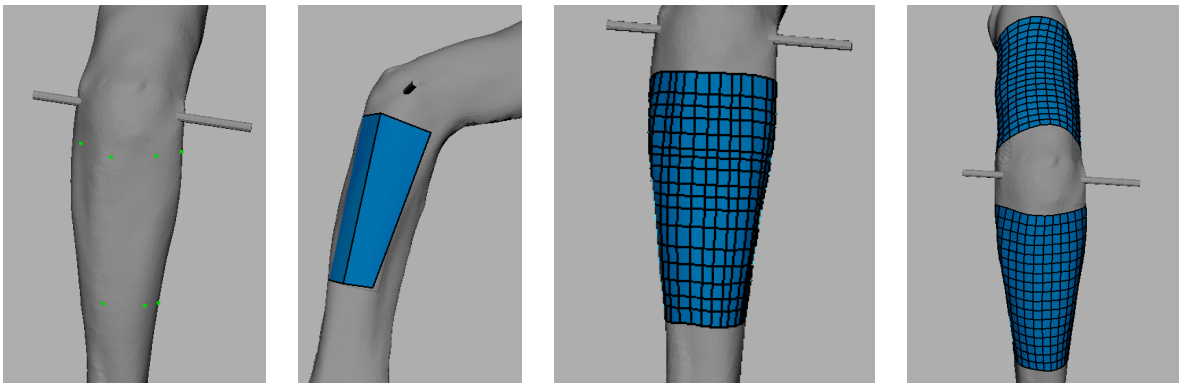


Figure 55: From left to right: 1) The vertexes are placed to define the shape of the splint on the limb 2) The polygons are drawn 3) The polygons are subdivided 4) The polygons are relaxed

6. a) The counter part is imported and placed (near the shoulder in the middle of the splint) as in Figure 56.1.
b) This step is not done for the blocking hinge design.

7. Four polygon cubes are created, and their dimensions are changed to 35x35x150mm. They are placed at the position of the straps and added to a layer, modified to be displayed in wire frame (see Figure 56.2).
8. The polysurface is copied and some faces of this new polysurface are deleted to create the alveoli. Their shape are then modified depending on the designer or the OT choice but the following procedure is advised. For the upper part:
 - (a) Faces are deleted to create two alveoli on the side of the upper part that will be against the patient's torso (see Figure 56.3). Those alveoli are rectangular and placed where the boxes show the straps position. The dimensions that should be respected are displayed in Figure 56.4.

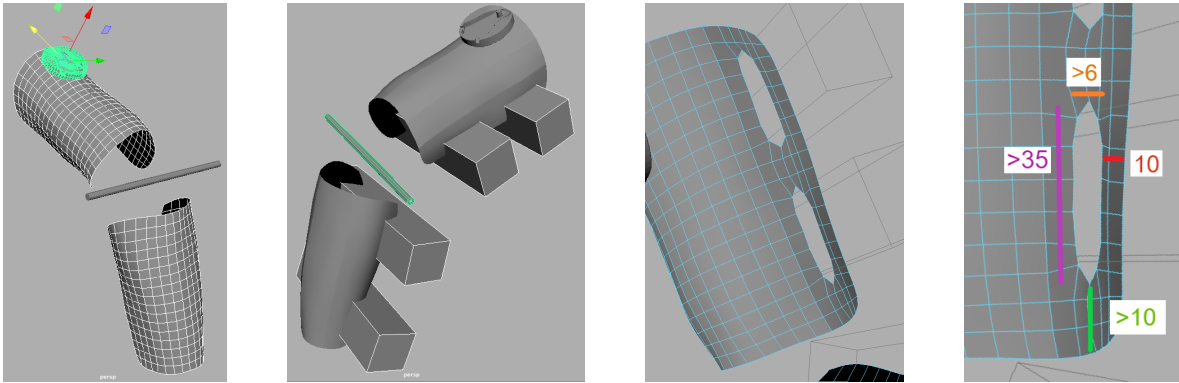


Figure 56: From left to right: 1) The counterpart for the BOA is imported and is placed near the shoulder, centered on the splint 2) Boxes are created to give the position of the straps 3) On the upper part, the two alveoli that will be used as belt loops are created on the side near the patient's torso 4) Dimensions that should be respected for the alveoli near the torso.

- (b) a) Three alveoli are created as displayed in Figure 57.1 just below the BOA counterpart. Their shape should be optimized for the printing (droplets with the pointed side towards the elbow).
 - b) Two columns of three alveoli are added on the upper part of the splint.
 - (c) On the side near the torso, three alveoli are created (elongated droplets). On the opposite side, three larger but still elongated alveoli are made by letting enough space for the belt loops (see Figure 57.2 and 57.3)
- For the forearm part, three columns of 4 droplet alveoli are created, as displayed in Figure 57.4. Care must be taken to leave enough space for the belt loops and for the canals that will pass between the columns.
9. The drawing is then detached from the scan and slightly pulled away from the skin to create a gap to avoid too tight splints (see Figure 58.1). The faces are then extruded by 5mm in the local translate Z (0mm of thickness and of offset, 1 division), as can be seen in Figure 58.2.
 10. a) The extrusion is created by extruding the faces in front of the elbow (approximately 40mm), as displayed in Figure 58.3. The edges are then moved to have a smoother transition and the faces are pulled away to guarantee that the elbow will not touch it (see Figure 58.4).
 - b) This step should not be done for the blocking hinge design.

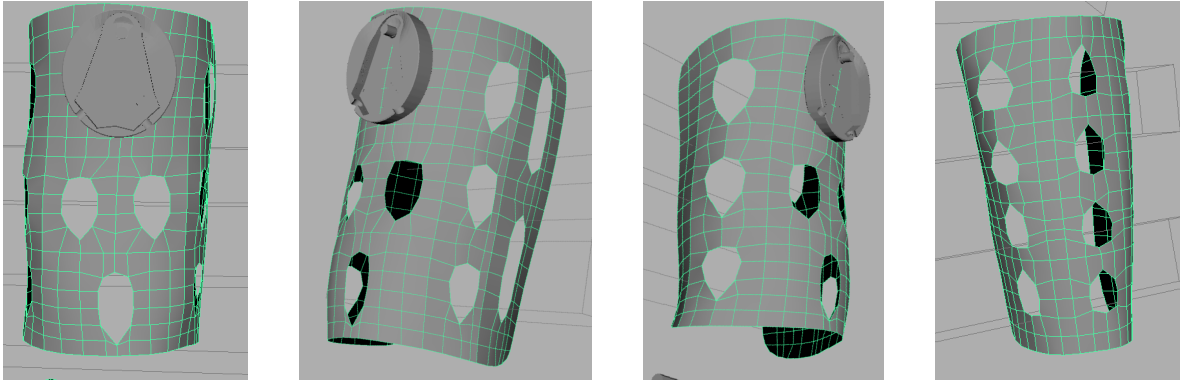


Figure 57: From left to right:1)Three droplet alveoli are designed under the counterpart 2) Three alveoli are drawn on the side near the torso, next to the alveoli acting as belt loops 3) Three alveoli are drawn on the opposite side 4) Three columns of four alveoli are designed on the forearm part. 4) The splint is extruded (5mm) and boxes are drawn to indicate the straps position 4) Belt loops are created

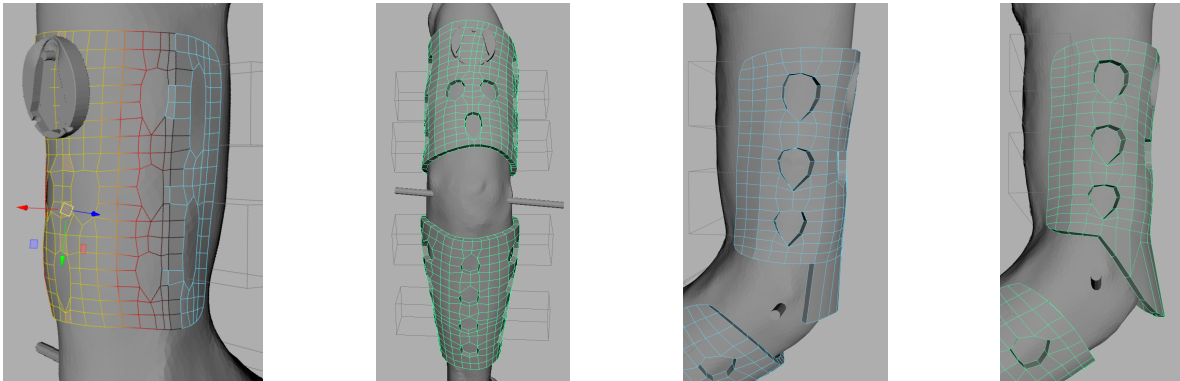


Figure 58: From left to right:1) The Polysurface is pulled to be detached from the skin, depending on the gap wanted, an offset could be added at this step 2) The splint is extruded (5mm in the local translate Z) 3) The extrusion is created by extruding the faces in front of the elbow 4) Smooth transition to the extrusion and gap to not touch the elbow

11. Belt loops are created. The faces defining the belt loops feet are extruded (8mm in local translate Z, with 2 divisions and no offset). The upper internal face of each feet is joined to the one in front using the *bridge* tool (with 0 division) as displayed in Figure 59.1). The three edges forming the corner are then selected and the *edit edge flow* tool is applied three times. The edges of the belt loops can be moved to ensure the good measures (minimum 35mm wide, 8mm depth and 5mm height), as seen in Figure 59.2.
12. a) The counterpart is positioned to be out of the splint and the edges of the splints are moved for the counterpart to be embedded. It is not needed to sew the vertexes of the two parts, but the counterpart should be smoothly included in the orthosis to be well printed (see Figure 59.3).
b) This step should not be done for the blocking hinge design.
13. a) Four free hinges are imported. The hinges of the upper arm are external, and the ones of the forearm are internal. Attention must be paid to not touch the elbow (a gap is advised to ensure no injury). This is displayed in Figure 59.4. b) Two free hinges are imported to be placed on the

side closest to the torso.

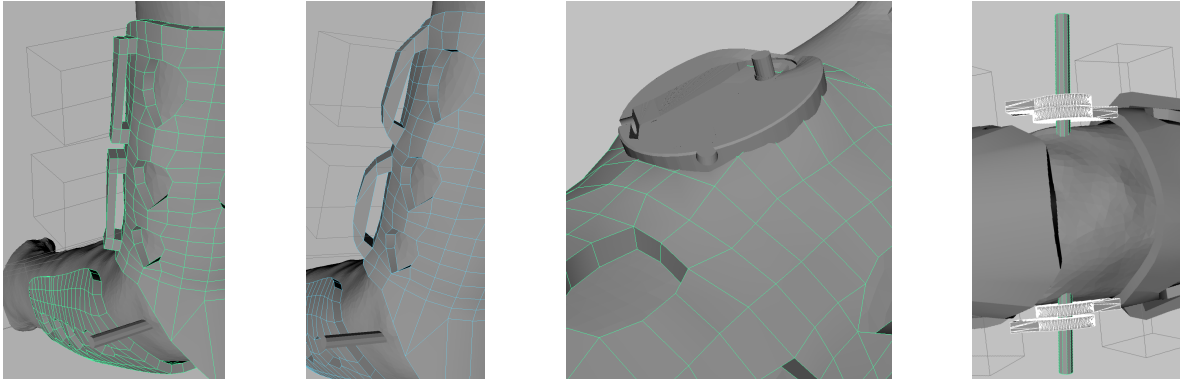


Figure 59: From left to right 1) Beltloops are created 2) Beltloops are adapted to be smoother 3) The counterpart is positioned to be embedded in the splint 4) Four free hinges are imported and centered on the cylinder with their arm facing the part of the splint where they should be embedded.

14. The faces near the hinges are extruded (8 to 10mm depending on the design) and moved to fully embrace the arm of the hinge as displayed in Figure 60.1.
15. The two splint are smoothed (with 2 divisions), as can be seen in Figure 60.2. Pay attention to only smooth the orthosis and not the hinges and counterpart. The free hinges must be checked to see if they are still correctly embedded in the splint. Indeed, the splint moves when it is smoothed. If they are not included properly, go back to the non-smooth step and move the vertexes.
16. a) To create the tunnels, first define the splint as a *live surface*, then draw a curve using the *EP curve* tool in the shape of the tunnel wanted (shown in Figure 60.3). Then draw a circle of radius 1.25mm anywhere. Select first the circle than the curve and extrude the surface (fixed path on, component pivot) as can be seen in in Figure 60.4.
- b) The counterparts of the blocking hinges are imported and placed to the side the farthest from the body. The faces of the splint should be moved for this counterpart to be fully embedded.

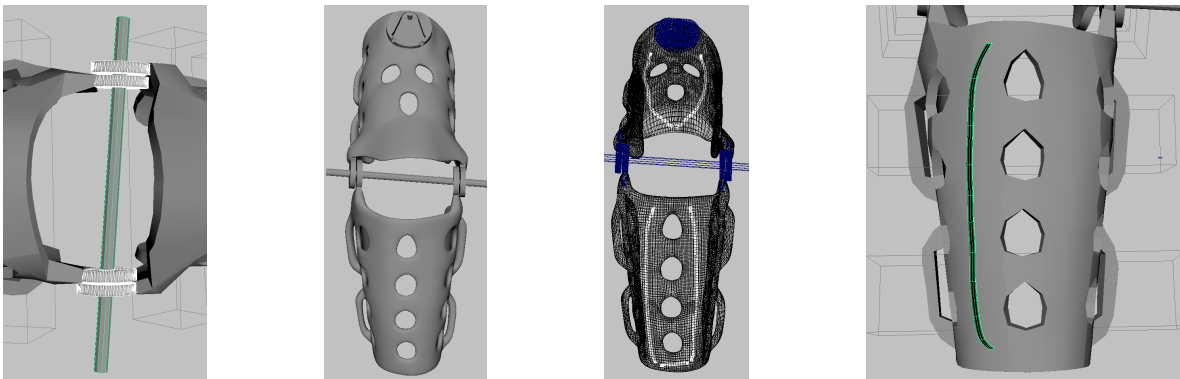


Figure 60: From left to right 1) Embedded free hinges 2) The splints are smoothed 3) Location of the tubes to be embedded 4) A curve is drawn and extruded

17. a) The extruded surface created should be converted using the *NURBS to polygons* tool. The ends of the tunnels are pulled away from the splint to create an entrance for the cables (see Figure 61.1). The entire tube is then moved to be embedded in the splint (see Figure 61.2).
b) This step should not be done for the blocking hinge design.
18. a) To be sure the cables cannot go out of the splint, the thickness is locally increased where the tubes are by pulling on the faces of the splint (see Figure 61.3).
b) This step should not be done for the blocking hinge design.
19. The mesh of the splint is separated to have the mesh of the upper arm and the one of the forearm separately.
20. Select the mesh of the forearm part and its two hinges and export this selection as an obj file. The same should be done for the upper part, its hinges and the counterpart. All tubes should also be exported into one obj file for the BOA design.
21. a) The forearm part and the tubes are imported in *3D Builder*, the tubes are subtracted and the splint is embossed with the name of the product if desired, as shown in Figure 61.4. The same is done for the upper part.
b) Both parts and the counterpart of the blocking hinges are imported in *3D Builder*, the counterparts are subtracted and the splint is embossed with the name of the product if desired.

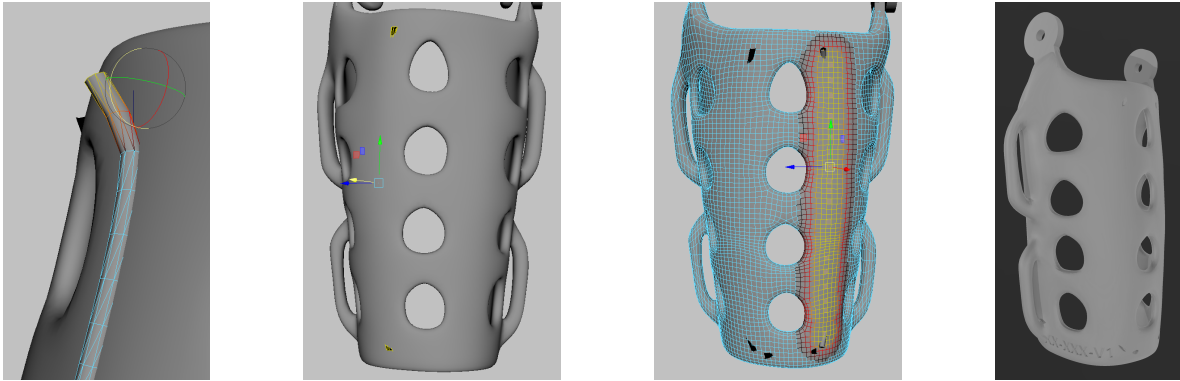


Figure 61: From left to right 1) Pull the extremities of the tube out of the splint 2) Embed the tubes in the orthosis 3) Pull out the faces where the tubes are 4) Emboss the name of the model and subtract the tubes

2.3 At Spentys, by the production operator

Both files are then imported in *Cura* to be sliced and printed. The splints are placed vertically, with the free hinges towards the top of the printer.

a) For the BOA design, the supports are added manually to avoid having any of them blocking the tunnels. Once both parts are printed, the splints are post-processed, using a scalpel to remove the supports. Binding screws are placed to attach both parts of the splint. The cable is pushed into the tubes and the length of the cables is adjusted depending on the range of motion desired. The BOA is glued in the counterpart using a bi-component epoxy glue [67] and the velcro straps are added.

b) For the blocking hinge design, once both parts are printed, the splints are post-processed with a scalpel to remove the supports. Both parts can then be polished in Rosler. The blocking hinges printed separately can be clipped into each part of the splint. Binding screws are placed to attach both parts of the splint and velcro straps are added.

The main information are displayed in Table 24 and the printing parameters used are displayed in the appendix, in Table 5.



Figure 62: Left: Binding screw keeping the two parts of the orthosis together. Center: BOA glued into the counterpart. Right: Velcro straps are added

| | |
|------------------------------------|--|
| FOR BOTH DESIGNS | |
| Printer | Ultimaker 3 |
| Material | Transparent PP (or Fortis) |
| Printing of the splint | Printed in two pieces, vertically with the free hinges upwards |
| Padding | Should be added by the OT |
| Temperature of the head | 210 °C |
| FOR THE BOA DESIGN | |
| Supports | Supports should be added manually to avoid having supports in the tubes (important to check that the tubes are free) |
| Post-printing | Do not put the splint in the Rosler, use the scalpel for a smooth finish |
| FOR THE BLOCKING HINGE | |
| Position for the printing (hinges) | Horizontal, laid down on the printer bed |
| Supports | Automatic supports (Check that there is none in the clip hole) |
| Post-printing | The splint can be post-printed in the Rosler |

Table 24: Summary of the main information to think about at the production step.

2.4 Restitution to the patient

The orthosis is given to the patient with the following recommendations:

1. The orthosis should be worn everyday. Ideally several times a day for short periods but the duration of those periods should be defined by the care provider.
2. The splint should be worn during rest or non-physical activities such as watching TV or reading.
3. The brace should be put on in the closest position (maximal flexion) and then gently and slowly extended by turning the BOA.

4. The opening angle should be decided with the OT. If he desires, the OT can give a range of angle to let the patient decide, depending on his current perception and pain.

Part IV

Feedback from patients

The BOA design was tested by two patients suffering from elbow spasticity due to a stroke. Since only two patients were available for the trial, only the BOA model is tested (since it is the most promising). It would be interesting to test the blocking hinge design on patients. Both patients gave their consent to try the orthosis and to share the relevant information about their health.

1 Details of the trials

The information of the two patients is given in Table 25. It should be highlighted that both patients are hemiplegic (left side), that their MAS correspond to the ones targeted²¹ and both patients received Botulinum toxin injections. After discussion with the occupational therapist, both were advised to wear the orthosis each day, once in the morning and once in the afternoon, for one hour, during rest periods. This trial period lasted 8 days (from the 27th of May to the 3rd of June 2021 included).

Note that the Balcofen (sold under the brand name Lioresal [84]) taken by Patient 2 is a muscle relaxant and anti-spastic that is commonly used in the management of spasticity. Neither of them will probably gain back the control of their arm but care must be taken to avoid deterioration of their state. Indeed the range of motion and the flexibility of their elbow should be maintained and could even be improved.

The splints of each patient was made according to the scans done and including a small offset for comfort. The splint can be worn over clothes or on the skin but the offset should be adjusted depending on the patient's preferences.

2 Results of the trials

This trial is important to have a feedback on the comfort of the splint. The trial period and the number of participants are not sufficient to obtain significant results but it can already be interesting to have these feedback.

2.1 First short trial

Both patients first tried their orthosis for 15 minutes to see if it fitted and if the splint was comfortable enough to consider a longer trial period. Patients wearing the splints are shown in Figure 63.

The patients tried the orthoses over their clothes since they were thin. Putting the orthoses on and adjusting the BOA was easy. Both patients said that the splint was comfortable and that there was no painful region. They also stated that keeping the arm elongated was not painful.

2.2 Longer trial period

As the trial is only done on a small period, its goal is mainly to assess the comfort of the orthoses rather than analyze its long-term effects. However, the physical therapists treating the patients were interviewed after the trial to give their opinion on the device and its possible effects.

²¹The MAS is not the same with or without Botulinum toxin injections but in both cases, the MAS was in the [1+ ; 3] range.

| | Patient 1 | Patient 2 |
|---|---|--|
| Sex | Male | Male |
| Date of birth | 13/10/1964 | 09/08/1962 |
| Age | 56 | 58 |
| Date of the stroke | 2/01/2021 | 17/05/2020 |
| Time since the stroke | 5 months | 12 months |
| Diagnosis | Hemiplegic (Left) | Hemiplegic (Left) |
| Modified Ashworth scale without injections | 2 or 3 | 2 or 3 |
| with injections | 1+ | 1+ |
| Active movement of the arm | Impossible | Impossible |
| Passive movement of the arm | Possible if very slow | Possible if slow |
| Pain as the arm is elongated | None | None if slow movement |
| Current medications | None linked to spasticity | Lioresal 25mg 3x/day [84] |
| Injections details | Botulinum toxin 300 units to the elbow's and fingers' flexors | Botulinum toxin 300 units to the elbow's and fingers' flexors |
| Date of the last injections | 7 May 2021 | 10 March 2021 |
| Current treatment | Physiotherapy, ergotherapy, neuropsychology, psychological counselling, speech and language therapy | Physiotherapy, ergotherapy, neuropsychology, psychological counselling |
| Evolution since the stroke | Walks better but no changes for the arm | No significant improvements |
| External help to wear the orthosis | The patient is hospitalized at the center (his physiotherapist will help him) | Regular appointments at the center but the patient will wear the splint at home (his wife will help him) |

Table 25: Information of the patients that tested the orthoses.

2.2.1 Patient 1

Due to his stroke, Patient 1 is suffering from diastasis (separation of parts of the body that are normally joined together [87]) of the shoulder. This means that, due to the lack of muscular tone, the humeral head is at risk of detaching itself from the shoulder if the load is not reduced by supporting the arm²². This information was not known at the time of the scanning or he would not have been selected for the trial. This might not be an issue if the orthosis is worn only for short periods but as the patient has already experienced pain due to this issue in the past months, it was decided to stop the trial. Note that none of the orthoses available on the market (presented in Part Section) would suit the patient.

2.2.2 Patient 2

Patient 2, on the other hand, was able to wear the orthosis and to give feedback on the eight-days trial. He was not able to wear it every day but only one day out of two since no one was available to help him put the orthosis on. His wife, who helped him, found the BOA dial easy to adjust. Even though

²²The patient has to keep his arm elevated for the shoulder to not bear the entire load. Usually, the patient rests his flexed arm on a foam placed on the plate fixed to his wheelchair. During the two first meetings with the patient, he did not have the equipment used to maintain his arm elevated as he was going to his physical therapy session.



(a) Patient 1



(b) Patient 2

Figure 63: Patients wearing their custom splints.



Figure 64: Patient 1 wearing his splint. On the left, the initial position in which the splint is put on. The BOA is then turned to force the extension and, on the right, the arm is in extension.

he was advised to wear it for one hour at a time, he decided to keep it for two hours each time as he felt comfortable in it. The patient found the orthosis comfortable (both on bare skin and on clothes) and did not have any complaints. However, the skin was slightly red (see Figure 65a) and marked (see Figure 65b) on the location of the straps and of the alveoli. Even when asked about these precise red/marked areas, the patient maintained that he did not feel any pain or lack of comfort. Those marks could have appeared because the patient wore the orthosis 2h instead of the 1h recommended. If the marks are visible after a 1h period, it might be needed to change the alveoli size/shape or use wider Velcro straps to increase the area on which the pressure is applied.

The physical therapist noticed that the arm was getting more relaxed. This is very encouraging but this observation should be interpreted with great caution. Indeed, the relaxation could come from the Botulinum toxin injection. However, the injection was done on 10 March 2021, it would thus be surprising to see the effects of the injection changing from one week to the other, 11 weeks after the injection.

2.3 Conclusion of the trial

In conclusion, only one patient out of the two was able to wear the orthosis for the entire period of the trial. Patient 1, that did not proceed with the trial, was suffering from diastasis of the shoulder²³ so his arm could not be elongated for more too long periods. However, he found the splint comfortable for the short period he tried it. Patient 2 gave a feedback on the eight-days trial. He could not put

²³This information was not known at the time of the scanning or he would not have been selected for the trial. During the two first meetings with the patient, he did not have the equipment used to maintain his arm elevated as he was going to his physical therapy session.



(a) The skin near the elbow of Patient 2 is slightly red.



(b) The location of the straps and of some alveoli can be seen on the skin of the patient.

Figure 65: Redness and marks on Patient 2 arm. Note that the patient wore the orthosis 2h instead of the 1h recommended.

the splint on by himself so wearing every day was not possible but he found it comfortable and his physical therapist saw an improvement of flexibility (but it could come from the injection received). The orthosis seems to leave small marks on the patient's arm and even though he says it does not hurt, caution must be taken.

Part V

Conclusion

This section concludes this work and gives ideas for future improvements.

1 What has been done

Two models of custom 3D printed orthoses have been created to force the arm's extension of patients suffering from elbow spasticity. The elbow flexors of the targeted patients are constantly contracted and they should be regularly elongated, to avoid permanent shortening of the muscles' fibers [3].

Two models are developed, both 3D printed and modeled on the patient 3D scan to fit perfectly. The proposed designs are adapted to the pathology. Indeed, depending on both short-term factors (time of the day and tiredness or stress of the patient for example) and long-term factors (such as treatments, improvements or worsening of the contracture), the opening angle can be adjusted [5]. To not rush the muscles, the increments between two opening angles are small²⁴.

The first model uses a BOA dial, a small device able to shorten or lengthen a cable embedded in the splint. As the length of the cable changes, the splint's opening angle increases or decreases. The second model uses a blocking hinge that allows the splint to be blocked to a finite number of opening angles (two models with different increment size are available).

Once the ideas were initially defined, both solutions were optimized by changing the design and parameters according to the issues encountered. Most issues were encountered during the design and the printing tests (bad quality due to the printing orientation and the printer, problems with the tubes to pass the cable, post-printing deformations etc.). For both designs, the splint is 3D printed in polypropylene: a light, waterproof, semi-flexible, and resistant material. This choice was easily made for the BOA model but several trials and modifications were needed for the blocking hinge model. Ultimately, the forearm and the upper arm parts are printed separately and are then combined using

²⁴Increments of 16.4° or 18° for the blocking hinge (Small and Large models) and around 1.5° for the BOA design.

simple binding screws. This reduces the printing time, improves the finishing quality and the resistance of the models. Some post-processing is needed but it is quick and simple in comparison to fixing an external hinge.

One patient did an eight-days trial with a BOA model. The patient could not put on the splint by himself (his wife needed to help him so it was not possible to wear it every day) but he found the splint comfortable and the external helper found the BOA easy to adjust. His physical therapist saw an improvement of flexibility (caution must be taken as it could come from the injection received). The patient wore the splint for a longer period than recommended and it seems to leave small marks on his arm. Even though he said it did not hurt, some parameters might need to be adjusted if the problem remains when the splint is worn 1h at a time.

In conclusion, the two models of orthoses are promising but additional studies on more patients are needed to properly assess their effects.

2 Further improvements

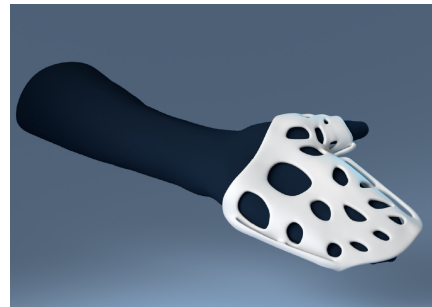
In this section, some ideas for further improvements are described.

2.1 Inclusion of the hand in the orthosis

As most patients suffering from elbow spasticity also suffer from wrist and fingers spasticity, it would be interesting to complete the orthosis designed in this work with a second part that extends to the wrist and fingers. The fingers could be maintained elongated by being laid down on a slightly curved surface without including a hinge to move them. Some products already produced by Spentys could be used such as the H3 or the H5 model displayed in Figure 66.



(a) The H3 model is attached to the hand to support the fingers into the desired position. The fingers can be in independent positions.



(b) The H5 model provides palmar support of the hand and fingers.

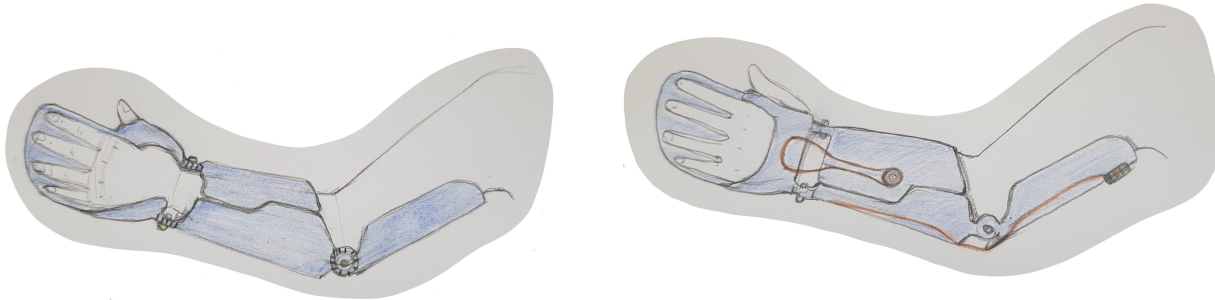
Figure 66: Two models already available in the Spentys to provide support for the fingers [10]. Those models are already tested and approved and they could be integrated into this new design.

However, the position of the wrist should be adjustable, as the one of the elbow, using hinges. This could be done using the BOA or the blocking hinge system. Since there will be two articulations that need to be controlled, the elbow and the wrist, the same system (both the blocking hinges or both a BOA) or a combination of the two (one blocking and one BOA) can be used. With the ideas developed in this section, the opening of the wrist and the opening of the elbow are controlled independently. An additional challenge is that when the arm is in a relaxed and natural position, the axis of rotation

of the wrist and the one of the elbow are not parallel and are almost perpendicular.

Examples of two models are displayed in Figure 67. The model in Figure 67a uses blocking hinges both for the wrist and the elbow. In this case, the forearm part of the orthosis should be longer, to be connected to the part supporting the hand through hinges. The difficulty here would be to avoid touching the wrist articulation and salient bones. As the rotation axes of both articulations are not parallel, the splint should cover the ventral and the dorsal part of the forearm to support the hinges. Two shells can be clipped together to entirely cover the forearm.

A model with two BOA is displayed in Figure 67b. As for the blocking hinges, the forearm should be entirely covered to allow the fixation of the free hinges of both the wrist and the elbow articulations. The BOA controlling the elbow opening is positioned near the shoulder (as in this project) and the one from the wrist is placed on the dorsal part of the forearm with its cable passing through the splint on the dorsal part of the hand.



(a) With the blocking hinge system, the forearm part of the splint is longer and connected to the part supporting the hand through a second blocking hinge. The forearm part should have a second shell covering the radius as the two articulations will not be in the same orientation.

(b) With the BOA system, the forearm part of the orthosis should be longer to be connected to the part supporting the hand through free hinges. The forearm part should have a second shell on the dorsal part as the two articulations will not be in the same orientation and the BOA of the wrist has to be in the direction of the fingers.

Figure 67: Ideas of models to control both the wrist and the elbow opening angles while supporting the hand.

2.2 Automation of the process

GrassHopper can be used to write a script that uses *Rhino3D* to model the orthosis "automatically". This is already done at Spentys for several common models (hand and forearm models). Writing those scripts is time-consuming but allows the designers to save time on each order and to deliver a consistent design. It is important to invest time in the elaboration of these scripts for models that are very often ordered but not for complicated and rarely ordered designs.

2.3 Long term tests

It would be interesting to see the impact of these orthoses in the long term. A study with several subjects, with different profiles, should be carried out to assess the efficiency of that technique. The maximum range of motion, which gives the maximum angles both in extension and flexion, can be measured using a goniometer (an instrument that measures precise angles). The ROM could be regularly measured, to see the evolution of the patients as they wear, or not, the orthosis. Attention

must be paid as the patients usually engage in more than one treatment at a time. The combination of treatments (medication/physical therapy/immobilization device/surgery...) must be taken into account in this study.

2.4 Adapt the splint for children

As many children suffer from cerebral palsy (0.21% of children are touched worldwide [30]), the orthosis could be adapted to suit them as well. The design should be slightly modified but the overall look might be similar. However, a specific literature research should be carried out to ensure that all aspects of the problems are understood. Moreover, as children are active and restless, it might more difficult to find slots in the day when they could wear the orthosis.

Part VI

Appendix

1 Technical drawings

The technical drawings of the two models of blocking hinges designs are given in this appendix. Both the designs and the drawings are made in *Solidworks*. The dimensions are given in mm.

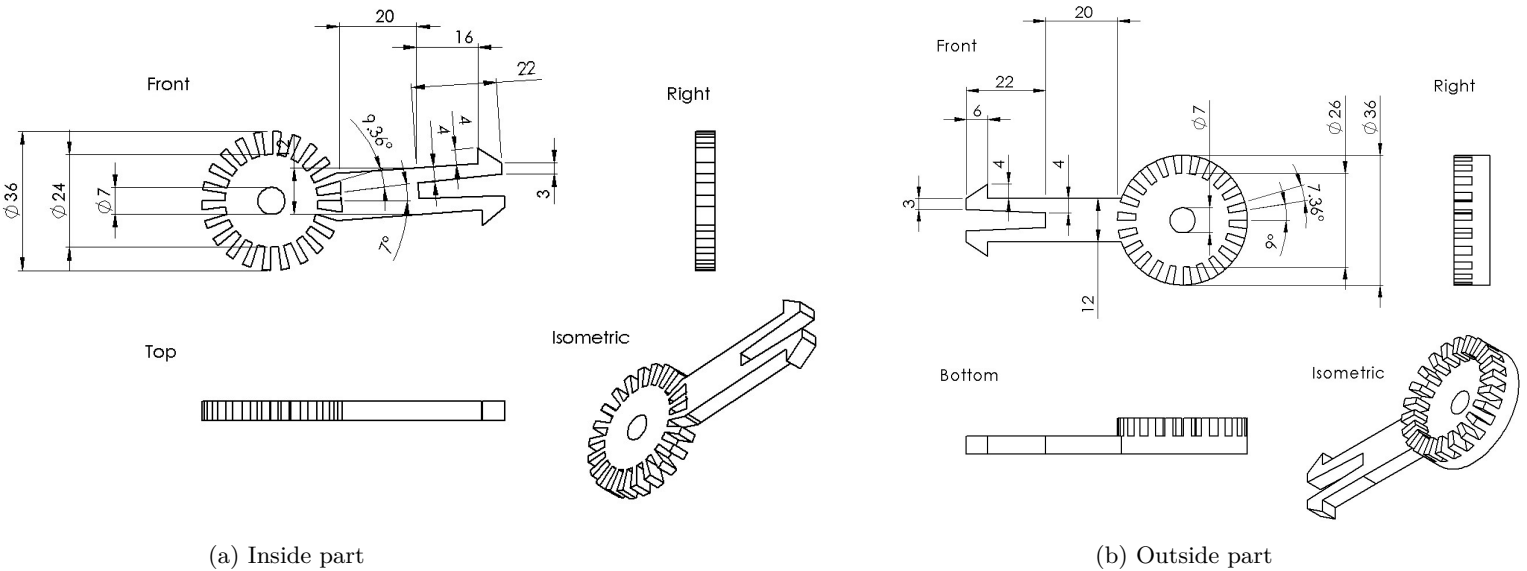


Figure 68: Technical drawings of the Small model of the blocking hinge design.

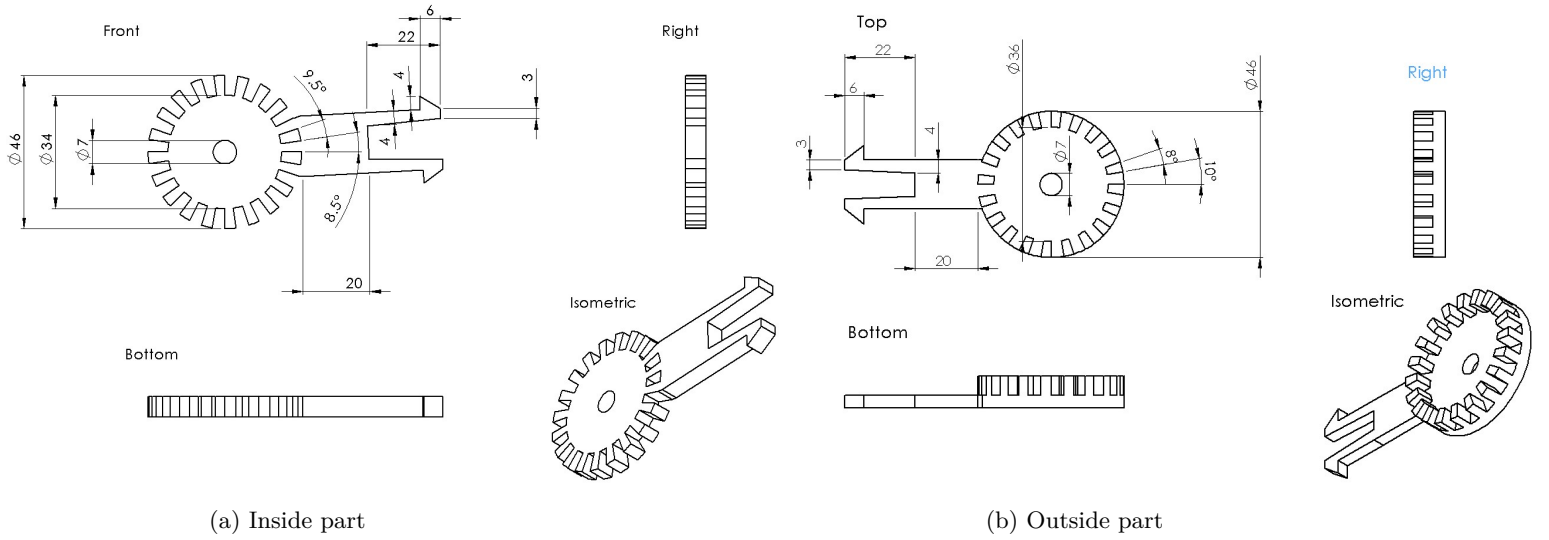


Figure 69: Technical drawings of the Large model of the blocking hinge design.

2 Internship at Spentys

This Master thesis is linked to an industrial internship done at Spentys [10] and is divided into two main parts. The creation of common models of orthoses for Spentys' costumers and the elaboration of this project.

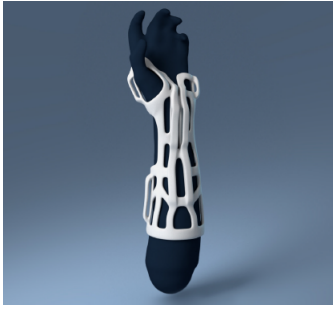
2.1 Help with the orders

To get used to the 3D modeling software and help the designers, I took care of some orders for Spentys' clients. This was interesting to understand the workflow, from the patient to the designer passing by the orthopedist and the sales agent. I learned how to clean a scan and prepare it for the modeling in *Meshmixer* [56]. The scan is cleaned by removing holes, artifacts, and unwanted anatomical parts and smoothing.

As I was asked to do hand and forearm models, *Rhino3D* [57] was used with a script from *Grasshopper* [58]. These scripts facilitate the modeling of those common models, displayed in Figure 70. The following steps should be done. Detailed explanations are not provided but each step is briefly described:

- Import the scan, manually align it in the correct position, and give the important information (order number, version number, side of the limb...)
- Mark the important anatomical points on the scan (elbow and wrist cease, extremities of the phalanges of each finger, etc.). The circumference of the thumb is also needed to ensure good comfort.
- Pick the model layout chosen by the client.
- Make the splint fit the scan. The software uses the scan and the anatomical points given to create an orthosis that fits but the proposed design has to be adjusted manually. Several parameters can be changed (width, rounding...) if needed²⁵.

²⁵The time needed for this step highly depends on the OT's desires, the anatomy of the patient, and the scan quality.



(a) A1 model for the forearm. The A1 attaches to the forearm and immobilizes the wrist with a dorsal opening.



(b) A3 model for the forearm with medial opening. The A3 attaches to the forearm and immobilizes the wrist with a medial opening.



(c) H1 model for the thumb. The H1 attaches to the hand and immobilizes the thumb.

Figure 70: Some common models from Spentys catalog.

- Once the overall shape is good, the next step allows the designer to smooth the angles of the model, to close some unwanted alveoli, or to widen some belt loops if the previous model did not allow them to be large enough for the velcro straps to fit (usually the case for hand orthosis of small patients)²⁵.
- A different closure system can be added. This closure system does not use velcro straps and belt loops but an embedded system with three different closure positions.
- The KPI ²⁶ should be filled to highlight the potential problems encountered. This is important to give a feedback to improve the scripts.
- The model is then exported, once on the scan so the client can see a preview on the platform and validate the design and once alone to engrave its id and to print it. All files are then uploaded on the platform.

2.2 New product

The second part of this internship consisted of the creation of the new product described in this Master thesis and that could be added to the company's catalog.

The elaboration of this product is highly detailed in this document and is the work done for my Master thesis. The internship being separated from this, it mainly helped me to understand the typical steps to develop a new product for the market. As the company is already well implemented and already offers a wide catalog of braces, their expertise was highly valuable. The main steps are the following: This internship helped to understand the typical steps to develop a new product for the market. Indeed, the company is already well implemented and already offers a wide catalog of braces. The main steps are the following:

1. Definition of the need and analysis of the market: The first step was to find a pathology/issue that was not already fully addressed. Then, literature research was carried out to understand the medical aspect of the pathology but also to analyze the current solutions for this problem. The new solution proposed has to be innovative and advantageous compared to the alternatives already on the market. The market size had to be assessed to motivate this project.

²⁶Key performance indicators (KPIs) are targets that help you measure progress against your most strategic objectives [89].

2. Deeper literature research: To correctly design the product and fit the desires of the clients and the needs of the patients, all the features needed should be clearly understood.
3. Learning of the different 3D modelling software: This step was done both for the elaboration of the new product and the work done at Spentys (see Section 2.1). Indeed, some unexpected issues arose during the modelling, and having a good understanding of the software features helps to tackle them. Being able to ask questions to the designers help this learning process.
4. Optimization of the design: The initial ideas should be modified to obtain the best results possible. For this, a lot of trials were done, the opinions of many health care professionals, but also of other employees from Spentys, were taken into account.
5. Feedback from the patients: Meeting patients helped to understand other unexpected constraints (production time, psychological aspects,...). Having their feedback is precious to validate the product or to change some of its aspects.

The resistance analysis performed in this work (see Part III Section 4) were not advised by the company but are carried out for the academic part of this work.

3 Production costs and reimbursement process

As this orthosis is initially conceived to be included in Spentys catalog, the production costs and the reimbursement process are important. Custom orthoses for chronic pathologies are reimbursed by the health insurance, renewable every five years and every year for the children. In Belgium, INAMI is in charge of the reimbursement system [86]. Each year, depending on the "the housewife's shopping basket", the value of several coefficients are defined²⁷. These coefficients are used in formulas that do not change, to define the amount of reimbursement of each product. In this way, products' reimbursement change depending on the cost of life in a proportional manner. Three scenario are compared, a prefabricated orthosis, a custom orthosis without the articulation and a custom orthosis with the articulation. The prefabricated scenario is given in comparison. Both the amount for the two parts with and without the articulation are given. Indeed, as the BOA is not a usual articulation, it might not be reimbursed as one.

The INAMI nomenclature is given in French (and Dutch)²⁸

Spentys would sell the orthoses to 50% of the reimbursed price and the production cost should be between 20% and 30% of the selling price. Overall, the production cost should be around 10% (and maximum 15%) of the reimbursed price. The three scenarios are compared in Table 26.

²⁷The amount are computed for 2021, so the coefficient are defined as $T_1 = 3,308571$ and $T_2 = 1.732316$

²⁸In the section "*Chapitre VI. Lunettes et autres prothèses de l'oeil, appareils auditifs, bandages, appareils orthopédiques et autres prothèses - Art. 29. § 1er. Sont considérés comme relevant de la compétence des orthopédistes (T) - C. MEMBRES SUPERIEURS*", we find:

- 649574: *Groupe principal VII: Poignet et avant-bras - Topographie:(CVII1) De l'articulation métacarpienne aux deux tiers proximaux de l'avant-bras - Sur mesure: Segment du poignet et de l'avant-bras CVII1*. This code is reimbursed $T_1 * 141.6\text{€}$.
- 649736: *Groupe principal IX: Bras - Topographie: (CIX1) De l'articulation du coude aux deux tiers proximaux du bras. Les points de mesure sont les plis du coude et de l'aisselle - Sur mesure: Segment-bras*. This code is reimbursed $T_1 * 141.6\text{€}$
- 650016: *Groupe principal XIV: Suppléments pour articulations - Sur mesure: Suppléments pour articulations ou systèmes de traction: Coude*. This code is reimbursed $T_1 * 94.4\text{€}$.
- 649655: *Groupe principal VIII: Coude - Topographie: (CVIII1) De la moitié de l'avant-bras à mi-bras. Les points de mesure sont les plis du poignet, du coude et de l'aisselle - Préfab: Orthèse du coude; Orthèse du coude avec système de charnière*. This code is reimbursed $T_2 * 187.4\text{€}$. As previously said, this is given as a comparison.

| Scenario | Formula | Reimbursed TVA included (€) | Reimbursed TVA non-included (€) | Sold (€) | Production cost desired (€) |
|----------------------------|---------------|-----------------------------|---------------------------------|----------|-----------------------------|
| 649574 and 649736 | $T_1 * 283.2$ | 936.98 | 883.94 | 441.97 | [88.39;132.59] |
| 649574, 649736 and 650016 | $T_1 * 377.6$ | 1,249.3 | 1,178.58 | 589.29 | [117.85;176.79] |
| Prefabricated one (649655) | $T_2 * 187.4$ | 324.6 | 306.22 | 153.11 | [30.62;45.93] |

Table 26: Amount reimbursed, TVA included and not included as well as the maximum price at which the orthoses should be sold and the maximum production costs for each scenario. The first scenario accounts for the forearm and the upper arm parts but not for the articulation, the second accounts for both parts and the articulation and the third, for prefabricated orthoses, is given as a comparison.

To compute the production costs, the following components are taken into account²⁹:

- A designer would work between 60 and 90min to create the BOA model and around 60 minutes for the blocking hinge design. The cost of an employee is 29.6€/h for Spentys so the modeling cost would be between 29.6 and 44.4€ for the BOA model and 29.6€ for the blocking hinge model.
- The polypropylene used. As the polypropylene costs 34.97€/kg and the splint weights approximately³⁰ between 250 and 350g, it will cost between 8.74 and 12.24€.
- The BOA costs 12€
- The Ultimaker 3 extended costs 3,695€ and the depreciation period is approximated to 3 years (5 days a week of printing 24h : 18,720h) it would take maximum 40h³¹ to print the full orthosis. This means that 468 full orthoses could be printed by one printer and the cost of the printer for one orthosis would be 7.89€.
- Four Velcro straps cost 9.16€.
- Two free hinges, bought at 2€ but they could easily be found at a lower price³².
- The epoxy glue tube costs around 8.7€ but can be used for many orthoses so the price for one splint is under 1€.

The total cost of the production of the orthosis (considering the most expensive possibilities³³) with the BOA design is thus 88.69€ and 60.89€ for the blocking hinge design. We see that, whether or not the articulation is reimbursed, the production cost is lower than the one desired.

4 Inconclusive finite element simulations

This Section describes the inconclusive simulations done on the assembly of the two parts of the hinge. These results are interesting to understand the choices made in the final simulation explained in Part II Section 42. The first simulations were done with only the arm of the external part fixed. The internal part and the cylinder "jumped" out of the assembly and underwent huge displacements (up

²⁹All prices are given excluding taxes.

³⁰The weight of the different splints printed: Prototype: 266g, Patient 1: 263g, Patient 2: 322g

³¹The prototypes for the patients (see Section IV) took 30 and 37 hours to be printed. Each prototype was printed using only one printer. By printing the upper arm part and the forearm part simultaneously in two different printers, the printing time is reduced to 17 and 20 hours.

³²The hinges were found by the piece [88] but they can be bought in large quantities in a professional shop to reduce the cost of individual pieces.

³³The prices are computed considering 90 minutes for the modeling of the BOA and 60min for the blocking hinge design and prices of the pieces are taken as if they were bought individually.

to $8e + 6mm$) since they were no longer in contact with the external part of the hinge.

A trial was also done by forbidding the external face of the internal part of the hinge to move but the results obtained were not conclusive (see Figure 71). Indeed, the stresses are mostly localized on this face and does not appear deeper in the volume of the teeth, which does not represent reality. Moreover, the stresses distribution is unrealistic as some points of the internal part that are not in contact with the external part experience very high stresses while other points that are in contact do not.

Other problems arose, due to solver issues, leading to simulations artifacts, as displayed in Figure 72a. Changing the boundary conditions and the size of the mesh reduced those artifacts.

As the face should not be restricted, it was decided to fix the internal cylinders of the parts (where the binding screw is). However, taking the surfaces of the internal cylinders as fixed, in all directions, does not work as it forbids the rotation around the binding screw so the load is entirely taken by the arms of the hinges and the teeth are not subjected to any stress (as displayed in Figure 72b)³⁴. As explained in Part II Section 4.3.1, the best solution was to forbid the internal cylinders and the cylinder mimicking the screw to move perpendicularly from the pieces. As the face should not be restricted, it was decided to fix the internal cylinders of the parts (where the binding screw is). However, taking the surfaces of the internal cylinders as fixed, in all directions, does not work as it forbids the rotation around the binding screw so the load is entirely taken by the arms of the hinges and the teeth are not subjected to any stress (as displayed in Figure 72b)³⁵. As explained in Part II Section 4.3.1, the best solution was to forbid the internal cylinders and the cylinder mimicking the screw to move perpendicularly from the pieces.

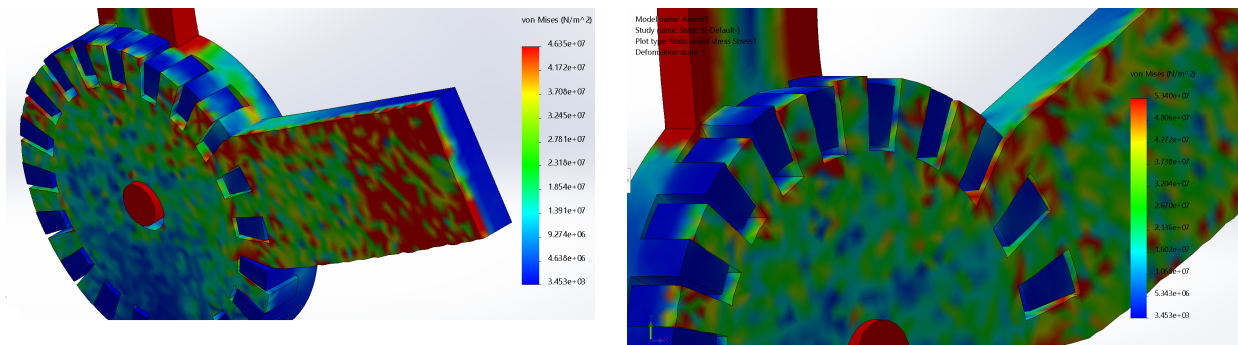


Figure 71: Von mises stresses as movements along the perpendicular direction of the face of the internal part are forbidden.

Note that the promising simulation done in Part II Section 4.3.1 with an element size of 1mm was also carried out with an element size of 0.5mm. Even though the mesh quality was improved, the results were unrealistic, as displayed in Figure 73. This is probably explained by the fact that the solver was not able to use the *Large displacements* option.

³⁴Note that for this simulation, the load and fixed points were different but, as it was not conclusive, the idea was not developed any further.

³⁵Note that for this simulation, the load and fixed points were different but, as it was not conclusive, the idea was not developed any further.

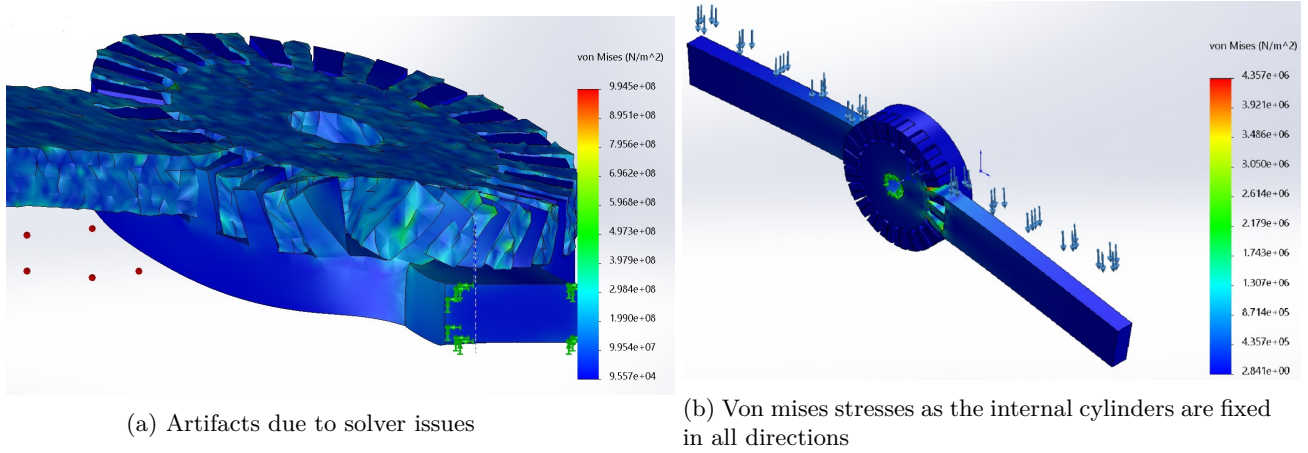


Figure 72: Errors during the simulation of the assembly.

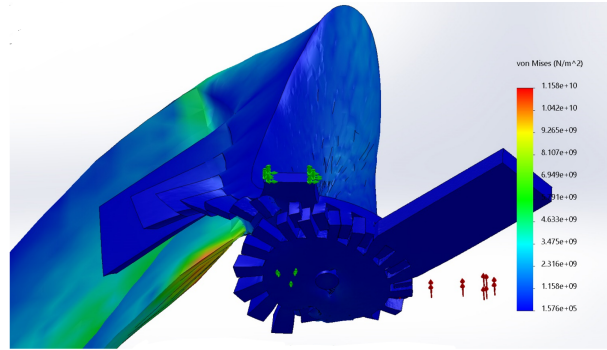


Figure 73: Von mises stresses of the assembly simulation using a very thin mesh (0.5mm of element size). The deformed geometry does not reflect reality due to issues of the solver.

5 Parameters used for the printing

The parameters shown in Figure 74 were the one used for most designs. Note that the thickness of the layers was the only changing parameter. Indeed, thinner layers give a slightly better finishing but the quality does not tremendously change as the thickness is increased. On the other hand, the printing time is proportional to the thickness, so, most prototypes were printed with a 0.2mm thickness but some small tests were done with a 0.3mm thickness.

| Quality | | | |
|------------------------------------|-------------------------------------|-----------------|--|
| Layer Height | 0.2 | mm | |
| Shell | | | |
| Wall Thickness | 1.1 | mm | |
| Wall Line Count | 3 | | |
| Top/Bottom Thickness | 1.1 | mm | |
| Top Layers | 6 | | |
| Bottom Layers | 6 | | |
| Fill Gaps Between Walls | Everywhere | | |
| Infill | | | |
| Infill Extruder | Extruder 1 | | |
| Infill Density | 99 | % | |
| Infill Pattern | Octet | | |
| Infill Overlap Percentage | 0 | % | |
| Material | | | |
| Default Printing Temperature | 210 | °C | |
| Printing Temperature | 210 | °C | |
| Printing Temperature Initial Layer | 215 | °C | |
| Initial Printing Temperature | 200 | °C | |
| Final Printing Temperature | 195 | °C | |
| Build Plate Temperature | 95 | °C | |
| Diameter | 2.85 | mm | |
| Flow | 100 | % | |
| Enable Retraction | <input checked="" type="checkbox"/> | | |
| Retraction Distance | 7 | mm | |
| Retraction Speed | 35 | mm/s | |
| Retraction Prime Speed | 35 | mm/s | |
| Retraction Extra Prime Amount | 0.8 | mm ³ | |
| Retraction Minimum Travel | 0.76 | mm | |
| Nozzle Switch Retraction Distance | 16 | mm | |
| Nozzle Switch Prime Speed | 35 | mm/s | |

| Speed | | | |
|-------------------------------|-------------------------------------|-------------------|--|
| Print Speed | 30 | mm/s | |
| Infill Speed | 35 | mm/s | |
| Wall Speed | 30 | mm/s | |
| Outer Wall Speed | 25 | mm/s | |
| Inner Wall Speed | 30 | mm/s | |
| Travel Speed | 300 | mm/s | |
| Print Acceleration | 2000 | mm/s ² | |
| Travel Acceleration | 2000 | mm/s ² | |
| Print Jerk | 25 | mm/s | |
| Cooling | | | |
| Enable Print Cooling | <input checked="" type="checkbox"/> | | |
| Fan Speed | 20 | % | |
| Regular Fan Speed | 20 | % | |
| Maximum Fan Speed | 20 | % | |
| Support | | | |
| Generate Support | <input type="checkbox"/> | | |
| Build Plate Adhesion | | | |
| Build Plate Adhesion Type | Brim | | |
| Build Plate Adhesion Extruder | Extruder 1 | | |
| Brim Width | 16 | mm | |

Figure 74: Printing parameters used for most of the printing tests and for the final designs.

References

- [1] Beaumont Health *Conditions - Spasticity* Retrieved on 10 March 2021, from <https://www.beaumont.org/conditions/spasticity#:~:text=Spasticity%20is%20usually%20caused%20by,sclerosis%20and%20hereditary%20spastic%20paraplegias>.
- [2] Vijay Patel *UPPER VS. LOWER MOTOR NEURON LESIONS*, Illinois Chiropractic Society. Retrieved March 10, 2021 from <https://ilchiro.org/upper-vs-lower-motor-neuron-lesions/#:~:text=An%20upper%20motor%20neuron%20lesion,1>
- [3] Hefter, H., Jost, W. H., Reissig, A., Zakine, B., Bakheit, A. M., & Wissel, J. (2012). *Classification of posture in poststroke upper limb spasticity: a potential decision tool for botulinum toxin A treatment?* International journal of rehabilitation research, 35(3), 227-233.
- [4] American Association of Neurological Surgeons (2021) *Spasticity* Retrieved March 21, 2021 from <https://www.aans.org/en/Patients/Neurosurgical-Conditions-and-Treatments/Spasticity>
- [5] Andringa, A., van de Port, I., & Meijer, J. W. (2013). *Long-term use of a static hand-wrist orthosis in chronic stroke patients: a pilot study*. Stroke research and treatment, 2013.

- [6] Össur. Retrieved March 17, 2021 from <https://www.ossur.com/en-ca/bracing-and-supports/upper-extremity/innovator-x-post-op-elbow>
- [7] Donjoy Retrieved March 17, 2021 from <https://www.djoglobal.com/products/donjoy/x-act-rom-elbow>
- [8] Guyton GP. *Een analyse van de iatrogene complicaties van het totale contact gegoten*. Voetklem Int. 2005; 26(11):903-907.
- [9] BOA dialed in *Le BOA FIT SYSTEM*. Retrieved March 14, 2021 from <https://www.boafit.com/fr-fr/>
- [10] <https://www.spentys.com/>
- [11] Lance, J. W. (1980). *The control of muscle tone, reflexes, and movement: Robert Wartenbeg Lecture*. Neurology, 30(12), 1303-1303.
- [12] Human Anatomy and Physiology Lab, Lumen learning *The spinal cord*. Retrieved March 18, 2021 from <https://courses.lumenlearning.com/ap1x94x1/chapter/the-spinal-cord/>
- [13] Wikipédia, l'encyclopédie libre. *Faisceau pyramidal*. Retrieved May 17, 2021 from http://fr.wikipedia.org/w/index.php?title=Faisceau_pyramidal&oldid=166460706
- [14] Liu, J., Sheng, Y., & Liu, H. (2019). *Corticomuscular coherence and its applications: a review*. Frontiers in human neuroscience, 13, 100.
- [15] Stephen Kishner (November 2017) *Elbow Joint Anatomy* Medscape. Retrieved from <https://emedicine.medscape.com/article/1898896-overview#showall>
- [16] Tim Taylor (July 3, 2018) *Muscles of the Elbow* Innerbody Research. Retrieved from <https://www.innerbody.com/image/musc07.html#:~:text=Two%20muscles%20%2D%20the%20triceps%20brachii,the%20extensors%20of%20the%20forearm.&text=The%20anconeus%20is%20a%20much,and%20ends%20at%20the%20olecranon.>
- [17] The Lecturio Medical Concept Library *Elbow Joint*. Retrieved March 30, 2021 from <https://www.lecturio.com/concepts/elbow-joint/>
- [18] Ghai, A., Garg, N., Hooda, S., & Gupta, T. *Spasticity-Pathogenesis, prevention and treatment strategies*. Saudi J Anaesth. 2013; 7 (4): 453-60.
- [19] Harb, A., & Kishner, S. (2020). *Modified Ashworth Scale*. StatPearls. Retrieved from <https://www.ncbi.nlm.nih.gov/books/NBK554572/>
- [20] Physiopedia, *Tardieu Scale*. Retrieved April 4, 2021 from https://www.physio-pedia.com/Tardieu_Scale
- [21] Akpınar, P., Atici, A., Özkan, F. U., Aktas, I., Kulcu, D. G., Sarı, A., & Durmus, B. (2017). *Reliability of the Modified Ashworth Scale and Modified Tardieu Scale in patients with spinal cord injuries*. Spinal Cord, 55(10), 944-949.
- [22] Haugh, A. B., Pandyan, A. D., & Johnson, G. R. (2006). *A systematic review of the Tardieu Scale for the measurement of spasticity*. Disability and rehabilitation, 28(15), 899-907.
- [23] World Health Organization (2012) *Global Health Estimates*. Retrieved March 28, 2021 from http://www.who.int/healthinfo/global_burden_disease/en/
- [24] Devroey, D., Van Casteren, V., & Buntinx, F. (2003). *Registration of stroke through the Belgian sentinel network and factors influencing stroke mortality*. Cerebrovascular Diseases, 16(3), 272-279.

- [25] World Stroke Organization (2019) *Global Stroke Fact Sheet 2019*. Retrieved March 28, 2021 from <https://www.world-stroke.org/publications-and-resources/resources/global-stroke-fact-sheet>
- [26] Rizzo, M. A., Hadjimichael, O. C., Preiningerova, J., & Vollmer, T. L. (2004). *Prevalence and treatment of spasticity reported by multiple sclerosis patients*. Multiple Sclerosis Journal, 10(5), 589-595.
- [27] Huangling Zeng†, Jian Chen†, Yang Guo and Sheng Tan (20 January 2021) *Prevalence and Risk Factors for Spasticity After Stroke: A Systematic Review and Meta-Analysis* Retrieved from Neurorehabilitation, a section of the journal Frontiers in Neurology. doi: 10.3389/fneur.2020.616097
- [28] Sommerfeld, D. K., Gripenstedt, U., & Welmer, A. K. (2012). *Spasticity after stroke: an overview of prevalence, test instruments, and treatments*. American Journal of Physical Medicine & Rehabilitation, 91(9), 814-820.
- [29] Walton, C., King, R., Rechtman, L., Kaye, W., Leray, E., Marrie, R. A., ... & Baneke, P. (2020). *Rising prevalence of multiple sclerosis worldwide: Insights from the Atlas of MS*. Multiple Sclerosis Journal, 26(14), 1816-1821.
- [30] Oskoui, M; Coutinho, F; Dykeman, J; Jetté, N; Pringsheim, T (June 2013). "An update on the prevalence of cerebral palsy: a systematic review and meta-analysis". Developmental Medicine & Child Neurology. 55 (6): 509–19. doi:10.1111/dmcn.12080. PMID 23346889. S2CID 22053074.
- [31] My child at CerebralPalsy.org *Prevalence of Cerebral Palsy*. Retrieved March 30, 2021 from <https://www.cerebralpalsy.org/about-cerebral-palsy/prevalence-and-incidence>
- [32] The American Society of Health-System Pharmacists, *Baclofen* Retrieved May 2, 2021 from <https://medlineplus.gov/druginfo/meds/a682530.html>
- [33] Christopher Melinosky (March 2021) *Spasticity* WebMD, LLC Retrieved from <https://www.webmd.com/pain-management/pain-management-spasticity>
- [34] Hillman, M. (2004). *Rehabilitation robotics from past to present: A historical perspective*. In Z.Z. Bien & D. Stefanov (Eds.), *Advances in Rehabilitation Robotics* (25-44). Berlin: Springer-Verlag.
- [35] UC San Diego, School of Medicine. Regents of the University of California. *Selective Peripheral Neurotomy*. Retrieved May 26, 2021 from <https://health.ucsd.edu/specialties/neuro/specialty-programs/paralysis-center/Pages/peripheral-neurotomy.aspx>
- [36] Symmetric designs *Canadian Serial Orthoses, Flexion contracture management*. Retrieved March 19, 2021 from <https://www.symmetric-designs.com/knee-and-elbow-extension>
- [37] Rosenmann, G., et al. (2018). *Development and Evaluation of Low-Cost Custom Splint for Spastic Hand by Additive Manufacturing*. 701-711.
- [38] Orfit: The personal fit *ORFILIGHT® 3.2 mm*. Retrieved April 22, 2021 from <https://www.orfit.com/app/uploads/80004-ORFILIGHT.pdf>
- [39] Jost, W. H., Hefter, H., Reissig, A., Kollwe, K., & Wissel, J. (2014). *Efficacy and safety of botulinum toxin type A (Dysport) for the treatment of post-stroke arm spasticity: Results of the German-Austrian open-label post-marketing surveillance prospective study*. Journal of the neurological sciences, 337(1-2), 86-90.
- [40] Li, S. (2017). *Spasticity, motor recovery, and neural plasticity after stroke*. Frontiers in neurology, 8, 120. Retrieved from <https://www.frontiersin.org/articles/10.3389/fneur.2017.00120/full>

- [41] Graham, K. S., Golla, S., Gehrmann, S. V., & Kaufmann, R. A. (2019). *Quantifying the center of elbow rotation: implications for medial collateral ligament reconstruction*. HAND, 14(3), 402-407.
- [42] Alonso, A., & Hernán, M. A. (2008). *Temporal trends in the incidence of multiple sclerosis: a systematic review*. Neurology, 71(2), 129-135. doi: 10.1212/01.wnl.0000316802.35974.34
- [43] Chantraine, F., Kolanowski, E., Filipetti, P. (2014) *Spasticité: Définition, Evaluation et Traitement* CNRFR – Rehazenter, Laboratoire d'Analyse du Mouvement et de la Posture, Luxembourg
- [44] National Rheumatoid Arthritis Society, *Elbow Surgery* Retrieved April 2, 2021 from <https://nras.org.uk/resource/elbow-surgery/>
- [45] Human Anatomy and Physiology Lab, Lumen learning *Muscles of the upper arm*. Retrieved May 8, 2021 from <https://courses.lumenlearning.com/ap1x94x1/chapter/muscles-of-the-upper-arm/>
- [46] Manosplint Catalog *Velcro straps : M600000001-2192 STRAP ELASTIC 295x38mm / Blue/gray*
- [47] All3DP, *3D Printing Technology Guide: The Types of 3D Printing Technology* (February 2020) Retrieved from <https://all3dp.com/1/types-of-3d-printers-3d-printing-technology/>
- [48] Ultimaker Support (February 2020) *Ultimaker 3 maintenance schedule* Retrieved from <https://support.ultimaker.com/hc/en-us/articles/360011597119-Ultimaker-3-maintenance-schedule>
- [49] Fast Radius *All about vat photopolymerization* Retrieved from <https://www.fastradius.com/resources/vat-photopolymerization/>
- [50] J. Flynt (March 2019) *All About SLS Printing: Advantages, Disadvantages, History, and more* 3D insider. Retrieved from <https://3dinsider.com/sls-printing/>
- [51] materialise *Multi Jet Fusion* Retrieved from <https://www.materialise.com/en/manufacturing/3d-printing-technology/multi-jet-fusion>
- [52] 3D sourced (December 2019) *Multi Jet Fusion: Everything You Need To Know About MJF 3D Printing*. Retrieved from https://www.3dsourced.com/3d-printing-technologies/multi-jet-fusion-mjf/#Multi_Jet_Fusion_Advantages
- [53] Autodesk, Inc. *Maya Software, 3D computer animation, modeling, simulation, and rendering software* Downloaded March 13, 2021 from <https://www.autodesk.com/products/maya/overview?term=1-YEAR>
- [54] Dassault Systèmes SolidWorks Corporation *Solidworks software* Downloaded May 3, 2021 <https://www.solidworks.com/>
- [55] Software developed by Microsoft Corporation to view, create, and personalize 3D objects. Downloaded March 13, 2021 from <https://www.microsoft.com/en-us/p/3d-builder/9wzdnrcrfj3t6?activetab=pivot:overviewtab>
- [56] *Meshmixer Software* Downloaded March 13, 2021 from <https://www.Meshmixer.com/>
- [57] Robert McNeel & Associates *Rhino 6 from Rhinoceros 3D* <https://www.rhino3d.com/>
- [58] Grasshopper *Algorithmic modeling for Rhino* <https://www.grasshopper3d.com/>
- [59] Cuiro *Catalogue: rehabilitation part: Handtherapy: Elbow R.O.M. Joint*. Retrieved March 20, 2021 from http://cuiro.ch/all/pdfs/Handtherapie_Part_1_S-001-094.pdf
- [60] Ultimaker BV *3D printers* Retrieved April 4, 2021 from <https://ultimaker.com/3d-printers>

- [61] Raise printer model Raise 3D Pro2 Plus. <https://www.raise3d.com/>
- [62] Wasp 3D printer model Delta WASP 4070 Industrial 4.0. <https://www.3dwasp.com/en/>
- [63] <https://de.rosler.com/en-en/products/mass-finishing/rotary-vibrators/>
- [64] All3DP *3D PRINTER LAYER SHIFTING: What's the Problem?* Retrieved May 3, 2021 from <https://all3dp.com/2/layer-shifting-3d-printing-tips-tricks-to-solve-it/#:~:text=Layer%20shifting%20is%20when%20the,model%20might%20turn%20out%20perfect.>
- [65] Magigoo Pro PP - The 3D printing adhesive for Polypropylene. Retrieved from <https://magigoo.myshopify.com/collections/all/products/magigoo-pp-the-3d-printing-adhesive-for-polypropylene>
- [66] Shaoxing Xinshan Science Technology Co.,Ltd. *How To 3D Print With Polypropylene PP Material?* (Feb 17, 2020) Retrieved from <http://m.xslightings.com/news/how-to-3d-print-with-polypropylene-pp-material-31628557.html>
- [67] Araldite® *Cristal 24ml seringue*. Retrieved May 12, 2021 from <https://www.go-araldite.com/fr/produits/epoxy-adhesives/araldite-crystal-2-x15ml-tube>
- [68] Sardelli, M., Tashjian, R. Z., & MacWilliams, B. A. (2011). *Functional elbow range of motion for contemporary tasks*. The Journal of bone and joint surgery. American volume, 93(5), 471-477. <https://doi.org/10.2106/JBJS.I.01633>
- [69] Loss, J. F., & Candotti, C. T. (2008). *Comparative study between two elbow flexion exercises using the estimated resultant muscle force*. Brazilian Journal of Physical Therapy, 12(6), 502-510.
- [70] MatWeb, material property data *Steels, General Properties*. Retrieved April 20, 2021 from <http://www.matweb.com/search/datasheet.aspx?bassnum=MS0001&ckck=1>
- [71] S. Cescotto (2017-2018) *Mécanique du solide, syllabus de théorie* Université de Liège, Faculté des Sciences Appliquées, Département ArGEnCo
- [72] Massonet C. and Cecotto S. (edition 2009) *Mécanique des matériaux* Université de Liège
- [73] Dassault Systems *Solidworks Help Strain Components*. Retrieved May 20, 2021 from http://help.solidworks.com/2017/english/solidworks/cworks/c_Strain_Components_2.htm
- [74] John Mitchell (October 18, 2018) *Yield Strength of Plastics – basic principles, the tensile test and material property table*. Retrieved from <https://www.engineeringclicks.com/yield-strength-of-plastics/>
- [75] Jenna Boyle (2013) *SolidWorks Simulation: What is Von Mises Stress?* Design point, Retrieved from <https://www.design-point.com/resource/blog/solidworks-simulation-what-is-von-mises-stress-part-2-of-2/>
- [76] BASF 3D Printing Solutions BV (Revised in November 2019) *Technical Data Sheet Ultrafuse PP*
- [77] BASF 3D Printing Solutions BV (Revised in November 2019) *Technical Data Sheet Ultrafuse PET*
- [78] Woern, A. L., Byard, D. J., Oakley, R. B., Fiedler, M. J., Snabes, S. L., & Pearce, J. M. (2018). *Fused particle fabrication 3-D printing: Recycled materials' optimization and mechanical properties*. Materials, 11(8), 1413.
- [79] Dassault Systems Solidworks Help *Running studies*. Retrieved May 22, 2021 from https://help.solidworks.com/2018/english/SolidWorks/cworks/c_Running_Studies.htm

- [80] De Leva, P. (1996). Adjustments to Zatsiorsky-Seluyanov's segment inertia parameters. *Journal of Biomechanics*, 29(9), 1223–1230. doi:10.1016/0021-9290(95)00178-6
- [81] Dehem, S., Gilliaux, M., Lejeune, T., Detrembleur, C., Galinski, D., et. al. *Assessment of upper limb spasticity in stroke patients using the robotic device REAplan*. In: *Journal of Rehabilitation Medicine*, Vol. 49, no. 7, p. 565–571 (2017) DOI:10.2340/16501977-2248
- [82] Li, X., & Eichinger, L. J. K. (2015). *Clinically Relevant Elbow Anatomy and Surgical Approaches*. In *Elbow Ulnar Collateral Ligament Injury* (pp. 1-10). Springer, Boston, MA.
- [83] Brinckmann, P., Drerup, B., Kretschmer, T., Schulze-Frenking, D., Wohlatz, A., & Wetz, H. H. (2007). *Locating the axis of rotation when fitting an elbow orthosis: A comparison of measurement and palpation*. *Prosthetics and orthotics international*, 31(1), 36-44.
- [84] WebMD LLC. *Lioresal Tablet* Retrieved May 26, 2021 from <https://www.webmd.com/drugs/2/drug-12240/lioresal-oral/details>
- [85] Centre Neurologique et de Réadaptation Fonctionnelle de Fraiture-en-Condroz. <http://www.cnrf.be/>
- [86] Institut national d'assurance maladie-invalidité. *La nomenclature des prestations de santé* Retrieved March 15, 2021 from <https://www.inami.fgov.be/fr/nomenclature/Pages/default.aspx>
- [87] Wikipédia, l'encyclopédie libre. *Diastasis* Retrieved June 6, 2021 from <https://en.wikipedia.org/wiki/Diastasis>
- [88] BricoPlanit Rocourt *Vis de reliure Vynex laiton 10 mm - 2 pcs*
- [89] QlikTech International AB *What is a KPI?*. Retrieved May 26, 2021 from [https://www.qlik.com/us/kpi#:~:text=Key%20performance%20indicators%20\(KPIs\)%20are,the%20success%20of%20your%20business.](https://www.qlik.com/us/kpi#:~:text=Key%20performance%20indicators%20(KPIs)%20are,the%20success%20of%20your%20business.)